PNAS RESEARCH ARTICLE | ECOLOGY OPEN ACCESS

Wild canids and felids differ in their reliance on reused travel routeways

William F. Fagan[a,1], Ananke G. Krishnan[a], Christen H. Fleming[a,b,c,d], Elizabeth Ferreira[a], Stephanie Chia[a], Anshuman Swain[a,e,f], Briana Abrahms[g,h], Chloe Bracis[i], Eliezer Gurarie[i], Thomas Mueller[k,l], Michael J. Noonan[m,n,o], Luiz Gustavo R. Oliveira-Santos[p], Marlee A. Tucker[q], Gayatri Anand[a], Qianru Liao[a], Sarah Na[a], Steven Su[a], Daisy Liao[a], Varun Chilukuri[a], Shreyas Ramulu[a], Luisa Maria Diele-Viegas[r], Michael Dougherty[s], David Illingworth[t], Dmitry Y. Alexandrov[u], Pamela Castro Antunes[p], Fernanda C. Azevedo[v,w], Christina Barrett[a], Matías Taborda Barroso[x], Dominik M. Behr[h,y], Jerrold L. Belant[z], Steven Bellan[aa], Dominique Berteaux[bb], Dean E. Beyer Jr.[z], Laura R. Bidner[cc,dd], Jacqueline Bishop[ee], J. David Blount[ff], Andrew Butler[gg], Andrew Carter[hh,ii], Marina Motta Carvalho[jj], Michael Chamberlain[kk], Maria D. Chistopolova[ll], Darren Clark[mm], L. Mike Conner[nn], Alayne Cotterill[oo], Gabriele Cozzi[h,y], Bogdan Cristescu[pp,qq], Calum X. Cunningham[rr], Emrah Çoban[ss], Siobhan Darlington[m], Ísis Zanini das Candeias[v], Christopher S. DePerno[tt], Jasja J. A. Dekker[uu], Colleen T. Downs[vv], Natalia Dronova[ll], Marine Drouilly[qq,ww,xx], Ernest Eblate[yy], Steve Ekwanga[dd], Morgan Swingen[tt,zz], Mohammad Farhadinia[aaa,bbb], Adam T. Ford[m], Jacqueline Frair[j,ccc], Laurence Frank[ddd], John M. Fryxell[eee], Todd K. Fuller[fff], Robert Fyumagwa[yy], Stefan Garthe[ggg], Wayne M. Getz[hhh,iii], Maria Jesus Palacios Gonzalez[x], TJ Gooliaff[jjj], Malte Götz[kkk], Rowena Hamer[lll,mmm], Mario Haberfeld[nnn], Mark Hebblewhite[ooo], Jose A. Hernandez-Blanco[ll], Mathias Herrmann[ppp], Marco Heurich[qqq,rrr,sss], Karen E. Hodges[m], AnnMarie Houser[ttt], Bruce Humphries[vv], Miguel Ángel López López Iglesias[uuu], Lynne A. Isbell[cc,dd], David Jachowski[gg], Craig Jackson[vvv], René Janssen[www], Kate E. Jenks[c], Jaime E. Jiménez[xxx], Maria Luisa S. P. Jorge[yyy], Rodrigo Jorge[zzz], Fernando Jubete[aaaa], Anjan Katna[bbbb,cccc], Roland Kays[tt,dddd], Andrew M. Kittle[eeee], Rebecca Klein[ttt], Raido Kont[ffff], Michelle J. C. Kral[ttt], Josip Kusak[ff,gggg,hhhh], Johannes Lang[iiii], Andrew David M. Latham[jjjj], Peter Leimgruber[c], Frederico G. Lemos[v,w], Taal Levi[kkkk,llll], Caio F. M. Lima[v,mmmm], Edson Lima[nnnn], Fernando Lima[oooo,pppp], John D. C. Linnell[sss,qqqq], David W. Macdonald[oo], Peter Mahoney[rr,rrrr], Peep Männil[ssss], Emmanuel Masenga[yy], Jenny Mattisson[vvv], Roel F. May[tttt], Roy T. McBride Jr.[uuuu], Robbie A. McDonald[vvvv], J. Weldon McNutt[h], Karl Miller[kk], Alexander Minaev[wwww], Dale G. Miquelle[xxxx], Christopher E. Moorman[tt], Ronaldo G. Morato[zzz], Ricardo Moreno[yyyy,zzzz], Guilherme Mourão[aaaaa], Bariushaa Munkhtsog[bbbbb], Bayaraa Munkhtsog[bbbbb,ccccc], Sergey V. Naidenko[ll], Teresa Nava[iiii], John Odden[ddddd], Morten Odden[ssss], Francisco Palomares[eeeee], Brent R. Patterson[fffff], Bruce D. Patterson[ggggg], Rogerio Cunha de Paula[zzz], Agustin Paviolo[hhhhh,iiiii], Yury K. Petrunenko[jjjjj,kkkkk], Alim B. Pkhitikov[lllll], Andrey D. Poyarkov[ll], Laura R. Prugh[mmmmm], Kasim Rafiq[g,h], Emiliano Esterci Ramalho[nnnnn], Tharmalingam Ramesh[vv,ooooo], Nathan Ranc[ppppp], Dustin H. Ranglack[qqqqq,rrrrr], Anya Ratnayaka[sssss,ttttt], David Roshier[uuuuu], Eivin Røskaft[vvvvv], Viatcheslav V. Rozhnov[ll], Hector Ruiz-Villar[wwwww], Joel Ruprecht[lllll], Gustaf Samelius[xxxxx], Philipp Schwemmer[ggg], Çağan H. Şekercioğlu[ff,ss,hhhh], Laurel E. K. Serieys[pp,qq,ww], Ivan V. Seryodkin[yyyyy], Olaf Simon[zzzzz], Nucharin Songsasen[c], Pavel A. Sorokin[aaaaaa], Svetlana Soutryina[bbbbbb], Patrick Stent[jjj], David Stoner[rrrr], Jarryd Streicher[vv], Jack Tatler[cccccc], Kristine Teichman[m], Maria Thaker[dddddd], Katerina V. Thompson[a], Jeffrey J. Thompson[eeeeee,ffffff], Marcos Adriano Tortato[gggggg,hhhhhh], Manfred Trinzen[iiiiii], Leanne Van Der Weyde[ttt,jjjjj], Abi Tamim Vanak[bbbb,kkkkkk], Marianela Velilla[eeeeee,ffffff,llllll], Zea Walton[mmmmmm], Tyler J. Wheeldon[fffff], Tomas Willebrand[sss], Terrie M. Williams[nnnnnn], Christopher C. Wilmers[oooooo], Jared Wilson-Aggarwal[vvvv], Michael L. Wysong[pppppp], Anna A. Yachmennikova[ll], Julie K. Young[rrrr], and Justin M. Calabrese[a,b,qqqqqq]

Affiliations are included on p. 10.

Edited by William Murphy, Texas A&M University, College Station, TX; received January 31, 2024; accepted August 5, 2025

Diverse factors, including environmental features and cognitive processes, can drive animals' movements and space use, with far-reaching implications. For example, repeated use of individual-level travel routeways (directionally constrained but imperfectly aligned routes), which results in spatial concentration of activity, can shape encounter-based processes including predation, mate finding, and disease transmission. However, how much variation in routeway usage exists across species remains unknown. By analyzing GPS movement tracks for 1,239 range-resident mammalian carnivores—representing 16 canid and 18 felid species from six continents—we found strong evidence of a clade-level difference in species' reliance on repeatedly used travel routeways. Across the global dataset, tracked canids had a 15% (±7 CI) greater density of routeways within their home ranges than did felids, rising to 33% (±16 CI) greater in landscapes shared with tracked felids. Moreover, comparisons within species across landscapes revealed broadly similar home range routeway densities despite habitat differences. On average, canids also reused their travel routeways more intensively than did felids, with hunting strategies and spatial contexts also contributing to the intensity of routeway usage. Collectively, our results suggest that key aspects of carnivore routeway-usage have an evolutionary component. Striking interspecific and clade-level differences in carnivores' reliance on reused travel routeways within home ranges identify important ways in which the movement patterns of real-world predators depart from classical assumptions of predator-prey theory. Because such departures can drive key aspects of human-wildlife interactions and other encounter-based processes, continued investigations of the relationships between movement mechanisms and space use are critical.

Carnivora | home range | movement ecology | probability ridges | spatial ecology

The authors declare no competing interest.

This article is a PNAS Direct Submission.

[1]To whom correspondence may be addressed. Email: bfagan@umd.edu.

This article contains supporting information online at https://www.pnas.org/lookup/suppl/doi:10.1073/pnas.2401042122/-/DCSupplemental.

Published September 29, 2025.

Issues of space use by moving animals are foundational to diverse research topics at the interface of evolution, ecology, and behavior, including the evolution of territoriality, range residency, and migration (1, 2) as well as the ecology of foraging and predator–prey interactions (3, 4). Classically, many key theoretical results in these fields have required strong assumptions about the homogeneity of space use, with studies that allow for spatial heterogeneity often yielding strikingly different predictions (5–7). Despite the mathematical complications that spatial heterogeneity engenders, such considerations are often highly warranted from a biological perspective. For example, reliance on well-traveled routes (8–14) constitutes a specific way in which the movement of wild animals can depart radically from the ideal gas dynamics that provide the mathematical foundations of encounter-based processes in ecology (e.g., predation, mate finding, disease transmission) (15–18).

Depending on spatial scale, understanding when, where, and how strongly individual animals rely on repeatedly used travel routes through their landscapes can help identify foraging strategies (19), delineate conservation priorities for migrating species (20), and provide information about how learning and memory shape movements (10, 21–23). Among range-resident predators, repeated use of travel routes may emerge as animals navigate among preferred feeding regions (e.g., waterholes, rabbit warrens) or as animals use particular routes for both relocation and foraging (23–25). Questions about reliance on travel routes differ fundamentally from investigations of repeated site visitation, which, by emphasizing destinations and residency time, can be studied using periodograms and repeatability analyses (14, 26, 27). Given the operational demands of field research, however, studies of route-usage in wild species on large scales have typically involved only one or a few species instead of being broadly comparative. Consequently, a robust, cross-species understanding of (dis)similarities in route-usage and the spatial heterogeneity it engenders is lacking. However, increasing opportunities to combine GPS tracking data with publicly accessible remote sensing data mean that large-scale comparative analyses of space use by wild animals are now possible in rigorous and unprecedented ways (28–30).

Studies exploring repeated usage of particular travel routes for terrestrial species—variously discussed in terms of traplines (8, 11), trails (18), recursive paths (12, 13), hunt paths (14, 31), and other terms—focus on similarities in the spatial trajectories of animal movements over time, with recognition that both environmental factors (e.g., valleys, roads, cliff faces) and cognitive processes (e.g., perception, learning, memory) may underlie the emergence of particular reused routes (10, 14, 23–25, 32). The various terms used in the literature to characterize spatial consistency in animal movement often differ in connotation. For example, a "game trail" connotes a very narrow track wherein individuals are often stepping in one another's footsteps, even to the point of creating a bare-earth path through vegetation. In contrast, a "corridor" implies a passageway for migration or other movement through favorable habitat bounded by more hostile areas; corridor width is not restricted by definition, but is often interpreted as being narrow relative to the scale of animal movement (20, 25). A movement "route" is similarly not formally defined with regard to width, but a degree of narrowness is often implied (10, 12). No term in current usage seems to capture the idea that bundled sets of narrow routes with similar orientations may exist as animals traverse a given region of their home range repeatedly but with imperfect consistency. Recognizing that some would reserve the term route for use exclusively with narrow channels for movement, we introduce the term "routeway" to characterize cases where travel is directionally constrained but imperfectly aligned. Below, we introduce statistical methods for identifying routeways from GPS tracking data. We emphasize that routeways exhibit a heightened degree of directional persistence of motion and would be distinct from movement networks that can be characterized by the potential for changes in direction at intersection points.

Mammalian carnivores have long been subjects of space-use research because of their diverse environments and ecological niches, and their association with critical conservation issues (33–35). Within the order Carnivora, the dog and cat families (Canidae and Felidae, respectively) are members of two highly divergent lineages (respectively, the suborders Caniformia and Feliformia) that last shared a common ancestor 41 (36) to 51 Mya (37). The Canidae and Felidae constitute obvious choices for comparative research on predator space use because each family represents a substantial evolutionary radiation, and each includes diverse species whose movements in nature have been studied extensively by researchers worldwide via GPS tracking (29, 38). Collectively, canids and felids tend to be home range resident species (34, 39–41). Their strategies for locating food involve stereotyped movement behaviors (e.g., cursorial pursuit, patient stalking), which in turn reflect important evolutionary differences in biomechanics, physiology, and preferred resources

Significance

Animals' space-use patterns are central to eco-evolutionary theories of territoriality and foraging and to resource management practices, all of which can entail assumptions of spatial homogeneity. We found evidence for species- and clade-level variation in mammalian carnivores' reliance on re-used travel routeways within their home ranges, with canids having, on average, both a greater density of travel routeways and a greater probability of routeway usage than felids. Such marked variation in the heterogeneity of species' space-use patterns is important because it provides a strong empirical contrast to long-standing assumptions of mathematical models of predator-prey dynamics and, more broadly, highlights key issues of space use that are relevant for the conservation and management of at-risk mammalian carnivores globally.

(42–46). These strategies vary among carnivore species, but can also depend on prey species, habitats, and local conditions (39–41, 43, 44, 46). In addition, relationships between carnivores' movement behaviors and space use patterns can depend on cognitive processes such as perception and memory (13, 14, 21, 31, 33, 47–49), which also have an evolutionary basis (49–51). Overall, canids and felids share and even compete for many environments and food types, and present similar spatial planning challenges related to conservation and human–wildlife interactions (34, 52, 53), providing a broad context for comparative analyses.

We examined whether the many evolutionary, behavioral, and ecological dissimilarities among canid and felid species would translate into systematic differences in their use of space within their home ranges, particularly with regard to species' reliance on reused travel routeways. We focused on two aspects of routeway usage: the density of routeways within individuals' home ranges and the intensity with which individuals reused those routeways. If we found strong differences in the density, or use intensity, of routeways across wild carnivore species, it would suggest that at least one mechanistic (nonrandom) driver was at work. Absent such a driver, widespread variation in home range location and composition across taxa and landscapes would be expected to homogenize routeway usage across taxa, or at least obscure weak effects. Variation in routeway usage could arise mechanistically from behavioral differences in movement strategy while foraging, and relatedly, speed, both of which can be investigated in conjunction with GPS tracks. Diverse environmental features such as habitat structure, seasonality, topography, and human infrastructure might also contribute to variation in routeway usage, and such influences can be evaluated through investigations that link remote sensing and movement data. Through detailed analyses of a large database of GPS tracks representing diverse wild felid and canid species, we found evidence that differences in behavior and environmental factors are in fact important predictors of these carnivores' reliance on reused travel routeways. More intriguingly, however, we found robust support for the existence of clade-level differences in routeway density and routeway usage within home ranges. These differences, in which canids systematically exceed felids in their reliance on travel routeways, have important implications for both our understanding of predator–prey interactions and conservation planning.

Results

After leveraging an established workflow for estimating a home range distribution for an individual animal from its GPS track (Fig. 1 *A*–*C*), we characterized the location of reused routeways within the home range via statistical features called "probability ridges" (Fig. 1*D*). A ridge is a spatially contiguous curve of heightened probability in a smooth 2-D probability density function and is mathematically unsigned, indicating movement can progress "in both directions" along the ridge. Within a home range, probability ridges will emerge when an animal repeatedly traverses a region using similar trajectories. In this way, ridges delineate the center of a routeway along its length (*SI Appendix*, *SI Detailed Methods*).

To facilitate comparisons across individuals and species whose home range sizes vary widely, we adopted the nondimensional measure of 'ridge density', which scales total ridge length by home range size (*SI Appendix*, *SI Detailed Methods*). Furthermore, adding spatial buffers to identified probability ridges allowed us to then calculate 'ridge-associated probability mass' as the proportion of the probability mass in an individual's home range distribution that was ridge-associated for each of several buffer widths. Thus, we use ridge density to quantify the existence of routeways, and likewise, we use 'ridge-associated probability mass' to quantify the intensity of routeway usage. After establishing the performance of our routeway estimation methods via detailed simulation studies (*SI Appendix*, Figs. S11–S13 and Tables S5 and S6), we analyzed ridge densities and ridge-associated probability masses within and across clades, controlling for home range size, phylogeny, habitat types, GPS data quality, and other potentially explanatory (or confounding) covariates.

Clade-Level Effects for Ridge Density. Across all models, ridge density was significantly higher for canids than felids. The phylogenetically controlled mixed model revealed a 15% (±7 CI) ($P < 10^{-5}$) increase in ridge density among canids compared with felids when using the full dataset of 1,239 GPS tracks. This canid-felid clade-level difference is readily apparent when plotted on a phylogenetic tree, both for the empirical means and the predicted values (Fig. 2). We also extracted five subdatasets to assess potentially confounding effects associated with our aggregation of multispecies, multisite GPS track data. These subdatasets allowed us to address any effects of 1) data preprocessing, 2) animals' instantaneous speeds, 3) unknown phenological effects stemming from GPS tracks of duration < 1 y, 4) unmodeled spatial variation arising from individuals' heterogeneous landscapes, and 5) phylogenetic uncertainty. Analyses of these subdatasets yielded results that were broadly similar, with canids' heightened ridge density increasing from the above-mentioned results for the full-dataset to 33% (±16 CI) ($P < 10^{-5}$) for the "shared landscapes" subdataset (consisting of the GPS tracks from a set of nine landscapes in which one or more canid species and one or more felid species were studied together) (Fig. 3*B*). Collectively, these consistent clade-level effects indicate that the difference in ridge density between canids and felids is a robust feature that is not sensitive to the details of individual GPS tracks, species, or landscapes (*SI Appendix*, Table S1), nor to phylogenetic uncertainty (*SI Appendix*, *SI Detailed Methods*, *Phylogenetic Considerations*).

Predictive Model Fits for Ridge Density. To quantify the importance of the canid-felid clade effect relative to other possible sources of variation, we used statistical models that included a battery of terms as fixed and random effects within a phylogenetically controlled generalized linear mixed modeling framework (*SI Appendix*, *SI Detailed Methods*, *Statistical Analyses*). For the full dataset, predictions of ridge density reflected significant effects of home range size ($P < 10^{-4}$), terrain roughness ($P < 0.05$), and movement strategy while hunting (represented by the indicator variable slow walking; $P < 0.05$), but no other variables were significant predictors. Specifically, animals engaging in slow-walking behavioral strategies and possessing large home ranges featuring greater terrain roughness exhibited lower ridge density beyond the clade-level effect for the full dataset; effect size plots appear in Fig. 3*A*. Outside of the full dataset, tree cover was a significant predictor for the "year or longer" dataset ($P < 0.01$), and terrain roughness was a significant predictor for all datasets except the year or longer and shared landscapes datasets. Effects of movement strategies were not significant except for the slow-walking indicator variable in the "no-preprocessing" dataset ($P < 0.02$). Average instantaneous speed of travel was not a significant term in the model for the "including speed" dataset ($P > 0.8$), suggesting individual-level variation in speed is not contributing to the observed clade-level differences in ridge density. Effect size plots for the including speed subdataset and all other subdatasets appear in *SI Appendix*, Fig. S1.

Across the nine shared landscapes (which included temperate and tropical forests, temperate and tropical savannas, plus deserts

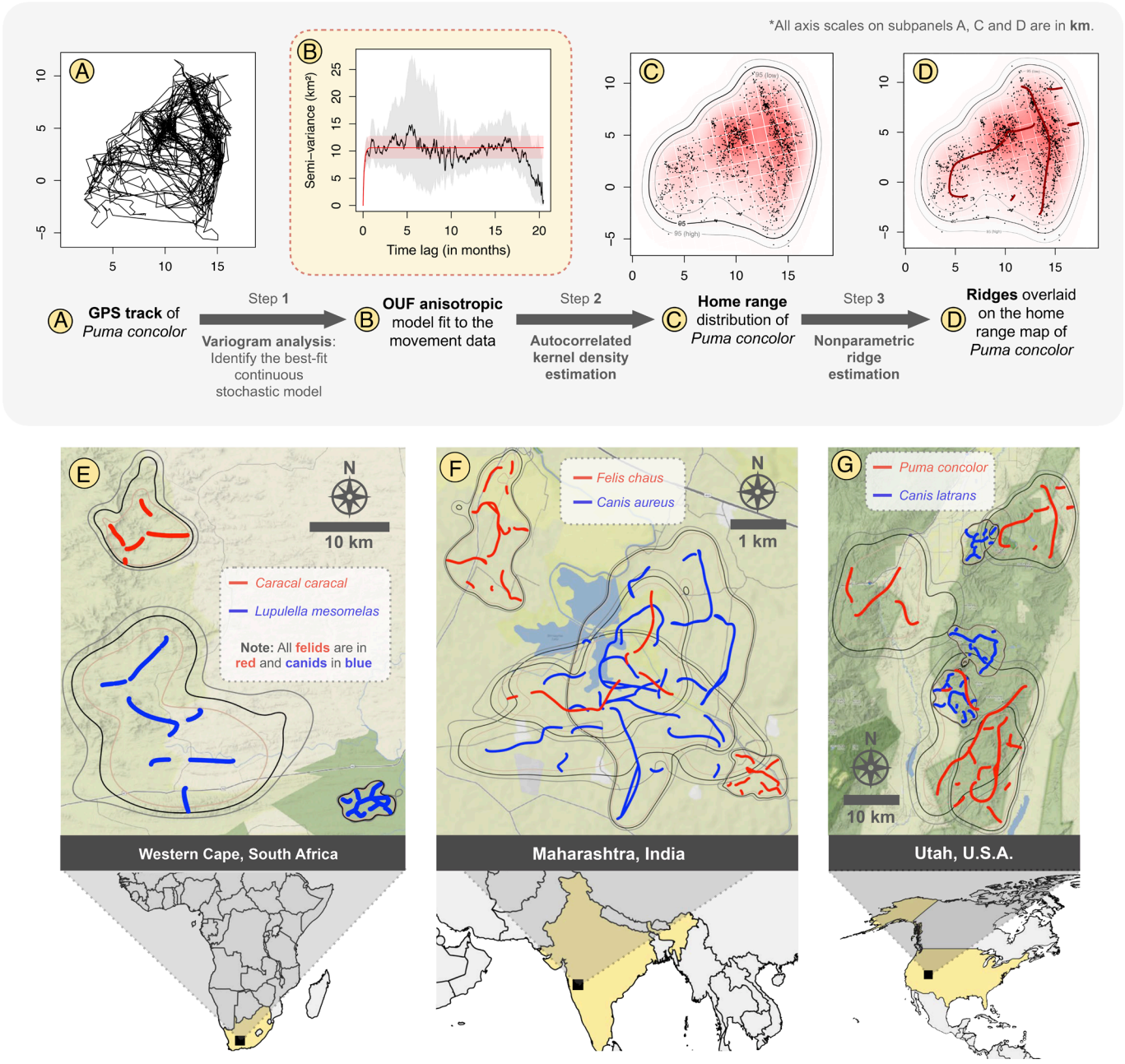

Fig. 1. Diagram of analysis workflow building maps of probability ridges from GPS tracking data (*A–D*) and sample maps showing home ranges and probability ridges overlaid on landscapes (*E–G*). Panel *A* shows the original movement track data for cougar F70 (*Puma concolor*) from Utah, USA (54). Panel *B* shows the empirical semivariance (black) for F70's movement track, together with 95% confidence limits (gray shading) and the best-fit variogram (red) and its 95% confidence limits (pale red shading) corresponding to an anisotropic version of the OUF continuous-time stochastic process (*SI Appendix*, *SI Detailed Methods*). As in geostatistical analyses involving semivariances, large lags involve the fewest datapoints and have little influence on model fit. Panel *C* depicts the cougar's estimated home range distribution including its boundary (black curve) and corresponding 95% confidence limits (gray curves), probability density surface (red hashing), and SD of the AKDEc bandwidth kernels (white grid lines). Original movement trajectories are represented as black dots for clarity. Panel *D* identifies the calculated probability ridges that indicate routeways of repeated usage (red curves) overlaid on the home range distribution. Note: Panels *A*, *C*, and *D* are mappable objects, but *B* is not. In Panels E-G, plots show mean home ranges (black contours), outer and inner 95% confidence bounds on the home ranges (gray and plum contours, respectively), and the location of probability ridges (red- and blue-colored curves) for individuals from six species in landscapes in which movements of both canids and felids were studied [Panels *E*: (55); *F*: (56); and *G*: (54)]. Backgrounds depict topographical relief and landcover type, ranging from arid (tan) to mesic (green) (Stadia Maps: https://stadiamaps.com/attribution/). Variograms, home ranges, and probability ridges were calculated via the R package *ctmm* as detailed under *Materials and Methods*. Cougar F70 appears in the *Upper Right* of panel *G*. Panels *D–G* show ridges calculated via the accurate but computationally inefficient *ks* algorithm (*SI Appendix*).

and xeric scrublands), mean ridge densities of canid species were routinely higher than those of felid species inhabiting the same landscapes (Fig. 4), providing additional support for the robustness of the clade-level differences. Similarly, for the 11 species with GPS tracks in three or more landscapes, we found remarkable consistency in mean ridge density within species across landscapes after controlling for other factors (*SI Appendix*, Fig. S2). Nine of the 11 species showed no significant differences in ridge density across landscapes, whereas only two species, *Lynx rufus* and *Felis silvestris*, exhibited any significant heterogeneity. Only one of seven landscapes differed from the others for *L. rufus*, and only one of four landscapes differed from the others for *F. silvestris* (*SI Appendix*, Fig. S2). This high degree of consistency within species across diverse landscapes suggests a strong role for

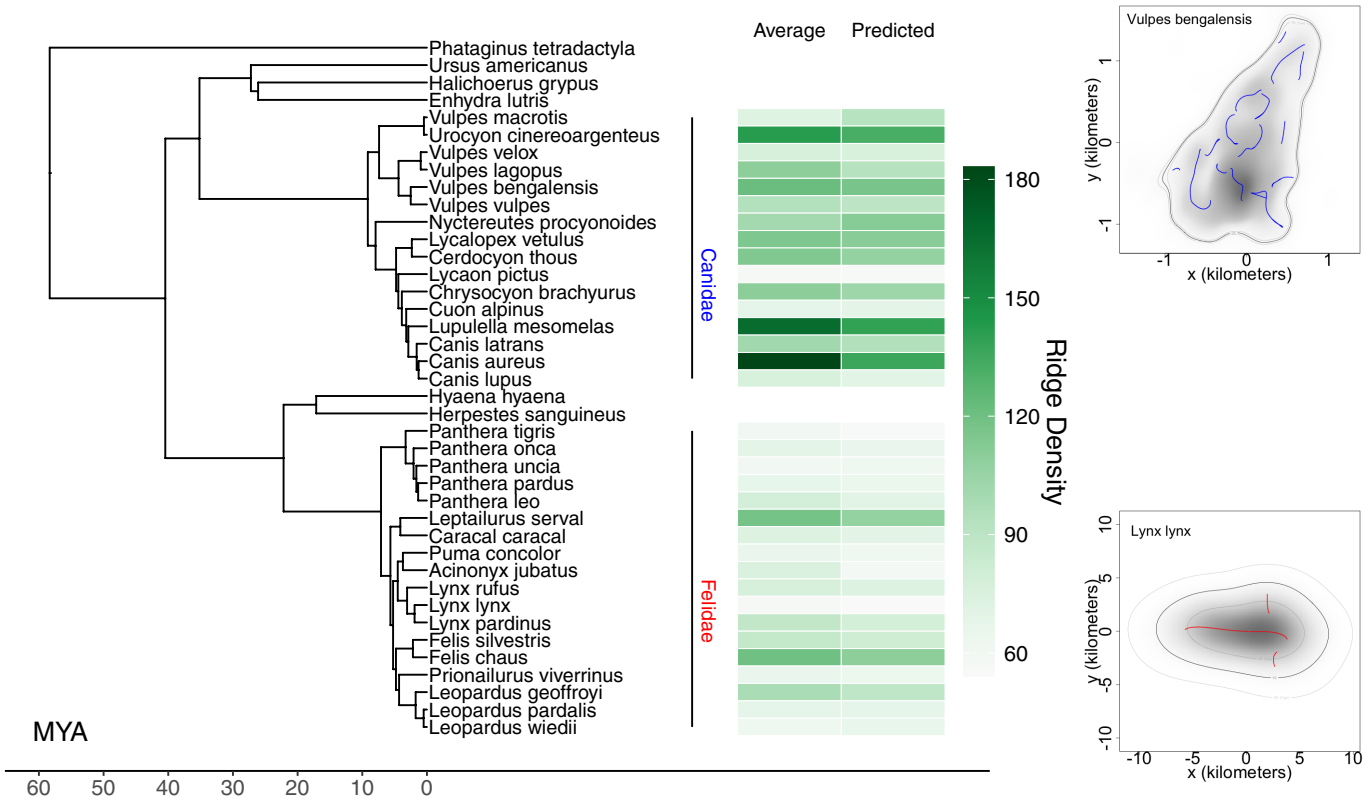

Fig. 2. Mean empirical ridge density for 34 species of canids and felids and the corresponding model-predicted mean values for the full dataset of 1,239 tracks (Dataset S1). Example plots for individuals whose home ranges feature very high ridge density [*Canis aureus*; "Jackal 08" (56)] and very low ridge density [*Lynx lynx*; "Kars" (57)] are shown next to the color key. Ridges appear as blue and red curves for the canid and felid exemplars, respectively, and the background gray hashing indicates probability density of space use with each home range. The phylogenetic tree includes outgroup and ingroup species (without movement data) used only to help structure the phylogenetic distance matrix and visualize the phylogenetic tree; these species were truncated from the phylogenetic distance matrix prior to statistical analyses. Ridges plotted were calculated via the accurate but computationally inefficient *ks* algorithm (*SI Appendix*).

biological species-level features in driving the pronounced clade-level effects (Fig. 3). Species-level mean ridge densities predicted by the model for the full dataset fell well within the empirical ranges for all species except the raccoon dog (*Nyctereutes procyonoides*), for which only two GPS tracks could be analyzed (*SI Appendix*, Fig. S3).

Separate analyses of the canid and felid groups were broadly similar, revealing few differences in the predictive models that could be interpreted as evidence of strong interaction effects (*SI Appendix*, Fig. S4). Engaging in the disruptive fast hunting movement strategy was associated with higher ridge density in canids, but with lower ridge density in felids. Other exceptions were that increasing terrain roughness decreased ridge density for felids ($P < 0.03$) but not for canids and that increases in seasonality (quantified by a measure of primary productivity, Var DHI GPP, see *SI Appendix*, Table S1) decreased ridge density for canids ($P < 0.02$) but not felids (*SI Appendix*, Fig. S4).

Ridge-Associated Probability Mass. By surrounding each ridge with a series of spatial buffers (*Materials and Methods*), we quantified the proportion of the probability mass in each individual's home range that was ridge-associated. Overall, the ridge-associated probability mass in an individual's home range roughly correlated with its ridge density. For narrowly defined ridge tops (i.e., probability ridges with 10 or 50 m fixed-width buffers on either side), canids had, on average, significantly more ridge-associated probability mass in their home range distributions than did felids (7.1 to 20.2% more for 10-m buffers and 5.3 to 14.9% more for 50-m buffers using the full dataset; *SI Appendix*, Fig. S5).

At the species level, ridge-associated probability mass varied widely, with diverse taxa, including several species of foxes and some forest-dwelling cats, averaging 20 to 40% of their probability mass associated with probability ridge tops, indicating a strong concentration of activity along those routeways (*SI Appendix*, Fig. S6). Individuals with larger home range sizes consistently had lower ridge-associated probability mass, regardless of buffer width (*SI Appendix*, Fig. S7). For 50-m buffers, increasing percent tree cover and human footprint index, plus the use of the pursuit and slow-walking strategies were all significant predictors of reduced ridge-associated probability mass (*SI Appendix*, Fig. S7*A*). As was true for ridge density (Fig. 3*B*), we found even larger interclade differences for ridge-associated probability mass when focusing on the shared landscapes dataset; in this case, the interclade differences were highly significant for buffer widths ranging from 10 m (95% CI: 17 to 42% more for canids) to 200 m (95% CI: 5 to 19% more) (*SI Appendix*, Figs. S5 and S7*F*). More broadly, the interclade differences in ridge-associated probability mass were a robust result evident across all subdatasets for narrowly defined ridge tops (≤50 m buffer width; *SI Appendix*, Fig. S7).

Discussion

Drawing on a dataset of 1,239 carnivore GPS tracks, representing 16 canid and 18 felid species across six continents, we found that on average, canid home ranges feature substantially greater densities of reused travel routeways (quantified as probability ridges, Figs. 1 and 3) compared to felid home ranges. Moreover, canids used these routeways more extensively than did felids, as quantified

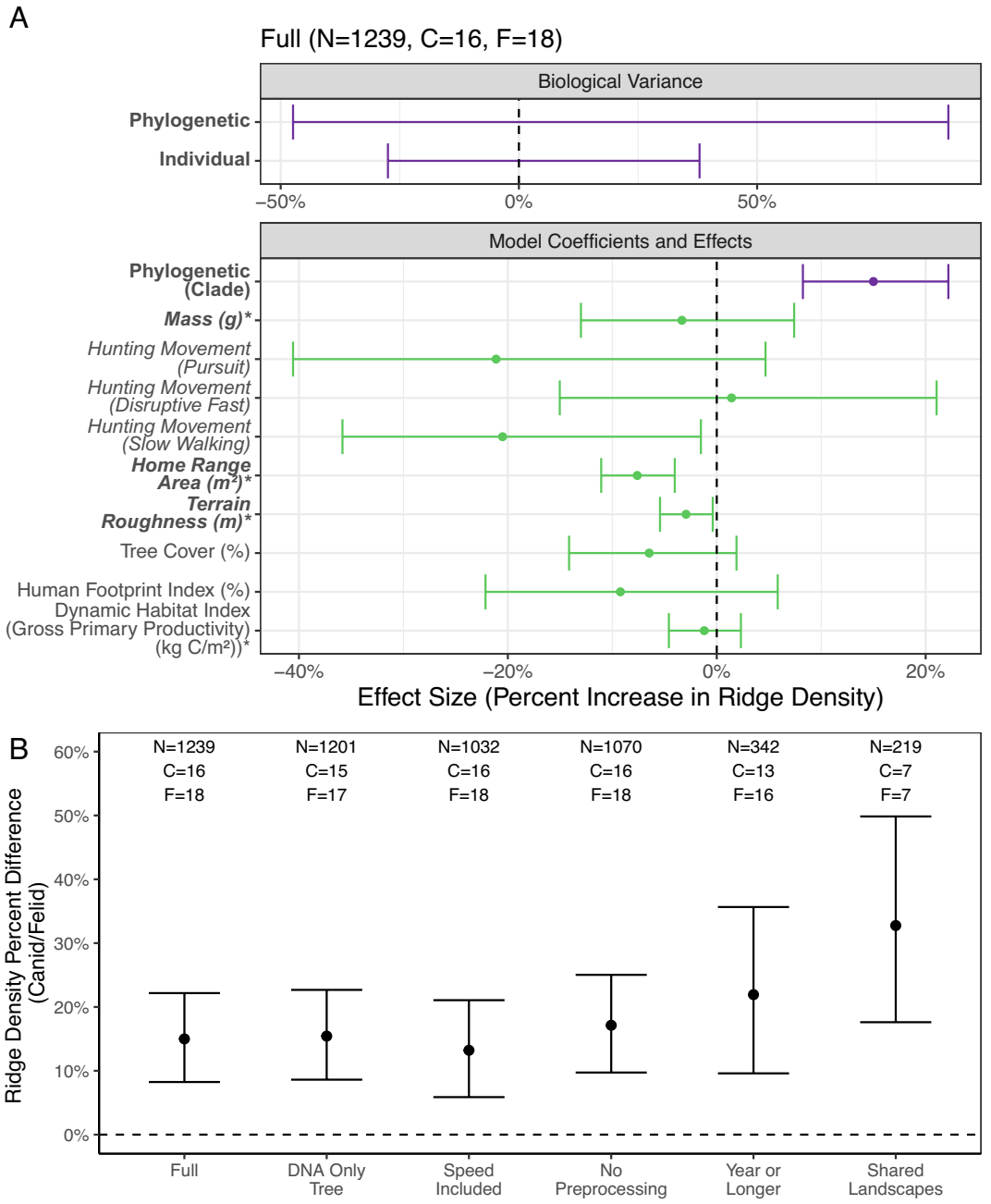

Fig. 3. Effect size plots for ridge density for the full dataset (*A*) and mean (±95% CI) clade-level percent differences from models for all datasets (*B*). In (*A*), continuous variables were standardized so that the effect size corresponds to 1 SD of the predictor, whereas for a variable expressed as a percentage, the effect size corresponds to the full effect of that predictor at 100%. Predictors in bold font and purple plotting represent biological variation, and the plots labeled Phylogenetic and Individual are prediction intervals. The plotting labeled Phylogenetic (Clade) is part of the overall phylogenetic variation, but it is expressed as a mean and CI alongside other model coefficients. Model covariates are in green, including indicator variables (italics), variables log transformed for analysis (bold-italics), and standardized variables (asterisk). In (*B*), clade effects are plotted as canids minus felids, with y = 0.0 indicating no difference between clades and positive values indicating increased ridge density in canids. Clade effects are highly significant ($P < 0.0003$) in each of the six datasets). N, C, and F are the number of individuals, canid species, and felid species, respectively.

by the greater ridge-associated probability mass in their home ranges (*SI Appendix*, Figs. S5–S7). These results, which control for variation in home range size, contrasting hunting strategies and landscape characteristics, as well as variation in the quantity and quality of movement track data, identify striking differences in carnivores' space use with regard to reliance on reused travel routeways and the resulting internal heterogeneity of their home ranges. The magnitude and consistency of these differences are remarkable given the diverse challenges of collecting and working with field data across so many different species and landscapes.

Collectively, clade-level differences in carnivore movement and space use, together with species-level variation attributable in part to different hunting strategies and landscape contexts (*SI Appendix*, Figs. S3 and S6), have a variety of implications, with connections to such diverse topics as the mathematical modeling of predator–prey interactions and the practical implementation of conservation plans. Canids' higher average ridge densities (Fig. 3*B*) and higher average ridge-associated probability masses (*SI Appendix*, Fig. S5) serve to concentrate their activities along particular routeways within their home ranges, which will influence the pace and pattern

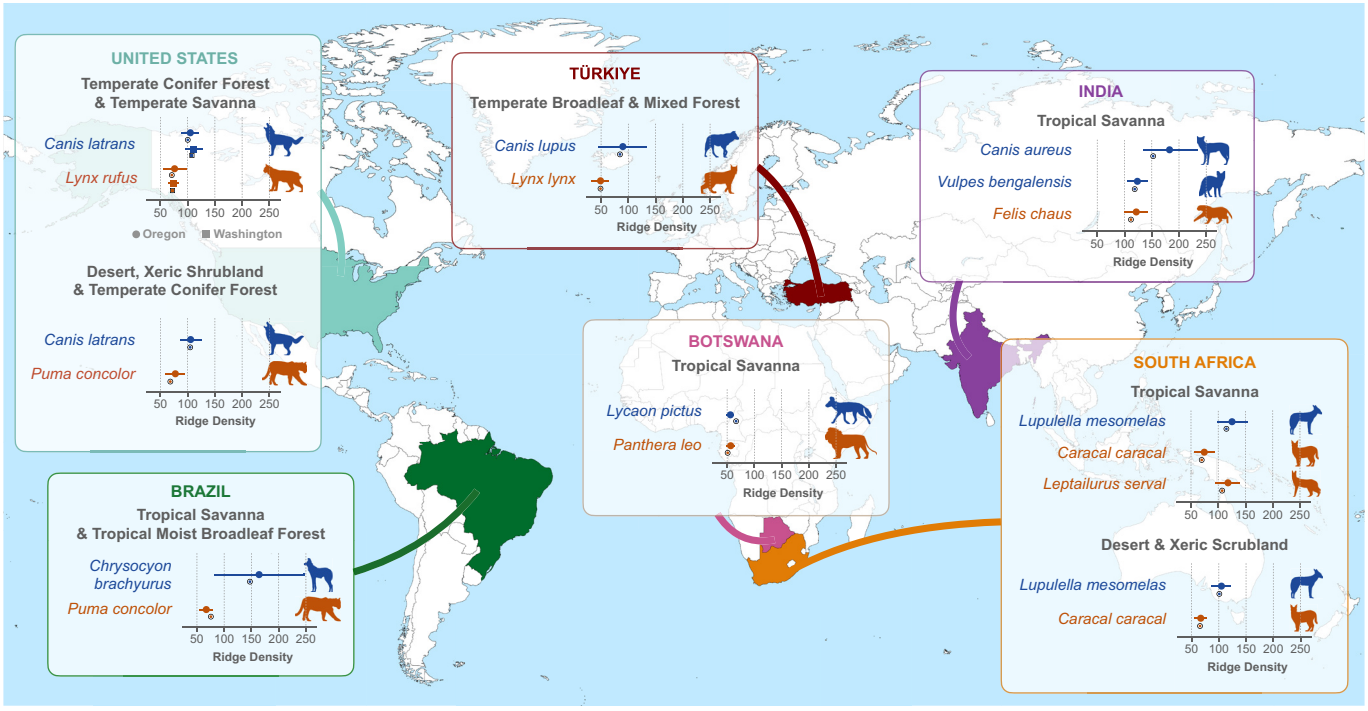

Fig. 4. Ridge densities for canids and felids for the nine landscapes in which at least one species from each clade was tracked together (the shared landscapes dataset; n = 219 individuals total). Solid symbols are empirical means (±95% CI), whereas black-bordered, open symbols (offset lower) indicate means predicted by the statistical model for this dataset (*SI Appendix*, Table S3). At the clade level, canid ridge densities are on average 33% (±16 CI) higher than felids across the shared landscapes dataset (Fig. 3*B*).

of their encounters with conspecifics and with prey (58–60). Such concentrations of movement and activity represent striking departures from the dynamics of ideal gases, which have long provided the theoretical foundations of predator–prey dynamics, mate finding, and other encounter-based processes in ecology, but which are increasingly challenged by models with alternative reaction kinetics (15–17, 61, 62). For example, interclade differences in reliance on travel routeways could mean that the linkages between animal movement and disease transmission operate quite differently across taxa (63, 64), as species that concentrate movement along well-traveled routeways would have different exposure profiles for depositing or acquiring infective agents than would species whose movements were not so spatially constrained. Variation in carnivores' reliance on travel routeways could also have important trophic consequences via impacts on the spatial distribution of prey species, which often avoid areas of heightened predator activity (65, 66).

Another consequence of carnivores' differential reliance on well-traveled movement routeways pertains to the risks associated with human interactions. For example, stricter adherence to reused routeways could reduce hunting efficiency as travel routeways are compromised through development or through increased contact with humans when established travel routeways overlap with new areas of human activity (67). Similarly, poaching with snares or traps along predictably reused travel routeways would be a greater threat to those species with greater ridge-associated probability mass (*SI Appendix*, Fig. S6). Of course, one potential benefit of some species' greater affinities for routeway-attuned travel is that negative interactions with human infrastructure might be more easily addressed for such species, such as through construction of highway wildlife crossing structures at key locations (53, 68).

What Drives Variation in Carnivore Routeway Usage? The phylogenetically structured variation in routeway usage among carnivores could derive from several sources, including database artifacts, biases in our statistical modeling, environmental factors, and biological processes. The first possibility—that the differences we report between canids and felids are simple statistical artifacts—seems unlikely. Throughout our analyses, we have controlled for the effects of a diverse array of factors at the individual-, species-, and landscape levels that could affect the formation of travel routeways (*SI Appendix*, Tables S1 and S2), and our results still indicate the existence of strong phylogenetic structure. For example, when canids and felids occupied the same landscapes (reducing the potential for unmodeled spatial variables to affect the clade-level difference), ridge density for canids exceeded that of felids by 33% (±16% CI; Figs. 3*B* and 4) with a concomitant 10 to 30% mean increase in the intensity of ridge use (*SI Appendix*, Fig. S5). Nevertheless, we recognize that other factors, such as unmodeled environmental variables, unmodeled clade- or species-specific behaviors (e.g., site fidelity), and unknown differences among the particular populations of carnivores to which the GPS-tracked individuals belonged, could all contribute to the observed clade-level differences in route usage if those other factors occurred across individuals or taxa in just the right way (see *SI Appendix* for further discussion of potential sources of bias).

Moving beyond statistical artifacts and biases, environmental features constitute a key alternative explanation for routeway-following behavior in home ranges (23), and features like creek valleys, forest roads, and cliff faces are known to shape carnivores' routeway-like movements in particular settings (25, 68, 69). However, the identity and importance of physical landscape features capable of creating or refining animals' travel routeways will vary strongly across biomes, habitats, and even individual home ranges (23), and additional variation will emerge due to species- and individual-level sensitivities and behavioral reactions to those features (47, 60, 66, 70, 71). With so many factors at play, the ways by which diverse environmental contexts (and individuals' heterogeneous responses to environmental features) could scale

up to yield the observed clade-level differences in ridge density and ridge-associated probability mass are unclear.

Potential biological drivers of the clade-level difference in routeway usage include issues of morphology, perception, and cognition. The skeletal architectures of canids and felids differ in key ways, including major differences in shoulder joints, hind limbs, and orbital morphology, and these differences have been previously interpreted with regard to both movement and hunting strategies (42, 44, 45, 72, 73). For example, felids have "floating" clavicles that may increase their maneuverability relative to canids, whereas canids have a rigid shoulder structure restricting lateral limb movement and encouraging straightforward linear travel (74). Whether phylogenetic differences in joint morphology or visual perceptual fields could scale up to influence travel patterns within carnivore home ranges remains unclear.

Canids' increased reliance on movement routeways could also be mediated by their greater capabilities for olfactory perception (75). Although canids, felids, and indeed other carnivores routinely scent mark for purposes of social communication and identification, canids' enhanced abilities to detect scents (76) could reinforce movement along particular routeways, as modeled in ref. 77. Differences in diet may also play a role, in that all felids are carnivores, but many canids can be omnivorous, exploiting a wider range of resources depending on availability. Successful foraging via the latter, more generalized strategy could rely more heavily on memory, particularly when resources, or access to them, varies seasonally (19, 24, 78).

A Link to Cognition? Given our phylogenetic modeling, and our finding that ridge densities are generally consistent within species across landscapes and biomes (*SI Appendix*, Fig. S2), it seems plausible that the observed clade-level differences in ridge density and ridge-associated probability mass have a biological, perhaps cognitive, component. In this context, clade-level differences in species' reliance on routeways for navigation could be linked to different cognitive strategies, with canids using routeways more heavily and felids exhibiting more flexible, less repetitive, or more random movement. Routeway-based movement allows for easier and more efficient movement for some species and environmental contexts (10, 12, 18, 28) and is widely considered a hallmark of the cognitive maps that some species employ for navigation (19, 21). The development of animals' travel routeways can hinge on experiential learning and memory (79–81), which have been experimentally demonstrated to drive the establishment of home ranges in pheasants and deer (82, 83).

As for a specific mechanism, one speculative possibility emerges from the animal cognition literature, where laboratory experiments suggest that domestic dogs (*Canis lupus familiaris*) have four to eight times longer working memory plus stronger spatial cognition and object permanence skills compared to domestic cats (*F. silvestris catus*) (84–86). Methodological concerns regarding the breeds and sources of animals used in those laboratory studies limit the extension of these ideas to wild animals. However, in humans, greater working memory is believed to be associated with memory retrieval structures that facilitate quick and accurate retrieval of large amounts of information from long-term memory (87, 88), and greater working memory predicts improved performance on navigational tasks (89, 90). Crucially, controlled search processes are believed to be regulated by working memory and executive control (91). Laboratory studies of rodents that examined relations between prefrontal and hippocampal function also suggest a tight coupling between prefrontal-regulated working memory processes and hippocampal-mediated long-term spatial memories (92, 93).

Future Directions. Additional understanding of the observed phylogenetic signals in routeway usage could perhaps be gained through targeted analyses of species not studied here. That is, are space-use patterns typical of other mammalian carnivore groups predictable from their relationships with canids and felids? For example, hyaenas, which have been studied extensively in the context of cognition (49), present an interesting case study for future work because they are behaviorally canid-like in many ways, but evolutionarily far closer to felids (34). The predictions are that hyaena species should have greater ridge density and greater ridge-associated probability mass than other members of the Feliformia, after controlling for other factors. Another testable hypothesis is that clade-level differences in routeway usage may map onto differential success in rebuilding carnivore populations via translocations and/or the release of captive-bred animals (52, 83, 94). In such settings, naïve carnivores must gain proficiency in spatial navigation as they establish home ranges in new landscapes, creating excellent opportunities for understanding how animals learn (80, 95–97).

Conclusion. We found that mammalian carnivores vary widely in their reliance on reused travel routeways within their home ranges and that this variation is predictable as a function of phylogeny, behavioral hunting strategies, and environmental context. Further efforts to delineate (and statistically associate) the location of probability ridges in real landscapes with specific, species-relevant landscape features should provide insight into the relative importance of anthropogenic features (e.g., roads, fences) versus natural features (e.g., forest edges, creek valleys, cliffs) in shaping animals' preferred travel routeways (25, 69, 98). Spatial concordance (or lack thereof) between an individual's probability ridges and the landscape features in its home range should also inform understanding of the relative biological and physical bases of least-cost movement paths inferred from energetics modeling (99–101). Putative cognitive differences between canids and felids suggest one possible mechanism behind the robust clade-level differences in routeway usage we quantified, but available methods do not allow for easy, en masse discrimination of routeway-based movements driven by cognition versus those deriving from physical constraints (23). Regardless of its source, however, pronounced heterogeneity in carnivores' use of travel routeways has a variety of far-reaching implications. Among other possibilities, these findings provide empirical justification for new approaches to mathematical modeling of encounter processes in wildlife ecology (e.g., disease dynamics, mate finding, consumer–resource interactions) and also suggest avenues by which improved understanding of animals' spatial behavior may benefit practical conservation efforts.

Materials and Methods

Collectively, the full dataset of 1,239 tracks entailed almost 4.60 million GPS fixes, with 2.24 million fixes for canids, and 2.35 million for felids. Durations of individual tracks ranged from 4.14 and 4.28 wk (canids and felids, respectively) to 163 wk and 516 wk (again, respectively). Nominal sampling rates ranged from 1/min to ~1/d for both carnivore families. See Dataset S1 for detailed track-level information on fixes, durations, fix rates, and other measures. We emphasize, however, that these data on the number of fixes, durations, and fix rates per track are potentially beguiling, as it is not these numbers themselves that determine data sufficiency for home range analysis, but rather the effective sample size (ESS) values, with sufficiency for ESS ≥ 5 [(38, 102); also see *SI Appendix, SI Detailed Methods*]. For canids, ESS values ranged from 5.1 to 6,728 with a mean of 412, whereas for felids, ESS ranged from 5.0 to 6,891 with a mean of 170. As detailed in *SI Appendix*, we control for track-level variation in ESS in all of our statistical analyses.

Delineation of an animal's reused travel routeways necessitates identification of its home range [i.e., the region where the animal spends its time; (81, 102)] and the intensity with which it uses space within that home range. As explained in *SI Appendix, SI Detailed Methods*, we made these determinations using an established workflow that delineates an animal's home range distribution from GPS tracking data as a 2-D probability density function (hereafter, 2-D PDF) (102, 103) together with an implementation of a recently developed statistical method for identifying so-called probability ridges in a 2-D PDF (104). All spatial statistical analyses involving home ranges and probability ridges were conducted using the R package *ctmm* (102, 103), which advantageously allows processing of highly heterogeneous GPS tracks and avoids any subjective postprocessing.

With analogies to landscape ridges in geomorphology, a probability ridge represents a spatially contiguous curve with heightened probability relative to other, adjacent areas within a PDF (104). That is, a probability ridge is a 1-D feature interpretable as a spatially extended mode. Whereas a simple statistical mode occurs at a point where probability density is maximal in all directions, ridge points occur where probability density is maximal in the direction perpendicular to the tangent of a ridge curve while density along the curve is not constrained. A sequence of adjacent ridge points need not be in a straight line, and a ridge curve will emerge as a function of curvature present in the 2-D PDF. Note that for a 2-D PDF that is not related to a movement process, probability ridges will not necessarily correspond to specific movement routes, as such ridges would merely indicate areas of heightened probability. In contrast, for a 2-D PDF derived from animal movement data, ridges will correspond to route-like structures because movement is constrained to be (mathematically) continuous and movement through regions of high probability is favored. Thus, biologically speaking, a probability ridge curve will emerge when an animal repeatedly uses similar, spatially localized routes to navigate a given region within its home range. Animals do not necessarily (and indeed, are unlikely to) exactly move along a probability ridge. Instead, probability ridges merely provide spatial summaries for the orientation of movement in particular portions of an animal's home range.

However, as in geomorphology where ridgelines can occur in geographical regions of either high or low average elevation, the existence of a probability ridge in a region of a home range does not characterize the overall probability mass in that region. To quantify the extent to which individuals used the probability ridges in their home ranges, we spatially "buffered" each ridge curve by several specific widths (10, 50, 100, and 200 m) to transform each one-dimensional ridge curve into a series of two-dimensional features. From those features, we then calculated a double integral (across the buffered ridge width and along the ridge) to estimate the probability mass encompassed by a particular buffered ridge. Summing the probability mass across all of an individual's ridges (but eliminating any double-counting of probability mass in areas where buffered ridges intersect within a home range), we obtained a total ridge-associated probability mass for each individual for each buffer width. These ridge-associated probability mass values (out of a maximum possible of 1.0 total probability mass for each home range) provide a measure of how intensively a given animal is moving via its set of routeways relative to the nonrouteway portions of its home range.

We thus focused our analyses on two measures of animal routeway usage within a home range: 1) ridge density (ranging from 0 upward, and quantifying how extensive the set of probability ridges is within a home range) and 2) ridge-associated probability mass (ranging from 0 to 1, and quantifying how intensively an individual travels along the ridges in its home range) (*SI Appendix, SI Detailed Methods*).

The flow diagram (Fig. 1 *A–D*) illustrates how the steps of our analyses work together to yield maps of probability ridges as reused travel routeways. After all processing, 1,239 tracks across 34 species (16 canids, 18 felids) were usable for comparative analysis of the density of probability ridges in each animal's home range via phylogenetically controlled generalized mixed effects modeling (*SI Appendix, SI Detailed Methods*). Our statistical approach allowed us to test for the existence of a clade-level difference in the density of probability ridges while also controlling for, and testing the potential importance of, a broad suite of individual-, species-, and landscape-level covariates, including those that provided alternative explanations for observed clade-level differences in ridge density and ridge-associated probability mass (*SI Appendix*, Tables S1 and S2). To evaluate the robustness of our findings, we also analyzed several subdatasets drawn from within the full dataset of 1,239 usable tracks (*SI Appendix, SI Detailed Methods*).

Because our ridge-based methods for delineating routeways rely on the asymptotic properties of continuous stochastic processes (*SI Appendix, SI Detailed Methods*), our methods are insensitive to the marked variation in "sampling schedules" that results from discontinuous GPS fixes, which can vary greatly across individuals, taxa, and landscapes. In contrast, existing methods for estimating high-traffic areas such as corridors, routes, and path networks for individual taxa, such as types of Brownian bridges (105, 106) and network analyses (23), yield metrics with inherent scale dependencies that would muddle and compromise comparisons across our highly heterogeneous multispecies data (107–111). For example, spatial thresholds necessary to define route networks (i.e., what specific network nodes are interconnected) could not remain consistent across diverse sampling schedules and movement behaviors without tremendous loss of information due to data coarsening to a common schedule. Indeed, coarsening all our tracks to a minimum common sampling frequency of 1/d would require discarding 93.4% of our 4.60 million datapoints.

Simulation studies (*SI Appendix*) make clear that, subject to minor errors stemming from the vagaries of finite sampling effort, our methods do not falsely identify probability ridges when they should not exist (*SI Appendix*, Fig. S11) and accurately identify both the location and length of probability ridges when they are known to exist analytically (*SI Appendix*, Fig. S12). Both the lengths and densities of probability ridges estimated for empirical tracking datasets far exceed the false positive errors expected from finite sampling effort in null models (*SI Appendix*, Fig. S13 and Tables S5 and S6).

Data, Materials, and Software Availability. Code for all analyses have been deposited in Zenodo (https://zenodo.org/records/16172335). Spatially anonymized versions of all movement tracks have been deposited in Zenodo (https://doi.org/10.5281/zenodo.11159169). Dataset S2 presents detailed information regarding the original sources of animal tracking data, the movement tracks used in this analysis (including their sources and availability), animal care and permit authorizations, and funding acknowledgements. As detailed in Dataset S2, many of the movement tracks we analyzed are already publicly available as supplemental material associated with previous species-specific publications or through the ecological repository https://www.movebank.org; such datasets are either openly accessible or available through communication with the data holders. Other datasets are, however, not publicly available in raw form because they are protected by national or state laws that prohibit their public release or because they detail the movements of endangered species. To facilitate further analyses, spatially anonymized versions of all movement tracks are available at https://doi.org/10.5281/zenodo.11159169. The anonymization process preserves the internal integrity of the track, but obscures the animals' locations inside parks and sanctuaries or with respect to landscape features. Such anonymization has no effect on the calculation of ridge density or ridge-associated probability mass within an animal's home range. Together with the summary of track-level information available in Dataset S1, these anonymized tracks will allow users to recreate the same or similar hypothesis tests that we report, and also conduct future analyses of some or all of the movement tracks and their pre-summarized environmental contexts. Collaborations with the original data holders detailed in Dataset S2 are generally encouraged, and in cases where data are held by Indigenous groups or institutions from regions that are under-represented in the global science community, collaboration may be required to ensure inclusion. Previously published data were used for this work [Some movement data is available on online repository Movebank (indicated in spreadsheet "Cat_Dog Data Analyzed.AnimalCare. Acknowledgements.csv"). Movement data associated with a publication includes refs. 112–114].

ACKNOWLEDGMENTS. W.F.F. thanks C. Delwiche for suggestions about the phylogenetic presentation, E. Slud for discussions on statistical analyses, L. Koralov for discussions on stochastic processes, C. Cosner, A. Gumel, and H. Berestycki for discussions about reaction kinetics, and S. Carroll for a lesson in philosophy. A. Safsten assisted with a draft graphic and C. Folta assisted with data preparations. Three anonymous reviewers provided constructive feedback that allowed us to

rework and sharpen the manuscript. W.F.F., C.H.F., and J.M.C. were supported by NSF IIBR (No. 1915347). The University of Maryland provided additional financial support, and we acknowledge the University of Maryland supercomputing resources (https://hpcc.umd.edu) made available for conducting the research reported in this paper. This work was partially funded by the Center of Advanced Systems Understanding (CASUS), which is financed by Germany's Federal Ministry of Education and Research (BMBF) and by the Saxon Ministry for Science, Culture, and Tourism (SMWK) with tax funds on the basis of the budget approved by the Saxon State Parliament. Original funding sources for the collection of animal tracking data synthesized here appear in *SI Appendix*.

Author affiliations: [a]Department of Biology, University of Maryland, College Park, MD 20742; [b]Center for Advanced Systems Understanding, Helmholtz-Zentrum Dresden-Rosendorf, Görlitz 02826, Germany; [c]Smithsonian National Zoological Park and Conservation Biology Institute, Front Royal, VA 22630; [d]Department of Biology, University of Central Florida, Orlando, FL 32816; [e]Department of Ecology and Evolutionary Biology, University of Michigan, Ann Arbor, MI 48109; [f]Museum of Paleontology, University of Michigan, Ann Arbor, MI 48109; [g]Center for Ecosystem Sentinels, Department of Biology, University of Washington, Seattle, WA 98195; [h]Botswana Predator Conservation, Wild Entrust, Maun, Botswana; [i]Université Grenoble Alpes, Laboratoire Recherche Translationnelle et Innovation en Médecine et Complexité, Computational Biology and Modeling, La Tronche 38700, France; [j]Department of Environmental Biology, State University of New York Environmental Science and Forestry, Syracuse, NY 13210; [k]Senckenberg Biodiversity and Climate Research Centre, Senckenberg–Leibniz Institution for Biodiversity and Earth System Research, Frankfurt 60325, Germany; [l]Department of Biological Sciences, Goethe University, Frankfurt 60629, Germany; [m]Department of Biology, University of British Columbia-Okanagan, Kelowna, BC V1V 1V7, Canada; [n]Okanagan Institute for Biodiversity, Resilience, and Ecosystem Services, The University of British Columbia-Okanagan, Kelowna, BC V1V 1V7, Canada; [o]Department of Computer Science, Math, Physics, and Statistics, The University of British Columbia-Okanagan, Kelowna, BC V1V 1V7, Canada; [p]Department of Ecology, Federal University of Mato Grosso do Sul, Campo Grande 79070-900, Brasil; [q]Department of Environmental Science, Radboud Institute for Biological and Environmental Sciences, Radboud University, Nijmegen 6525 AJ, The Netherlands; [r]Laboratory of (Bio)Diversity in the Anthropocene, Biology Institute, Federal University of Bahia, Salvador 40170-110, Brasil; [s]Department of Psychology, University of Maryland, College Park, MD 21036; [t]Department of Psychology, California State University, Long Beach, CA 90840; [u]Laboratory of Population Ecology, A.N. Severtsov Institute of Ecology and Evolution, Russian Academy of Sciences, Moscow 119071, Russia; [v]Programa de Conservação Mamíferos do Cerrado, Cumari, Goiás 76760-000, Brasil; [w]Departamento de Ciências Biológicas, Universidade Federal de Catalão, Goiás 75706-881, Brasil; [x]Junta de Extremadura, Consejería de Agricultura, Ganadería y Desarrollo Sostenible, Dirección General de Sostenibilidad, Mérida 06800, Badajoz, Spain; [y]Department of Evolutionary Biology and Environmental Studies, Zurich University, Zurich 8057, Switzerland; [z]Department of Fisheries and Wildlife, Michigan State University, East Lansing, MI 48824; [aa]Center for Computational Biology and Bioinformatics, The University of Texas at Austin, Austin, TX 78712; [bb]Department of Biology, Chemistry and Geography, Université du Québec à Rimouski, Rimouski, QC G5L 3A1, Canada; [cc]Department of Anthropology, University of California, Davis, CA 95616; [dd]Mpala Research Centre, Nanyuki 10400, Kenya; [ee]Institute for Communities and Wildlife in Africa, Department of Biological Sciences, University of Cape Town, Private Bag X3, Cape Town 7700, South Africa; [ff]School of Biological Sciences, University of Utah, Salt Lake City, UT 84112; [gg]Department of Forestry and Environmental Conservation, Clemson University, Clemson, SC 29634; [hh]Science Department, Australian Wildlife Conservancy, Subiaco East, WA 6008, Australia; [ii]Gulbali Institute of Agriculture, Water and Environment, Charles Sturt University, Albury NSW 2640, Australia; [jj]Instituto de Defesa e Preservação dos Felídeos Brasileiros, Corumbá de Goiás 72960000, Brasil; [kk]Warnell School of Forestry and Natural Resources, University of Georgia, Athens, GA 30602; [ll]Laboratory of Behavior and Behavioral Ecology of Mammals, A.N. Severtsov Institute of Ecology and Evolution, Russian Academy of Sciences, Moscow 119071, Russia; [mm]Oregon Department of Fish and Wildlife, La Grande, OR 97850; [nn]The Jones Center at Ichauway, Newton, GA 39870; [oo]Wildlife Conservation Research Unit, Department of Biology, University of Oxford, Abingdon OX13 5QL, United Kingdom; [pp]The Cape Leopard Trust, Cape Town 7966, Western Cape, South Africa; [qq]Institute for Communities and Wildlife in Africa, Department of Biological Sciences, Faculty of Science, Upper Campus, University of Cape Town, Cape Town 7700, Western Cape, South Africa; [rr]School of Environmental and Forest Sciences, University of Washington, Seattle, WA 98195; [ss]KuzeyDoğa Society, Kars 36000, Türkiye; [tt]Department of Forestry & Environmental Resources, North Carolina State University, Raleigh, NC 27695; [uu]Jasja Dekker Dierecologie, Arnhem 6843WZ, The Netherlands; [vv]Centre for Functional Biodiversity, School of Life Sciences, University of KwaZulu-Natal, Scottsville 3209, South Africa; [ww]Panthera USA, New York, NY 10018; [xx]Centre for Social Science Research, Faculty of Humanities, University of Cape Town, Cape Town 7700, South Africa; [yy]Tanzania Wildlife Research Institute, Lemara 2113, Arusha, Tanzania; [zz]1854 Treaty Authority, Duluth, MN 55811-1524; [aaa]Durrell Institute of Conservation and Ecology, School of Anthropology and Conservation, University of Kent, Canterbury, Kent CT2 7NR, United Kingdom; [bbb]Department of Biology, University of Oxford, Oxford OX1 3RB, United Kingdom; [ccc]Roosevelt Wildlife Station, State University of New York Environmental Science and Forestry, Syracuse, NY 13210; [ddd]Museum of Vertebrate Zoology, University of California, Berkeley, CA 94720; [eee]Department of Integrative Biology, University of Guelph, Guelph, ON N1G 2W1, Canada; [fff]Department of Environmental Conservation, University of Massachusetts, Amherst, MA 01003; [ggg]Research and Technology Centre, University of Kiel, Büsum 25761, Germany; [hhh]Department of Environmental Science, Policy and Management, University of California, Berkeley, CA 94720; [iii]Mammal Research Institute, Department of Zoology and Entomology, University of Pretoria, Pretoria 0028, South Africa; [jjj]Ministry of Water, Land and Resource Stewardship, Penticton, BC V2A 7C8, Canada; [kkk]German Wildlife Foundation, Hamburg 20457, Germany; [lll]School of Natural Sciences, University of Tasmania, Hobart, TAS 7001, Australia; [mmm]Tasmanian Land Conservancy, Sandy Bay, TAS 7005, Australia; [nnn]Projeto Onçafari Miranda, Mato Grosso do Sul 79380-000, Brasil; [ooo]Wildlife Biology Program, Department of Ecosystem and Conservation Science, College of Forestry and Conservation, University of Montana, Missoula, MT 59812; [ppp]OEKO-LOG Field Research, Joachimsthaler, Parlow D-16247, Germany; [qqq]Faculty of Environment and Natural Resources, University of Freiburg, Freiburg 79106, Germany; [rrr]Department of Visitor Management and National Park Monitoring, Bavarian Forest National Park, Grafenau 94481, Germany; [sss]Department of Forestry and Wildlife Management, Inland Norway University of Applied Sciences, Koppang 2480, Norway; [ttt]Cheetah Conservation Botswana, Gaborone, Botswana; [uuu]Sociedad de Gestión Pública de Extremadura, Mérida 06800, Badajoz, Spain; [vvv]Norwegian Institute for Nature Research, Trondheim 7485, Norway; [www]Bionet Natuuronderzoek, Stein 6171EL, The Netherlands; [xxx]Department of Biological Sciences and Advanced Environmental Research Institute, University of North Texas, Denton, TX 76203; [yyy]Department of Earth & Environmental Sciences, Vanderbilt University, Nashville TN 37235; [zzz]National Research Center for Carnivores Conservation, Chico Mendes Institute for the Conservation of Biodiversity, Atibaia 12952-011, São Paulo, Brasil; [aaaa]Asociación de Naturalistas Palentinos, Fuentes de Nava 34337, Palencia, Spain; [bbbb]Ashoka Trust for Research on Ecology and Environment, Bangalore 560064, India; [cccc]Manipal Academy of Higher Education, Manipal, Karnataka 576104, India; [dddd]Biodiversity Lab, North Carolina Museum of Natural Sciences, Raleigh, NC 27601; [eeee]The Wilderness & Wildlife Conservation Trust, 130 Reid Avenue, Colombo 04, Sri Lanka; [ffff]Department of Zoology, Institute of Ecology and Earth Sciences, University of Tartu, Tartu 50409, Estonia; [gggg]Veterinary Biology Unit, Veterinary Faculty, University of Zagreb, Zagreb 10000, Croatia; [hhhh]Department of Molecular Biology and Genetics, Koç University, Istanbul 34450, Türkiye; [iiii]Working Group for Wildlife Research, Clinic for Birds, Reptiles, Amphibians and Fish, Giessen University, Giessen 35392, Germany; [jjjj]Wildlife Ecology and Management, Manaaki Whenua–Landcare Research, Lincoln 7640, Canterbury, New Zealand; [kkkk]Department of Forest Ecosystems and Society, Oregon State University, Corvallis, OR 97331; [llll]Department of Fisheries and Wildlife, Oregon State University, Corvallis, OR 97331; [mmmm]Departamento de Medicina Veterinária, Faculdade de Zootecnia e Engenharia de Alimentos, Universidade de São Paulo, Pirassununga 13635-900, Brasil; [nnnn]Instituto Para a Conservação dos Carnívoros Neotropicais-Pro-Carnívoros, Atibaia 1030, São Paulo, Brasil; [oooo]Instituto de Pesquisas Ecológicas, Nazaré Paulista 12960000, São Paulo, Brasil; [pppp]Departamento de Biodiversidade, Laboratório de Ecologia Espacial e Conservação, Instituto de Biociências, Universidade Estadual Paulista, Rio Claro 13506900, São Paulo, Brasil; [qqqq]Norwegian Institute for Nature Research, Lillehammer 2624, Norway; [rrrr]Department of Wildland Resources and Ecology Center, Utah State University, Logan, UT 84322; [ssss]Wildlife Department, Estonian Environment Agency, Tartu 10616, Tallinn, Estonia; [tttt]Department of Terrestrial Ecology, Norwegian Institute for Nature Research, Trondheim 7034, Norway; [uuuu]Faro Moro Eco Research, km 230 PY16, Departamento de Boquerón, Paraguay; [vvvv]Environment and Sustainability Institute, University of Exeter, Penryn TR10 9FE, Cornwall, United Kingdom; [wwww]Laboratory of Ecology, Physiology, and Functional Morphology of Higher Vertebrates, A.N. Severtsov Institute of Ecology and Evolution, Russian Academy of Sciences, Moscow 119071, Russia; [xxxx]Russia Program, Wildlife Conservation Society, Bronx, NY 10460; [yyyy]Fundación Yaguara Panama, Ciudad del Saber 0801, Panama; [zzzz]Smithsonian Tropical Research Institute, Balboa 0843 03092, Ancón, Panama; [aaaaa]Embrapa Pantanal, Corumbá 79320-900, Mato Gosso do Sul, Brasil; [bbbbb]Institute of General and Experimental Biology, Mongolian Academy of Sciences, Ulan Bator 13330, Mongolia; [ccccc]Wildlife Institute of Beijing Forestry University, Beijing 100083, China; [ddddd]Norwegian Institute for Nature Research, Oslo NO-0855, Norway; [eeeee]Departamento de Biología de la Conservación, Estación Biológica de Doñana, Consejo Superior de Investigaciones Científicas, Sevilla 41092, Spain; [fffff]Ontario Ministry of Natural Resources, Wildlife Research and Monitoring Section, Provincial Services Division, Trent University, Peterborough, ON K9L 1Z8, Canada; [ggggg]Negaunee Integrative Research Center, Field Museum of Natural History, Chicago, IL 60605; [hhhhh]Instituto de Biología Subtropical–Nodo Iguazú, Universidad Nacional de Misiones and Consejo Nacional de Investigaciones Científicas y Técnicas, Misiones 3300, Argentina; [iiiii]Asociación Civil Centro de Investigaciones del Bosque Atlántico, Puerto Iguazú N3370, Misiones, Argentina; [jjjjj]Department of Zoology and Genetics, Faculty of Biology, Herzen State Pedagogical University of Russia, St. Petersburg 191186, Russia; [kkkkk]SILVIS Lab, Department of Forest and Wildlife Ecology, University of Wisconsin, Madison, WI 53706; [lllll]Tembotov Institute of Ecology of Mountain Territories of Russian Academy of Sciences, Nalchik 360051, Russia; [mmmmm]Department of Quantitative Wildlife Sciences, University of Washington, Seattle, WA 98195; [nnnnn]Instituto de Desenvolvimento Sustentável Mamirauá, Tefé 69553-225, Amazonas, Brasil; [ooooo]Division of Conservation Ecology, Sálim Ali Centre for Ornithology and Natural History, Coimbatore 641108, Tamil Nadu, India; [ppppp]Centre d'Études Fonctionnelles et Évolutives des Animaux Sauvages, Institut National de Recherche pour l'Agriculture, l'Alimentation et l'Environnement, Université de Toulouse, Castanet-Tolosan 31326, France; [qqqqq]Department of Biology, University of Nebraska at Kearney, Kearney, NE 68849; [rrrrr]United States Department of Agriculture Animal and Plant Health Inspection Service Wildlife Services National Wildlife Research Center, Predator Project, Millville, UT 84326; [sssss]School of the Environment, The University of Queensland, St. Lucia, QLD 4072, Australia; [ttttt]Small Cat Advocacy and Research, Bowalawatta, Kandy 20024, Sri Lanka; [uuuuu]School of Animal and Veterinary Sciences, University of Adelaide, Roseworthy, South Australia 5371, Australia; [vvvvv]Department of Biology, Norwegian University of Science and Technology, Trondheim NO-7491, Norway; [wwwww]Area of Zoology, Department of Biodiversity and Environmental Management, Faculty of Biological and Environmental Sciences, University of León, León 24071, Spain; [xxxxx]Snow Leopard Trust, Seattle, WA 98103; [yyyyy]Laboratory of Animals Ecology and Conservation, Pacific Geographical Institute, Far Eastern Branch of the Russian Academy of Sciences, Vladivostok 690041, Russia; [zzzzz]Institute of Animal Ecology and Nature Education, Gonterskirchen 35321, Germany; [aaaaaa]Molecular Diagnostics Center, A.N. Severtsov Institute of Ecology and Evolution, Russian Academy of Sciences, Moscow 119071, Russia; [bbbbbb]Sikhote-Alin Reserve, Settlement Terney, Primorskiy Kray 692150, Russia; [cccccc]East Coast Ecology, 169 Pennant Parade Epping, New South Wales 2121, Australia; [dddddd]Centre for Ecological Sciences, Indian Institute of Science, Bangalore 560 012, India; [eeeeee]Asociación Guyra Paraguay and Consejo Nacional de Ciencia y Tecnología de Paraguay, Parque Ecológico Asunción Verde, Asunción 1101, Paraguay; [ffffff]Instituto Saite, Coronel Cabrera 166, Asunción 1407, Paraguay; [gggggg]Instituto Tabuleiro, Florianópolis 88040-400, Santa Catarina, Brasil; [hhhhhh]Programa de Pós-Graduação em Ecologia e Conservação, Universidade Federal do Mato Grosso do Sul, Campo Grande 79070-900, Mato Grosso do Sul, Brasil; [iiiiii]In der Jennenbach 37, Buchet D-54608, Germany; [jjjjjj]San Diego Zoo Institute for Conservation Research, Escondido, CA 92027-7000; [kkkkkk]School of Biological Sciences, University of KwaZulu-Natal, Durban 4000, South Africa; [llllll]School of Natural Resources, University of Arizona, Tucson, AZ 85721; [mmmmmm]Department for the Ecology of Animal Societies, Max

Planck Institute for Animal Behavior, Konstanz, Baden-Württemberg 78467, Germany; [nnnnnn]Department of Ecology and Evolutionary Biology, Center for Ocean Health, University of California, Santa Cruz, CA 95060; [oooooo]Center for Integrated Spatial Research, Environmental Studies Department, University of California, Santa Cruz, CA 95064; [pppppp]School of Biological Sciences, University of Western Australia, Crawley, WA 6009, Australia; and [qqqqqq]Department of Ecological Modelling, Helmholtz Centre for Environmental Research, Leipzig 04318, Germany

Author contributions: W.F.F. designed research; W.F.F., C.H.F., M.N., and J.M.C. conceptualized research approaches; W.F.F., A.G.K., C.H.F., E.S., A.S., B.A., C. Bracis, E.G., T.M., M.J.N., L.G.R.O.-S., M.T., L.M.D.-V., M.D., D.I., D.Y.A., P.C.A., C. Barrett, M.T.B., D.M.B., J.L.B., S.B., D.B., D.E.B., L.R.B., J.B., J.D.B., A.B., A. Carter, M.M.C., M.C., M.D.C., D.C., L.M.C., A. Cotterill, G.C., B.C., C.C., E.C., S.D., I.Z.d.C., F.A., C.S.D., J.D., C.T.D., N.D., M.D., E.E., S.E., M.S., M.F., A.T.F., J.F., L.F., J.M.F., T.K.F., R.F., S.G., W.M.G., M.J.P.G., T.J.G., M.G., R.H., M. Haberfeld, M. Hebblewhite, J.A.H.-B., M. Herrmann, M. Heurich, K.E.H., A.H., B.H., M.A.L.L.I., L.A.I., D.J., C.J., R. Janssen, K.E.J., J.E.J., M.L.S.P.J., R. Jorge, F.J., A. Katna, R. Kays, A. Kittle, R. Klein, R. Kont, M.J.C.K., J.K., J.L., A.D.M.L., P.L., F.G.L., T.L., C.F.M.L., E.L., F.L., J.D.C.L., D.W.M., P. Mahoney, P. Männil, E.M., J.M., R. May, R.T.M., R. McDonald, J.W.M., K.M., A.M., D.M., C.E.M., R.G.M., R. Moreno, G.M., Bariushaa Munkhtsog, Bayaraa Munkhtsog, M.N., S.V.N., T.N., J.O., M.O., F.P., B.R.P., B.D.P., R.C.d.P., A.P., Y.P., A.B.P., A.D.P., L.R.P., K.R., E.E.R., T.R., N.R., D.H.R., A.R., D.R., E.R., V.V.R., H.R.-V., J.R., G.S., P. Schwemmer, Ç.H.S., L.E.K.S., I.S., O.S., N.S., P.A.S., S.S., P. Stent, D.S., J.S., J. Tatler, K.T., M. Thaker, K.V.T., J. Thompson, M. Tortato, M. Trinzen, L.V.D.W., A.T.V., Z.W., M.V., T.J.W., T.W., T.M.W., C.C.W., J.W.-A., M.W., A.A.Y., J.K.Y., and J.M.C. performed research; W.F., A.K., C.F., S.C., G.A., Q.L., S.N., S.S., D.L., V.C., and S.R. analyzed data; C.H.F. contributed new analytic tools; A.G.K., C.H.F., A.S., C. Bracis, E.G., T.M., M.J.N., L.M.D.-V., M.D., D.I., R.H., and J.M.C. revised the paper; B.A., L.G.R.O.-S., M.A. Tucker, F.A., D. Berteaux, A. Carter, L.M.C., G.C., B.C., C.X.C., I.Z.d.C., J.D., C.T.D., A.F., M.F., J. Fryxell, T.K.F, W.M.G., M. Hebblewhite, J.A.H.-B., K.E.H., L.A.I., D.J., J.E.J., R. Kays, R. Klein, M.J.C.K., J.L., A.D.M.L., F.G.L., C.F.M.L, J.D.C.L., D.W.M., E.M., R. May, J.W.M., C.E.M., R.G.M., J.O., M.O., F.P., B.D. Patterson, Y.P., A.B.P., L.R.P., T.R., N.R., D.H.R., H.R.-V., G.S., P. Schwemmer, Ç.H.S., D.S., M. Thaker, K.V.T., J. Thompson, A.T.V., Z.W., T.J.W., T.W., T.M.W., C.C.W., and J.K.Y. contributed data and revised the paper; D.Y.A., P.C.A., C. Barrett, M.T.B., J.L.B., S.B., D.B., L.R.B., J.B., J.D.B., A.B., M.M.C., M.C., M.D.C., D.C., A. Cotterill, E.C., S.D., C.S.D., N.D., M.D., E.E., S.E., M.S., J.F., L.F., R.F., S.G., M.J.P.G., T.J.G., M.G., M.H., M.H., A.H., B.H., M.A.L.L.I., C.J., R. Janssen, K.E.J., M.L.S.P.J., R. Jorge, F.J., A. Katna, A. Kittle, R.K., J.K., P.L., T.L., E.L., F.L., P. Mahoney, P. Männil, R. McDonald, J.W.M., K.M., A.M., D.M., R. Moreno, G.M., Bariushaa Munkhtsog, Bayaraa Munkhtsog, S.V.N., T.N., B.P., R.C.d.P., A.P., A.B.P., K.R., E.E.R., D.H.R., A.R., E.R., V.V.R., J.R., L.E.K.S., I.S., O.S., N.S., P.A.S., S.S., P. Stent, J.S., J.T., K.T., M. Tortato, M. Trinzen, L.V.D.W., M.V., J.W.-A., M.W., and A.A.Y. contributed data; and W.F.F. wrote the paper.

1. J. Maynard Smith, *Evolution and the Theory of Games* (Cambridge University Press, 1982).
2. A. K. Shaw, I. D. Couzin, Migration or residency? The evolution of movement behavior and information usage in seasonal environments. *Am. Nat.* **181**, 114–124 (2013).
3. D. W. Stephens, J. R. Krebs, *Foraging Theory* (Princeton University Press, 1986), vol. 6.
4. M. L. Rosenzweig, Habitat selection and population interactions: The search for mechanism. *Am. Nat.* **137**, S5–S28 (1991).
5. R. S. Cantrell, C. Cosner, *Spatial Ecology Via Reaction-Diffusion Equations* (John Wiley & Sons, 2004).
6. T. Hillen, K. J. Painter, "Transport and anisotropic diffusion models for movement in oriented habitats" in *Dispersal, Individual Movement and Spatial Ecology: A Mathematical Perspective*, M. A. Lewis, P. K. Maini, S. V. Petrovskii, Eds. (Springer, Berlin/Heidelberg, Germany, 2013), pp. 177–222.
7. B. G. Weiner, A. Posfai, N. S. Wingreen, Spatial ecology of territorial populations. *Proc. Natl. Acad. Sci. U.S.A.* **116**, 17874–17879 (2019).
8. S. D. Healy, T. A. Hurly, Spatial memory in rufous hummingbirds (*Selasphorus rufus*): A field test. *Anim. Learn. Behav.* **23**, 63–68 (1995).
9. N. P. Naumov, Signal (biological) fields and their significance for animals. *Zh. Obshch. Biol.* **34**, 808–817 (1973).
10. A. Di Fiore, S. A. Suarez, Route-based travel and shared routes in sympatric spider and woolly monkeys: Cognitive and evolutionary implications. *Anim. Cogn.* **10**, 317–329 (2007).
11. D. Janzen, Euglossine bees as long-distance pollinators of tropical plants. *Science* **171**, 203–205 (1971).
12. O. Berger-Tal, S. Bar-David, Recursive movement patterns: Review and synthesis across species. *Ecosphere* **6**, 1–12 (2015).
13. K. E. Ironside *et al.*, Quantifying animal movement for caching foragers: The path identification index (PII) and cougars, *Puma concolor*. *Mov. Ecol.* **5**, 1–17 (2017).
14. H. M. McPhee, N. F. Webb, E. H. Merrill, Hierarchical predation: Wolf (*Canis lupus*) selection along hunt paths and at kill sites. *Can. J. Zool.* **90**, 555–563 (2012).
15. J. M. Hutchinson, P. M. Waser, Use, misuse and extensions of "ideal gas" models of animal encounter. *Biol. Rev.* **82**, 335–359 (2007).
16. J. P. O'Dwyer, Beyond an ecological ideal gas law. *Nat. Ecol. Evol.* **4**, 14–15 (2020).
17. A. M. Hein, B. T. Martin, Information limitation and the dynamics of coupled ecological systems. *Nat. Ecol. Evol.* **4**, 82–90 (2020).
18. T. Kashetsky, T. Avgar, R. Dukas, The cognitive ecology of animal movement: Evidence from birds and mammals. *Front. Ecol. Evol.* **9**, 724887 (2021).
19. M. de Guinea, A. Estrada, K. A. I. Nekaris, S. Van Belle, Arboreal route navigation in a Neotropical mammal: Energetic implications associated with tree monitoring and landscape attributes. *Mov. Ecol.* **7**, 1–12 (2019).
20. M. F. Kauffman *et al.*, Mapping out a future for ungulate migrations. *Science* **372**, 566–569 (2021).
21. B. McKeown, Z. Walton, T. Willebrand, Does recursive use of resource locations shape a home range? Exploring the red fox's cognitive map. *Wildlife Biol.* **2020**, 1–9 (2020).
22. M. A. Lewis *et al.*, Learning and animal movement. *Front. Ecol. Evol.* **9**, 681704 (2021).
23. S. E. Alavi *et al.*, A quantitative framework for identifying patterns of route-use in animal movement data. *Front. Ecol. Evol.* **9**, 743014 (2022).
24. D. Boyer, P. D. Walsh, Modelling the mobility of living organisms in heterogeneous landscapes: Does memory improve foraging success? *Phil. Trans. R. Soc. A: Math., Phys. Eng. Sci.* **368**, 5645–5659 (2010).
25. M. Dickie *et al.*, Corridors or risk? Movement along, and use of, linear features varies predictably among large mammal predator and prey species. *J. Anim. Ecol.* **89**, 623–634 (2020).
26. L. Riotte-Lambert, S. Benhamou, S. Chamaillé-Jammes, Periodicity analysis of movement recursions. *J. Theor. Biol.* **317**, 238–243 (2013).
27. G. Péron *et al.*, Periodic continuous-time movement models uncover behavioral changes of wild canids along anthropization gradients. *Ecol. Monogr.* **87**, 442–456 (2017).
28. K. R. Janmaat *et al.*, Using natural travel paths to infer and compare primate cognition in the wild. *iScience* **24**, 102343 (2021).
29. R. Kays, M. C. Crofoot, W. Jetz, M. Wikelski, Terrestrial animal tracking as an eye on life and planet. *Science* **348**, aaa2478 (2015).
30. H. J. Griebling *et al.*, How technology can advance the study of animal cognition in the wild. *Curr. Opin. Behav. Sci.* **45**, 101120 (2022).
31. U. E. Schlägel, E. H. Merrill, M. A. Lewis, Territory surveillance and prey management: Wolves keep track of space and time. *Ecol. Evol.* **7**, 8388–8405 (2017).
32. D. Biro, J. Meade, T. Guilford, Familiar route loyalty implies visual pilotage in the homing pigeon. *Proc. Natl. Acad. Sci. U.S.A.* **101**, 17440–17443 (2004).
33. S. Benson-Amram, H. J. Griebling, C. M. Sluka, The current state of carnivore cognition. *Anim. Cogn.* **26**, 37–58 (2023).
34. R. A. Mittermeier, D. E. Wilson, *Handbook of the Mammals of the World. Vol. 1: Carnivores* (Lynx Ediciones, Barcelona, Spain, 2009).
35. S. Thomas *et al.*, Evaluating the performance of conservation translocations in large carnivores across the world. *Biol. Conserv.* **279**, 109909 (2023).
36. N. S. Upham, J. A. Esselstyn, W. Jetz, Inferring the mammal tree: Species–level sets of phylogenies for questions in ecology, evolution, and conservation. *PLoS Biol.* **17**, e3000494 (2019).
37. S. Álvarez-Carretero *et al.*, A species-level timeline of mammal evolution integrating phylogenomic data. *Nature* **602**, 263–267 (2022).
38. M. J. Noonan *et al.*, A comprehensive analysis of autocorrelation and bias in home range estimation. *Ecol. Monogr.* **89**, e01344 (2019).
39. D. Alderton, B. Tanner, *Foxes, wolves, and wild dogs of the world*. (Facts on File, 1994).
40. L. Hunter, *Cats of Africa: Behavior, Ecology, and Conservation* (Johns Hopkins University Press, Baltimore, MA, 2006).
41. M. Sunquist, F. Sunquist, *Wild Cats of the World* (University of Chicago Press, Chicago, IL, 2017).
42. B. Van Valkenburgh, Locomotor diversity within past and present guilds of large predatory mammals. *Paleobiology* **11**, 406–428 (1985).
43. J. L. Gittleman, Carnivore life history patterns: Allometric, phylogenetic, and ecological associations. *Am. Nat.* **127**, 744–771 (1986).
44. A. N. Iwaniuk, S. M. Pellis, I. Q. Whishaw, The relationship between forelimb morphology and behaviour in North American carnivores (Carnivora). *Can. J. Zool.* **77**, 1064–1074 (1999).
45. J. A. Schwab, J. Kriwet, G. W. Weber, C. Pfaff, Carnivoran hunting style and phylogeny reflected in bony labyrinth morphometry. *Sci. Rep.* **9**, 1–9 (2019).
46. M. R. Hirt, M. Tucker, T. Müller, B. Rosenbaum, U. Brose, Rethinking trophic niches: Speed and body mass colimit prey space of mammalian predators. *Ecol. Evol.* **10**, 7094–7105 (2020).
47. E. Gurarie *et al.*, Spatial memory drives foraging strategies of wolves, but in highly individual ways. *Front. Ecol. Evol.* **10**, 768478 (2022).
48. K. R. Vitale Shreve, M. A. Udell, What's inside your cat's head? A review of cat (*Felis silvestris catus*) cognition research past, present and future. *Anim. Cogn.* **18**, 1195–1206 (2015).
49. K. E. Holekamp, S. Benson-Amram, The evolution of intelligence in mammalian carnivores. *Interface Focus* **7**, 20160108 (2017).
50. J. A. Finarelli, Testing hypotheses of the evolution of encephalization in the Canidae (Carnivora, Mammalia). *Paleobiology* **34**, 35–45 (2008).
51. J. A. Finarelli, J. J. Flynn, Brain-size evolution and sociality in Carnivora. *Proc. Nat. Acad. Sci. U.S.A.* **106**, 9345–9349 (2009).
52. J. D. Linnell, R. Aanes, J. E. Swenson, J. Odden, M. E. Smith, Translocation of carnivores as a method for managing problem animals: A review. *Biodivers. Conserv.* **6**, 1245–1257 (1997).
53. D. Denneboom, A. Bar-Massada, A. Shwartz, Factors affecting usage of crossing structures by wildlife–A systematic review and meta-analysis. *Sci. Total Environ.* **777**, 146061 (2021).
54. P. J. Mahoney, J. K. Young, Uncovering behavioural states from animal activity and site fidelity patterns. *Methods Ecol. Evol.* **8**, 174–183 (2017).
55. M. Drouilly, N. Nattrass, M. J. O'Riain, Global positioning system location clusters vs. scats: Comparing dietary estimates to determine mesopredator diet in a conflict framework. *J. Zool.* **310**, 83–94 (2020).
56. A. Katna, A. Kulkarni, M. Thaker, A. T. Vanak, Habitat specificity drives differences in space-use patterns of multiple mesocarnivores in an agroecosystem. *J. Zool.* **316**, 92–103 (2022).
57. Movebank (2019), https://www.movebank.org/study/1247305994. Accessed 15 September 2022.
58. R. Martínez-García, C. H. Fleming, R. Seppelt, W. F. Fagan, J. M. Calabrese, How range residency and long-range perception change encounter rates. *J. Theor. Biol.* **498**, 110267 (2020).
59. M. J. Noonan *et al.*, The search behavior of terrestrial mammals. bioRxiv [Preprint] (2022). https://doi.org/10.1101/2022.12.31.521874. Accessed 15 September 2022.
60. H. McKenzie, E. Merrill, R. Spiteri, M. Lewis, How linear features alter predator movement and the functional response. *Interface Focus* **2**, 205–216 (2012).
61. E. Gurarie, O. Ovaskainen, Towards a general formalization of encounter rates in ecology. *Theor. Ecol.* **6**, 189–202 (2013).
62. Y. Chen, F. Liu, Q. Yu, T. Li, Review of fractional epidemic models. *Appl. Math. Model.* **97**, 281–307 (2021).
63. L. A. White, J. D. Forester, M. E. Craft, Disease outbreak thresholds emerge from interactions between movement behavior, landscape structure, and epidemiology. *Proc. Nat. Acad. Sci. U.S.A.* **115**, 7374–7379 (2018).
64. M. Q. Wilber *et al.*, A model for leveraging animal movement to understand spatio-temporal disease dynamics. *Ecol. Lett.* **25**, 1290–1304 (2022).
65. J. W. Laundré, L. Hernández, K. B. Altendorf, Wolves, elk, and bison: Reestablishing the "landscape of fear" in Yellowstone National Park, USA. *Can. J. Zool.* **79**, 1401–1409 (2001).
66. K. M. Gaynor, J. S. Brown, A. D. Middleton, M. E. Power, J. S. Brashares, Landscapes of fear: Spatial patterns of risk perception and response. *Trends Ecol. Evol.* **34**, 355–368 (2019).
67. J. Whittington *et al.*, Towns and trails drive carnivore movement behaviour, resource selection, and connectivity. *Mov. Ecol.* **10**, 17 (2022).

68. A. González-Gallina, M. G. Hidalgo-Mihart, V. Castelazo-Calva, Conservation implications for jaguars and other Neotropical mammals using highway underpasses. *PLoS ONE* **13**, e0206614 (2018).
69. C. E. Dunford *et al.*, Surviving in steep terrain: A lab-to-field assessment of locomotor costs for wild mountain lions (*Puma concolor*). *Mov. Ecol.* **8**, 1–12 (2020).
70. M. Valeix *et al.*, How key habitat features influence large terrestrial carnivore movements: Waterholes and African lions in a semi-arid savanna of north-western Zimbabwe. *Landsc. Ecol.* **25**, 337–351 (2010).
71. E. Gurarie, J. Suutarinen, I. Kojola, O. Ovaskainen, Summer movements, predation and habitat use of wolves in human modified boreal forests. *Oecologia* **165**, 891–903 (2011).
72. C. Casares-Hidalgo, A. Pérez-Ramos, M. Forner-Gumbau, F. J. Pastor, B. Figueirido, Taking a look into the orbit of mammalian carnivorans. *J. Anat.* **234**, 622–636 (2019).
73. J. A. Schwab *et al.*, Evolutionary ecomorphology for the twenty-first century: Examples from mammalian carnivores. *Proc. R. Soc. B, Biol. Sci.* **290**, 20231400 (2023).
74. M. E. Taylor, "Locomotor adaptations by carnivores" in *Carnivore Behavior, Ecology, and Evolution*, J. L. Gittleman, Ed. (Springer US, Boston, MA, 1989), pp. 382–409.
75. B. Van Valkenburgh *et al.*, Respiratory and olfactory turbinals in feliform and caniform carnivorans: The influence of snout length. *Anat. Rec.* **297**, 2065–2079 (2014).
76. M. L. Gorman, B. J. Trowbridge, "The role of odor in the social lives of carnivores" in *Carnivore Behavior, Ecology, and Evolution*, J. L. Gittleman, Ed. (Springer US, Boston, MA, 1989), pp. 57–88.
77. S. Benhamou, An olfactory orientation model for mammals' movements in their home ranges. *J. Theor. Biol.* **139**, 379–388 (1989).
78. C. A. Schloss, T. A. Nuñez, J. J. Lawler, Dispersal will limit ability of mammals to track climate change in the Western Hemisphere. *Proc. Natl. Acad. Sci. U.S.A.* **109**, 8606–8611 (2012).
79. B. R. Jesmer *et al.*, Is ungulate migration culturally transmitted? Evidence of social learning from translocated animals. *Science* **361**, 1023–1025 (2018).
80. M. A. Lewis *et al.*, Learning and animal movement. *Front. Ecol. Evol.* **9**, 681704 (2021).
81. W. H. Burt, Territoriality and home range concepts as applied to mammals. *J. Mammal.* **24**, 346–352 (1943).
82. R. J. P. Heathcote *et al.*, Spatial memory predicts home range size and predation risk in pheasants. *Nat. Ecol. Evol.* **7**, 461–471 (2023).
83. N. Ranc, F. Cagnacci, P. R. Moorcroft, Memory drives the formation of animal home ranges: Evidence from a reintroduction. *Ecol. Lett.* **25**, 716–728 (2022).
84. S. Fiset, C. Beaulieu, F. Landry, Duration of dogs' (*Canis familiaris*) working memory in search for disappearing objects. *Anim. Cogn.* **6**, 1–10 (2003).
85. S. Fiset, F. Y. Doré, Duration of cats' (*Felis catus*) working memory for disappearing objects. *Anim. Cogn.* **9**, 62–70 (2006).
86. F. Y. Doré, S. Fiset, S. Goulet, M.-C. Dumas, S. Gagnon, Search behavior in cats and dogs: Interspecific differences in working memory and spatial cognition. *Anim. Learn. Behav.* **24**, 142–149 (1996).
87. K. A. Ericsson, W. Kintsch, Long-term working memory. *Psychol. Rev.* **102**, 211 (1995).
88. N. Unsworth, G. A. Brewer, G. J. Spillers, Working memory capacity and retrieval from long-term memory: The role of controlled search. *Mem. Cogn.* **41**, 242–254 (2013).
89. C. Meneghetti, E. Labate, E. Toffalini, F. Pazzaglia, Successful navigation: The influence of task goals and working memory. *Psychol. Res.* **85**, 634–648 (2021).
90. S. M. Weisberg, N. S. Newcombe, How do (some) people make a cognitive map? Routes, places, and working memory. *J. Exp. Psychol. Learn. Mem. Cogn.* **42**, 768–785 (2016).
91. T. T. Hills, P. M. Todd, R. L. Goldstone, The central executive as a search process: Priming exploration and exploitation across domains. *J. Exp. Psychol. Gen.* **139**, 590 (2010).
92. T. Spellman *et al.*, Hippocampal–prefrontal input supports spatial encoding in working memory. *Nature* **522**, 309–314 (2015).
93. G. W. Wang, J. X. Cai, Disconnection of the hippocampal–prefrontal cortical circuits impairs spatial working memory performance in rats. *Behav. Brain Res.* **175**, 329–336 (2006).
94. W. F. Fagan *et al.*, Spatial memory and animal movement. *Ecol. Lett.* **16**, 1316–1329 (2013).
95. T. K. Ruth, K. A. Logan, L. L. Sweanor, M. G. Hornocker, L. J. Temple, Evaluating cougar translocation in New Mexico. *J. Wildl. Manage.* **62**, 1264–1275 (1998).
96. S. Thomas *et al.*, Evaluating the performance of conservation translocations in large carnivores across the world. *Biol. Conserv.* **279**, 109909 (2023).
97. P. Cisneros-Araujo *et al.*, Born to be wild: Captive-born and wild Iberian lynx (*Lynx pardinus*) reveal space-use similarities when reintroduced for species conservation concerns. *Biol. Conserv.* **294**, 110646 (2024).
98. R. Rosenbaum *et al.*, Spatial ecology of snow leopards (*Panthera uncia*) in the Altai Mountains of western Mongolia. *PLoS ONE* **18**, e0280011
99. S. J. Green, B. J. Boruff, T. R. Bonnell, C. C. Grueter, Chimpanzees use least-cost routes to out-of-sight goals. *Curr. Biol.* **30**, 4528–4533 (2020).
100. S. LaPoint, P. Gallery, M. Wikelski, R. Kays, Animal behavior, cost-based corridor models, and real corridors. *Landscape Ecol.* **28**, 1615–1630 (2013).
101. T. Barry, E. Gurarie, F. Cheraghi, I. Kojola, W. F. Fagan, Does dispersal make the heart grow bolder? Variation in habitat selection across wolf life history. *Anim. Behav.* **166**, 219–231 (2020).
102. I. Silva *et al.*, Autocorrelation-informed home range estimation: A review and practical guide. *Methods Ecol. Evol.* **13**, 534–544 (2022).
103. J. M. Calabrese, C. H. Fleming, E. Gurarie, CTMM: An R package for analyzing animal relocation data as a continuous-time stochastic process. *Methods Ecol. Evol.* **7**, 1124–1132 (2016).
104. C. R. Genovese, M. Perone-Pacifico, I. Verdinelli, L. Wasserman, Nonparametric ridge estimation. *Ann. Stat.* **42**, 1511–1545 (2014).
105. J. S. Horne, E. O. Garton, S. M. Krone, J. S. Lewis, Analyzing animal movements using Brownian bridges. *Ecology* **88**, 2354–2363 (2007).
106. S. Benhamou, Dynamic approach to space and habitat use based on biased random bridges. *PLoS ONE* **6**, e14592 (2011).
107. J. M. Alston *et al.*, Clarifying space use concepts in ecology: Range vs. occurrence distributions. bioRxiv [Preprint] (2022). https://doi.org/10.1101/2022.09.29.509951. Accessed 15 June 2023.
108. C. H. Fleming *et al.*, Estimating where and how animals travel: An optimal framework for path reconstruction from autocorrelated tracking data. *Ecology* **97**, 576–582 (2016).
109. J. Dall, M. Christensen, Random geometric graphs. *Phys. Rev. E.* **66**, 016121 (2002).
110. Z. Dong, M. Tian, J. Liang, Y. Fang, Y. Lu, Research on the connection radius of dependency links in interdependent spatial networks against cascading failures. *Physica A* **513**, 555–564 (2019).
111. Y. Liang, Y. Xia, X. H. Yang, Hybrid-radius spatial network model and its robustness analysis. *Physica A* **591**, 126800 (2022).
112. L. E. Farrell *et al.*, Landscape connectivity for bobcat (*Lynx rufus*) and lynx (*Lynx canadensis*) in the Northeastern United States. *PLoS ONE* **13**, e0194243 (2018).
113. R. G. Morato *et al.*, Jaguar movement database: A GPS-based movement dataset of an apex predator in the Neotropics. *Ecology* **99**, 1691–1691 (2018).
114. R. Moreno, R. Mares, E. Aliaga-Rossel, R. Kays, Data from: Ámbito de hogar y actividad circadiana del ocelote (*Leopardus pardalis*) en la Isla de Barro Colorado, Panamá. *Movebank Data Repository* (2020). https://doi.org/10.5441/001/1.pb653nk3. Accessed 15 September 2022.

PNAS

Supporting Information for

Wild canids and felids differ in their reliance on travel routeways

William F. Fagan, Ananke G. Krishnan, Christen H. Fleming, Elizabeth Sharkey, Stephanie Chia, Anshuman Swain, Briana Abrahms, Chloe Bracis, Eliezer Gurarie, Thomas Mueller, Michael J. Noonan, Luiz Gustavo R. Oliveira-Santos, Marlee Tucker, Gayatri Anand, Qianru Liao, Sarah Na, Steven Su, Daisy Liao, Varun Chilukuri, Shreyas Ramulu, Luisa Maria Diele-Viegas, Michael Dougherty, David Illingworth, Dmitry Y. Alexandrov, Pamela Castro Antunes, Christina Barrett, Matías Taborda Barroso, Dominik M. Behr, Jerrold L. Belant, Steven Bellan, Dominique Berteaux, Dean E. Beyer, Jr., Laura R. Bidner, Jacqueline Bishop, J. David Blount, Andrew Butler, Andrew Carter, Marina Motta Carvalho, Michael Chamberlain, Maria D. Chistopolova, Darren Clark, L. Mike Conner, Alayne Cotterill, Gabrielle Cozzi, Bogdan Cristescu, Calum X. Cunningham, Emrah Çoban, Siobhan Darlington, Ísis Zanini das Candeias, Fernanda Azevedo, Christopher S. DePerno, Jasja Dekker, Colleen T. Downs, Natalia Dronova, Marine Drouilly, Ernest Eblate, Steve Ekwanga, Morgan Swingen, Mohammad Farhadinia, Adam T. Ford, Jacqueline Frair, Laurence Frank, John M. Fryxell, Todd K. Fuller, Robert Fyumagwa, Stefan Garthe, Wayne M. Getz, Maria Jesus Palacios Gonzalez, TJ Gooliaff, Malte Götz, Rowena Hamer, Mario Haberfeld, Mark Hebblewhite, Jose A. Hernandez-Blanco, Mathias Herrmann, Marco Heurich, Karen E. Hodges, AnnMarie Houser, Bruce Humphries, Miguel Ángel López López Iglesias, Lynne A. Isbell, David Jachowski, Craig Jackson, René Janssen, Kate E. Jenks, Jaime E. Jiménez, Maria Luisa S.P. Jorge, Rodrigo Jorge, Fernando Jubete, Anjan Katna, Roland Kays, Andrew Kittle, Rebecca Klein, Raido Kont, Michelle J.C. Kral, Josip Kusak, Johannes Lang, Andrew David M. Latham, Peter Leimgruber, Frederico G. Lemos, Taal Levi, Caio F. M. Lima, Edson Lima, Fernando Lima, John D.C. Linnell, David W. Macdonald, Peter Mahoney, Peep Männil, Emmanuel Masenga, Jenny Mattisson, Roel May, Roy T McBride, Jr., Robbie McDonald, John Weldon McNutt, Karl Miller, Alexander Minaev, Dale Miquelle, Christopher E. Moorman, Ronaldo G. Morato, Ricardo Moreno, Guilherme Mourão, Bariushaa Munkhtsog, Bayaraa Munkhtsog, Sergey V. Naidenko, Teresa Nava, John Odden, Morten Odden, Francisco Palomares, Brent R. Patterson, Bruce D. Patterson, Rogerio Cunha de Paula, Agustin Paviolo, Yury Petrunenko, Alim B. Pkhitikov, Andrey D. Poyarkov, Laura R. Prugh, Kasim Rafiq, Emiliano Esterci Ramalho, Tharmalingam Ramesh, Nathan Ranc, Dustin H. Ranglack, Anya Ratnayaka, David Roshier, Eivin Røskaft, Viatcheslav V. Rozhnov, Hector Ruiz-Villar, Joel Ruprecht, Gustaf Samelius, Philipp Schwemmer, Çağan H. Şekercioğlu, Laurel E.K. Serieys, Ivan Seryodkin, Olaf Simon, Nucharin Songsasen, Pavel A. Sorokin, Svetlana Soutryina, Patrick Stent, David Stoner, Jarryd Streicher, Jack Tatler, Kristine Teichman, Maria Thaker, Katerina V. Thompson, Jeffrey Thompson, Marcos Adriano Tortato, Manfred Trinzen, Leanne Van Der Weyde, Abi Tamim Vanak, Zea Walton, Marianela Velilla, Tyler J. Wheeldon, Tomas

Willebrand, Terrie M. Williams, Christopher C. Wilmers, Jared Wilson-Aggarwal, Michael Wysong, Anna A. Yachmennikova, Julie K. Young, and Justin M. Calabrese

Corresponding Author:
William F. Fagan
Email: bfagan@umd.edu

This PDF file includes:

Supporting text
Figures S1 to S13
Tables S1 to S6
Legends for Datasets S1 to S2
SI References

Other supporting materials for this manuscript include the following:

Datasets S1 to S2

Supporting Information Text

Detailed Methods.

Dataset

We compiled GPS tracking data from the online repository Movebank (1), from journal publications, and from co-authors directly. Collectively, we obtained movement tracks for 1528 individuals across 36 species of canids and felids. All analyses were conducted at the species level; "Great Lakes wolves" *Canis lupus x lycaon* were treated as *Canis lupus*. We attempted to estimate a home range for each of the 1528 individuals by fitting a series of range-resident, continuous-time movement models to each GPS track and visually assessing their variograms, followed by home range delineation using autocorrelated kernel density estimation (AKDEc; 2), all via the R package *ctmm* (version 1.1.0; (2-4)). By design, *ctmm* facilitates comparative analysis of GPS datasets involving missing data, irregular sampling intervals, and differences in nominal sampling interval (2-3, 5). Tracks with GPS sampling intervals <1 minute were resampled to 1-minute intervals to facilitate analysis without a location-error model in *ctmm.*

This approach first estimates each animal's movement as one of three continuous time stochastic processes, and then uses model selection techniques to identify the most appropriate model for each individual. An IID (independent and identically distributed) movement process has no temporal autocorrelation. An OU ("Ornstein-Uhlenbeck"; (6)) process features autocorrelation in position but no autocorrelation in velocity. Lastly, an OUF ("Ornstein-Uhlenbeck Foraging") process features autocorrelation in both position and velocity (4, 7-8), which together allow for calculation of a scale-insensitive estimate of movement speed (5). GPS tracking datasets almost always exhibit some form of autocorrelation, and the IID process is exceptionally infrequent among range-resident individuals (9). Autocorrelation in velocity is detectable in movement tracks where the time interval between fixes is short relative to the timescale over which velocity autocorrelation decays (4,7).

Silva et al. (3) provide a detailed overview of the stochastic process models' utility, meaning, parameterization, and estimation; here we present only a brief synopsis. Stable, saturating variograms (plots of semi-variance in position as a function of time-lag between relocations) facilitate effective visualization of key features of movement processes and identification of range

residency. Range-resident behavior is evident when the variogram of a movement track exhibits a clear asymptote at long time lags (3,4). Each variogram was checked visually to ensure saturation (4) before range resident movement models were fit to the data via perturbative residual maximum likelihood (10). We then identified the best fit stochastic process model for each track using AICc-based model selection (2,11). Home range areas were then estimated conditional on the selected model for each movement track, via autocorrelated kernel density estimation (11) with small sample size correction (12) embodied in the AKDEc method for determining range distributions (2). Importantly, the range distributions estimated via *ctmm* are best interpreted as home ranges, not (often smaller) territories that are actively defended against intruders or maintained through scent-marking and other mechanisms. For home range size, we used the area enclosed within the mean estimate of the 95th percentile of each individual's home range distribution (2,9).

It is essential to understand that home ranges estimated via *ctmm* are asymptotic distributions. That is, the distributions represent where the animal will travel and how it will use space over the long run assuming that the movement behaviors observed during the tracking period remain constant over the long run. In contrast, a visualization of a movement track derived from GPS fixes will depend completely on that specific set of recorded locations. That is, such a visualization is merely a sampling-dependent depiction of locations. One should therefore expect visual disparities between a plotted set of relocations and an asymptotic prediction of space use based on the statistical properties of the observed track.

Of the 1528 movement tracks, 1070 were well-fit by *ctmm* as IID, OU, or OUF processes without any cleaning efforts beyond those originally undertaken by the dataowners themselves (e.g., removal of questionable GPS relocations with sparse satellite support or high dilution of precision) or by us to remove physically impossible 'teleportation events' in which animals moved >7 times their mean speed with return angles of 180 ± 5 degrees or moved >100km between consecutive GPS relocations. We obtained good model fits to an additional 169 tracks after: 1) fixing minor problems (e.g., GPS timestamp issues; n = 16), 2) cropping out extreme, non-residential foraying trips (defined as GPS fixes > 5 median absolute deviations [MAD] from the density of point data in keeping with Burt's definition of a home range, n = 113) (13), 3)

splitting the track to delineate the home range via a *ctmm* model with a time-weighted mean (useful when an individual clearly shifted the center of its range, n = 23), 4) splitting the track to eliminate a period of non-residency (such as when an individual was moving and then settled, or when it left its home range without resettling, n = 4), or 5) employing two or more methods from 1-4 (n = 13).

Overall, we eliminated 289 tracks where fitting of range-resident models was not possible within *ctmm* thereby inhibiting delineation of a home range; many of these individuals were clearly not range-resident upon visual inspection of their variograms. Of the 289 excluded tracks, 221 were unsuitable for home range analysis because they had a home range effective sample size less than five (3) or a duration of less than one month. Home range effective sample size (hereafter, ESS) measures the information content in a tracking dataset with autocorrelation in comparison to the information content of a dataset with the same number of observations, but where all observations are independent. The ESS of an autocorrelated movement track is always less (and sometimes dramatically less) than the number of observations in the movement track, with the magnitude of the decrease in ESS (relative to the same number of independent observations) being proportional to the strength of autocorrelation in the data. In the context of home range analysis, ESS is interpretable as the number of 'home range crossing equivalents' that occurred over the duration of the track, which is approximately the total duration of the dataset divided by the characteristic home range crossing time (3). Collectively, unsuitable tracks lack stable, saturating variograms, yielding highly uncertain home range boundaries. We therefore excluded a final 68 additional tracks that were sufficient in ESS and duration, but for which we were unable to obtain a satisfactory saturating variogram even after the aforementioned cleaning steps 1-5.

In total, 1239 tracks across 34 species (16 canids, 18 felids) were usable for analysis (Dataset S1), and these constituted the 'full' dataset. To ensure the robustness of our findings, we also conducted separate comparative statistical analyses using several subsets of these 1239 tracks, specifically: 1) the 1070 tracks (including all 34 species) that required no preprocessing (hereafter, the 'no preprocessing' dataset), 2) the 1032 tracks (all 34 species) that were best-fit by OUF models, allowing us to obtain a continuous-time speed estimate (5) (hereafter the 'including speed' dataset), 3) the 342 tracks (13 canids and 16 felids) with duration > 1 year thus eliminating

many potential phenological biases (hereafter the 'year or longer' dataset; see SI Potential Phenological Biases), and 4) the 219 tracks (9 landscapes, 7 canids and 7 felids) in which canids and felids were studied in the same landscape (hereafter, the 'shared landscapes' dataset). Analysis of the 'shared landscapes' dataset eliminated potential effects of spatial context beyond the five spatial covariates we included in all of our statistical models (detailed below).

Characterizing how extensively animals rely on travel routeways

To make effective multispecies comparisons involving re-used travel routeways using GPS tracking data, we introduce an approach that relies on statistical features known as 'probability ridges' (14) to characterize the internal structure of animals' home range distributions. For biological movement data, a probability ridge curve will emerge when an animal repeatedly uses similar, spatially localized routes to navigate a given region within its home range.

Importantly, probability ridges should be a predominant feature of space use for range-resident individuals, but not for transient or 'floating' individuals, and this distinction underpinned our emphasis on identifying range-resident behavior through the variogram analysis discussed above. Ridges could emerge as a consequence of animals repeatedly moving to or through favored regions to forage, via recurrent patrolling of territorial boundaries, or via revisitation to locations of interest via the same routes. Maps in Fig. 1 depict the location of ridges inside home ranges calculated for several individuals across landscapes in which movements of both canids and felids were studied.

When using *ctmm* to estimate the location of ridges within a home range, we replaced the accurate yet $O(n^2)$ computationally slow *ks* package (15) (which proved completely unworkable with our large GPS-based datasets) with an approximate yet $O(n)$ computationally fast algorithm developed for this project. This algorithm numerically calculated gradient and curvature information in probability density per pixel, allowing us to identify any neighboring ridge-line points from each pixel. For each pixel, we then tallied the estimated number of ridge-line points contained within its neighboring cells, and normalized each per-cell tally by the total number of neighbors to obtain a value between 0 and 1 that we could threshold with regard to how certain (numerically) an area of heightened probability had to be so as to be

scored a ridge. That is, the tunable threshold certainty value corresponded to our *tolerance* for what constituted an actual ridge of probability within a home range. For example, with a tolerance threshold very near 0, a broad, very nearly flat portion of a probability density surface would include a ridge inside it, whereas with a tolerance threshold very near 1, only the sharpest, steepest regions of a probability density surface would include a ridge. The qualitative outcomes of our multispecies analyses (see below) were broadly insensitive to this threshold (Table S4), and we adopted an intermediate value of 0.5 throughout.

Our reliance on the computationally fast *ctmm* algorithm for ridge identification created a particular type of estimation error in the form of a numerical (aliasing) artifact that led to the identification of a pair of non-intersecting disjunct ridge curves where one would expect only a single ridge curve. Generally speaking, a true probability ridge will fall between each pair of non-intersecting curves, but identifying its specific spatial alignment using the *ks* algorithm is only possible with enormous computational cost for all but the shortest movement tracks. The aliasing curves, which may appear circular, oval, crescent-shaped, or otherwise connected at some image resolutions (but are not connected), will appear widely separated in portions of an animal's home range with low average probability density. In contrast, for portions of the home range featuring relatively high probability density, the two non-intersecting curves will fall very close to one another and may not even be visually distinguishable.

Importantly, the numerical aliasing artifacts affected only the intercepts of the statistical models for ridge density described below, and had no bearing on the reported effect sizes or hypothesis tests. In contrast, the numerical aliasing artifacts do have the potential to introduce an upward bias in the calculation of ridge-associated probability mass. This would occur because the aliased ridges could create superfluous buffers that intercept more probability mass than the buffers along the corresponding true ridge curve would have intercepted (had it been calculable). However, the bias introduced by this aliasing is expected to be small because the aliased ridges are most widely spread (and thus create the greatest opportunity for non-overlapping buffer zones), when local probability densities are small. Nevertheless, because of this potential for upward bias, however small, the reported values of ridge-associated probability mass should be interpreted as upper bounds on the true values (Figs. S5,6).

231

232 To avoid confusion, the probability ridges plotted in Figures 1D-G and 2 are based on the
233 computationally slow *ks* algorithm that avoids plotting any aliasing artifacts.

234

235 For comparative analyses, we focused on two metrics: *ridge density* and *ridge-associated*
236 *probability mass.* Ridge density is determined by 1) total ridge length (m), calculated as a simple
237 sum of the lengths of all ridge elements in an individual's home range (interpretable as travel
238 routeways used more heavily than other, adjacent areas), and 2) a standardization that adjusts for
239 the size of that individual's home range. Mathematically, we have

240 $$\text{ridge density} = \frac{\text{total ridge length}^2}{\text{home range area}} \quad , \qquad \text{(S1)}$$

241 where home range area is calculated as the mean of the 95th percentile of the AKDEc range
242 distribution estimated through *ctmm* (see SI Detailed Methods: Dataset). As a variable, ridge
243 density is both dimensionless and intrinsic (in the sense that it does not scale trivially with home-
244 range size), making it a preferred choice for analysis in subsequent complex models. We opted for
245 this mathematical definition of ridge density instead of an alternative (total ridge length /
246 sqrt(home range area) to retain the greatest flexibility with regard to statistical transformations
247 that might have been necessary in the context of our analyses (described below). Our definition of
248 ridge density and the metric from the alternative definition are proportional under a logarithmic
249 transformation, and our decision to use Eq. S1 did not affect the significance of our results. We
250 obtained our second focal metric, ridge-associated probability mass, by placing spatial buffers of
251 various widths along each probability ridge, as detailed in Materials and Methods in the main text.

252

253 An animal with high (or low) density of ridges navigates via a large (or small) set of travel
254 routeways relative to the extent of its home range. Importantly, because the locations of ridges
255 within a home range distribution ultimately derive from a bandwidth-limited autocorrelated kernel
256 density estimate (AKDEc), ridges are asymptotically consistent predictions of where the most-
257 intensely used travel routeways will eventually be located, given the available GPS data. In all
258 statistical analyses (described below), we included a simple first-order bias-correction term,
259 1/ESS, to model the lack of resolution in ridge density in home ranges deriving from movement
260 tracks with low data density.

Ridges reflecting re-used paths could arise because biological processes (e.g., perception, memory) influence navigation through a home range) or because environmental features form natural corridors/barriers within the home range. For instance, if looking at an arboreal species, efficient travel routes from tree to tree could exist based on proximity, making it difficult to discriminate memory from environmentally constrained movement (16). Among carnivores, roads, cliff faces, and other physical features structure movement routes in some locations (17-19). As detailed below, our statistical analyses used a series of landscape metrics to assess the potential importance of environmental factors that differ across spatial contexts.

Phylogenetic considerations

Because we needed to simultaneously account for the evolutionary nonindependence among the species in our dataset and test for a clade-level difference in movement between canids and felids, we positioned all 34 of the species on the maximum clade credibility (MCC) consensus tree of the completed phylogenetic tree for mammals downloaded from the VertLife database (20). We used the long-tailed pangolin (*Phantaginus tetradactyla*) as an outgroup not included in the Carnivora, the sea otter (*Enhydra lutris*), the grey seal (*Halichoerus grypus*), and the American black bear (*Ursus americanus*) as members of the Caniformia outside the Canidae, and the striped hyaena (*Hyaena hyaena*) and common slender mongoose (*Herpestes sanguineus*) as members of the Feliformia outside the Felidae. (Note: we included these in/outgroup species to structure and aid visualization of the phylogenetic distance matrix, which was then trimmed to include only canid and felid species before any statistical calculations; in/outgroup species did not involve any movement data). The 34 species movement dataset included at least one species from all major lineages of the Canidae and all major lineages of the Felidae, except one, the little-known bay cat lineage consisting of the genera *Catopuma* and *Pardofelis*. The MCC consensus tree we used in our focal clade-level analyses (detailed below) involves some phylogenetic uncertainty because, when the VertLife database was being developed, DNA data were not available for 2 of the 34 species for which we obtained movement data (*Leopardus geoffroyi, Vulpes bengalensis*; 20). To examine the potential influence of this phylogenetic uncertainty on our primary analyses, we conducted separate clade-level analyses on a reduced movement dataset using the MCC consensus tree of DNA-only distributions (20) for the 32 species whose DNA data informed the

VertLife database. Hereafter, we refer to this reduced movement dataset (1201 tracks, 15 canids, 17 felids) as the 'DNA only tree' dataset. For phylogenetic data manipulations, we relied on the R packages *ape* (version 5.7.1) (21) and *phytools* (version 1.2-0) (22).

Covariates and alternative hypotheses

Diverse factors could influence the extent and location of ridges within an individual's home range. Examples include tree cover, topography, or human infrastructure that could shape movement routeways by favoring or disfavoring certain areas (17-18, 23), body mass or hunting strategies that influence how animals move through their landscapes (24-27), or aspects of the GPS tracks themselves such as data density or the predicted home range size. We considered nine variables as fixed-effect covariates in our comparative models, and organized them according to whether they derived from species-level differences arising from each species' unique evolutionary biology or individual-level factors that depended on each organism's unique GPS track. Table S1 provides detailed information about these nine variables, including descriptions, justifications, and citations. Briefly, we considered 1) three individual-level variables calculated directly from *ctmm* (home range size, ESS, and speed), 2) four individual-level spatial variables (terrain roughness, tree cover, human footprint index, and variation dynamic habitat index for gross primary productivity "Var DHI GPP"), each of which was spatially averaged over each individual's estimated home range, and 3) two species-level factors (body mass and movement strategy while hunting). In preliminary analyses, we substituted road cover (one of the components of the human footprint index (28)) for the complete human footprint index. Finding only the most minimal differences, we used the complete human footprint index in all subsequent analyses because it captures more dimensions of human activity and infrastructure to which animals might respond by changing their movement (23).

Of these potential covariates, movement strategy while hunting requires special attention because similar variables have appeared in earlier comparative studies of carnivore locomotion and predatory niches (29-31). Other resources provide additional detailed species-level descriptions of canid and felid movement (24-27), and several coauthors provided their expert assessments for this analysis based on extensive direct observation of hunting strategies. However, different sets of terms have been used in different sources, established term sets exclude some movement

strategies reported in some sources, and movement behaviors are not detailed in any one resource for all 34 species in our full dataset. Consequently, we integrated across the varied terminology used in previous comparative analyses, species narratives, and additional sources to arrive at a set of three generalized terms describing canid and felid movement strategies while hunting that were simultaneously behaviorally distinct and inclusive of variations (Table S2). These were 1) *pursuit* (in which prey are actively chased, sometimes for many hundreds of meters), 2) *slow walking* (which, upon discovery of prey, would typically involve some elements of stalking, ambushing, and pouncing), and 3) *disruptive fast hunting* (in which carnivores move quickly through an area attempting to startle and flush prey). We treated these strategies as indicator variables, which meant that (unlike previous categorizations) a species could be classified as employing more than one strategy. Importantly, however, we emphasize that our analyses used all location data available from each GPS track, not just portions that could be defined as hunting.

Statistical analyses

We modified the R package *metafor* (version 3.8-1) to conduct phylogenetically controlled generalized linear mixed model (PGLMM) analyses of ridge density. In all analyses, we tested for a clade-level difference between canids and felids while using one random effect to accommodate the phylogenetic autocorrelation and another random effect (a Normal regression error, not included by default in *metafor*) to control for interspecific differences in numbers of individuals (SI Methods: Sample Code). The nine covariates discussed above appeared as fixed effects, including effects at the level of the species and the individual (Table S1). In these models, ESS is effectively a bias correction to the intercept; that is, the combination of intercept and 1/ESS sets the overall scale (with bias correction), but does not explain any biological variation.

Movement data for the same species but from different environments (and therefore different external conditions) could further clarify the extent to which biological processes (such as memory) versus environmental factors are driving clade-level differences in ridge density. One simple hypothesis is that ridge density should be similar for the same species in different landscapes if there is a strong role for carnivore biology, but dissimilar across landscapes if the density of re-used routeways is driven more by local prey and spatial context. However, any intraspecific differences across landscapes would not necessarily be independent of biology

because context can have a strong influence on cognitive processes (32). We explored this issue using a dataset of 11 species (five canids and six felids), each of which was studied in at least three landscapes. We used GLMs to conduct separate analyses for each species, testing for evidence of heterogeneity in ridge density across the particular landscapes from which GPS track data for that species were available. For each species, the fitted GLM included home range area, 1/ESS, and a study-level indicator variable.

We also conducted separate analyses in which the full statistical model, including all nine fixed effects covariates, was applied separately to the canid and felid groups. This is the functional equivalent of putting the clade effect in interaction with all variables, but is more easily understood and far easier (and faster) to estimate numerically. We looked for differences in the relative importance of the different predictor variables between the two carnivore families while controlling for evolutionary non-independence within families.

SI Methods: Sample Code provides sample code illustrating our approach to the complex phylogenetically controlled mixed-effects models that allow for tests of clade-level differences in ridge density between canids and felids. The full code for all analyses is available at https://github.com/anagkrish/cat_dog_mem and a permanent repository at https://zenodo.org/records/16172335.

Figure S9 presents results from standard methods for assessing the appropriateness of the PGLMM statistical model for ridge density presented in the previous subsection. Collectively, these results indicate that the linear modeling assumptions of our method are satisfied.

Potential Limitations

The continuous time movement models we used to delineate individuals' home ranges assume both a random movement process and statistical stationarity of the process. The random movement assumption could be violated if physical features of landscapes constrain movements in ways not represented in *ctmm* models. For example, margays (*Leopardus wiedii*), which routinely hunt arboreally, may be influenced by tree-to-tree connectivity, while snow leopard (*Panthera uncia*) movement may reflect coarser-scale physical constraints in some areas (19,26).

The stationarity assumption could be violated if carnivores exhibit spatial biases in their rates and linearity of movement in some conditions (e.g., wolves will follow forest roads in winter (17)). If our assumptions are broadly violated, the most generic interpretation of our results would be that canids exhibited greater ridge density in our study because they make more structured movements through landscapes.

Sample Code

Here we present sample R code and output for phylogenetically controlled mixed model analysis using a version of the package *metafor* specifically modified for this purpose. In this example, we use the best-fitting mixed model for the full dataset of 1239 individuals, which are spread across 34 species. Ridge density was modeled as

```
#setting up random effects
random <- list(~ 1|phylo, ~ 1|point)
 # these will be the only fitted variances in metafor, the latter is a normal regression error (not
included by default) that addresses the influence of radically different sample sizes per species
R <- list(phylo=ph_corr)

#fixed effects
mods <- ~ log_mass_st + pursuit + disruptfast + slowwalking + log_hr_st + inv_ess +
log_roughness_st + mean_treecover + mean_hfi + seasonality_dhi_gpp_st

#model call
FIT <- metafor::rma.mv(log_ridge,V=0,mods=mods,random=random,R=R,data=ridge)
```

This model yielded output of :

```
Multivariate Meta-Analysis Model (k = 1239; method: REML)

   logLik   Deviance        AIC        BIC       AICc
-376.7287   753.4574   779.4574   845.9282   779.7572

Variance Components:

            estim    sqrt  nlvls  fixed  factor    R
sigma^2.1  0.4129  0.6426     34     no   phylo  yes
sigma^2.2  0.1033  0.3214   1239     no   point   no

Test of Moderators (coefficients 2:11):
QM(df = 10) = 326.1984, p-val < .0001

Model Results:

                        estimate      se      zval    pval    ci.lb    ci.ub
intrcpt                   4.6862  0.5092    9.2026  <.0001   3.6881   5.6843  ***
log_mass_st              -0.0339  0.0538   -0.6308  0.5282  -0.1393   0.0715
pursuit1                 -0.2373  0.1444   -1.6439  0.1002  -0.5203   0.0456
disruptfast1              0.0141  0.0903    0.1558  0.8762  -0.1629   0.1910
slowwalking1             -0.2295  0.1093   -2.1001  0.0357  -0.4437  -0.0153    *
log_hr_st                -0.0791  0.0194   -4.0691  <.0001  -0.1172  -0.0410  ***
inv_ess                  -4.6404  0.3569  -13.0013  <.0001  -5.3400  -3.9409  ***
log_roughness_st         -0.0298  0.0133   -2.2514  0.0244  -0.0558  -0.0039    *
mean_treecover           -0.0668  0.0437   -1.5311  0.1257  -0.1524   0.0187
mean_hfi                 -0.0968  0.0783   -1.2355  0.2166  -0.2503   0.0567
seasonality_dhi_gpp_st   -0.0120  0.0178   -0.6765  0.4987  -0.0469   0.0228

---
Signif. codes:  0 ‘***’ 0.001 ‘**’ 0.01 ‘*’ 0.05 ‘.’ 0.1 ‘ ’ 1
```

In the above output, sigma^2.1 represents the effect of the overall phylogenetic variation and sigma^2.2 represents the random effect of differential sampling across species. With an estimated effect of 0.4129, the magnitude of the phylogenetic variation is much stronger than all of the fixed effects except effective sample size (ESS), which we use as a bias correction term accounting for differences in GPS track quality. Home range size, the slow-walking categorical strategy of hunting movement, and terrain roughness were also all significant as predictors of ridge density.

The next step in the analysis uses the fitted mixed effects model to resolve the overall phylogenetic effect into a specific test of a clade-level difference between canids and felids. We used the custom *ranef2()* function to extract both the predicted random effects and their covariance matrix, which is not a user feature of *metafor.* With this information we calculated optimal predictions of the clade differences.

The code to estimate a clade-level effect was

```
EFF <- ranef2(FIT)$phylo
REST <- EFF$est # random effects
RCOV <- EFF$COV # error covariance

CANINE <- ridge$clade=="canidae"
CANINE <- unique(ridge$phylo[CANINE])
FELINE <- ridge$clade=="felidae"
FELINE <- unique(ridge$phylo[FELINE])

iCOV <- ctmm:::PDsolve(RCOV) # safe matrix solver
dW.dl <- iCOV %*% cbind( names(REST) %in% CANINE , names(REST) %in% FELINE )
M <- rbind( colSums( dW.dl[CANINE,] ) , colSums( dW.dl[FELINE,] ) )
lambda <- c( solve(M) %*% c(1,-1) )
W <- c(dW.dl %*% lambda)
names(W) <- rownames(dW.dl)

# W[CANINE,] # check +1
sum(W[CANINE])
#
# W[FELINE,] # check -1
sum(W[FELINE])

# point estimate
DIFF <- c(W %*% REST)
VAR.DIFF <- c(W %*% RCOV %*% W)

# relative impact on ridge density (back transform)
ctmm:::norm.ci(DIFF, VAR.DIFF)  # normal confidence intervals
exp(ctmm:::norm.ci(DIFF, VAR.DIFF))
```

This analysis concluded that, on average, home ranges of canids featured ~15% (95% CI: 8 - 22%) greater ridge density than did home ranges of felids, after fully controlling for species-level traits (body mass, movement strategies), and individual-level variation in home range size, the effective sample size of the movement tracks, and spatial environmental covariates (terrain roughness, tree cover, human footprint index, and seasonality of gross primary production). The output was

```
> ctmm:::norm.ci(DIFF, VAR.DIFF)
       low        est       high
0.07923327 0.13974562 0.20025798
>  exp(ctmm:::norm.ci(DIFF, VAR.DIFF))
     low      est     high
1.082457 1.149981 1.221718
```

Potential artifacts due to database structure and potential sources of bias due to statistical estimation.

The dataset we aggregated for this analysis reflects diverse forms of heterogeneity that have the potential to impact our results, either directly or through interactions with potential sources of bias in our statistical estimation procedures. We addressed the most straightforward of these potential problems through our analyses of the DNA Only, Speed Included, No Preprocessing, Shared Landscapes, and Year or Longer subdatasets. In this section we report on 1) the potential biases leading up to decision to analyze the Year or Longer subdataset, 2) the potential for 'false positive' probability ridges due to finite sampling effort when ridges should not exist in a Null Model, 3) our ability to reconstruct both the location and the length of probability ridges when they are known to exist analytically in a Alternative Ridge Model, 4) a comparison of results among the Null Model, the Alternative Ridge Model, and the empirical datasets, and 5) suggestions for future improvements to our methods.

1) *Potential phenological biases leading up to the Year or Longer subdataset*.

Phenological biases in the availability of GPS tracks could potentially affect our results. For example, if individual animals exhibited strongly divergent space use at different times of the season, and the available GPS data only reflected a portion of the annual cycle that was unrepresentative of the rest of the year, then the location and extent of probability ridges in the home range distributions could be biased or incomplete.

To address this possibility, we used circular statistics approaches to characterize the availability of GPS track data by day of year for the dataset as a whole and for each species separately. At the level of the whole dataset, canids and felids were nearly identical in the seasonal availability of movement data, with slightly more felid data available between January and April and slightly more canid data available between June and December (Fig. S9).

At the species level, seasonal data availability for wolves (*Canis lupus*) and cougars (*Puma concolor*) was most circularly uniform in their respective clades, so these species served as reference points for comparisons (Fig. S10). In contrast, data for Arctic foxes (*Vulpes lagopus*) exhibited the most extreme divergence from complete annual availability, mostly due to the seasonality of Arctic field work combined with the short life of batteries allowing high-intensity GPS tracking. Among canids, dhole (*Cuon alpinus*) and crab-eating fox (*Cerdocyon thous*) exhibited lesser degrees of seasonal asymmetry in data availability. Seasonal asymmetry was less extreme among felids overall, with ocelot (*Leopardus pardalis*) and margay (*Leopardus wiedii*) exhibiting the strongest divergence from circularity (Fig. S10).

Ultimately, to ensure that any clade-level effects we found in the full dataset were not due to phenological differences across GPS tracks, we extracted and analyzed a reduced subdataset consisting only of those individuals whose GPS tracks had durations > 1 year (n = 342). Results from analyses of this 'year or more' subdataset were broadly consistent both qualitatively and quantitatively with results from the full dataset (Figs. 3B, S1, S7).

2) Potential for 'false positive' probability ridges due to finite sampling effort when they should not exist in a Null model

To demonstrate the performance of our methods when probability ridges should not exist, we consider the case of a stationary Gaussian stochastic process as a Null Model. A Gaussian stochastic process is a stochastic process (a collection of random variables indexed by time or space) such that any subset of those random variables is jointly Gaussian. A Gaussian

stochastic process can be completely defined by its mean and (kernel) covariance functions, and (in two dimensions) the stationary distribution of a stationary Gaussian stochastic process is simply a two-dimensional Gaussian distribution *(83)*. Mathematically, this definition means that the stationary (i.e., asymptotic) distribution of a stationary Gaussian stochastic process has no probability ridges. Consequently, when one estimates a home range from a finite set of points produced by a stationary Gaussian stochastic process, any probability ridges identified by *ctmm* from that home range are false positives. In our parlance, such false positives would indicate the presence of a movement routeway when in fact there was none from a statistical perspective. For example, false positives of probability ridges could occur for a stationary Gaussian stochastic process whose estimated distribution deviated in some way from the corresponding stationary distribution as a result of finite sampling effort.

We used the R package *ctmm* to create 6 sets of 100 sequences of points sampled from a stationary OUF (Ornstein-Uhlenbeck with Foraging) Gaussian stochastic process *(4)*. These sets of sequences varied with respect to temporal duration as a gauge of the completeness of sampling effort relative to what would be expected from the stationary distribution. In all cases, we would expect to find probability ridge lengths equal to zero in the corresponding stationary distributions, but we might in reality find very low probability ridge lengths due to artifacts evident in the sample sequence due to finite sampling effort. Such false positives would be predicted to decrease toward zero with increasing sampling duration.

Parameter values chosen for these simulations agree with those estimated from the empirical movement tracks. To explore the effect of short duration, we simulated from an OUF model with 24 samples/day (comparable to our dataset, which had min-average-max of 1-82-1440 locations/day, respectively), τ_v= 43200 seconds (comparable to our dataset, which had min-average-max of 0-2376-86678 seconds, respectively), and the duration ranging from 32 to 1024 days (comparable to our dataset, which had min-average-max of 30-294-3612 days, respectively).

Our Null Model results (Table S5) matched our predictions, indicating that our methods do not identify false positive probability ridges in the absence of a movement model except for understandable small effects (probability ridge lengths of ~2 - 12km) that arise due to the

effects of finite sampling effort. We show below how small these estimated lengths are compared to an Alternative Ridge Model where ridges should exist, and compared to our empirical data.

Table S5 illustrates that the false positive probability ridge length due to finite sampling effort was as a function of track duration, and that false positives were greatest for tracks with the shortest durations. We note that, for our analyses, 1) we only considered tracks of at least 30 days duration, and 2) we have already controlled for variation in track duration (and concomitant effects on false positive ridge density) through our inclusion of the predictor variable ESS (effective sampling size, a measure that includes effects due to varied track duration (3) in all of our comparative statistical analyses.

Figure S11 provides an illustration of probability ridges that emerge as artifacts of finite sampling in our Null Model consisting of an OUF Gaussian stochastic process in the absence of a movement model. Note that the probability ridges artifactually evident due to finite sampling size are small and scattered across the distribution range. They look nothing like the probability ridges observed in our empirical datasets (Figs. 1-2 from the main text).

3) Reconstructing the location and length of probability ridges when they are known to exist analytically in an Alternative Ridge Model

To demonstrate the performance of our methods when probability ridges are known to exist, we require a case where the expected length of probability ridges in a home range can be determined analytically for the case of finite sampling effort. We do this for the case of an Alternative Ridge Model involving a periodic OUF process with circular motion that approximates a maned wolf, *Chrysocyon brachyurus,* patrolling a territorial boundary *(84)*.

Asymptotically, this type of routeway-based motion yields a stationary distribution consisting of an annular 2D probability density function aligned around a circular path of known location that specifies the center of the animal's patrolling effort. Stochasticity around

this circular path creates a wider routeway of movement. Moreover, in the stationary distribution of the Alternative Ridge Model, there should exist a single, circular probability ridge that extends along the ridgetop of the aforementioned annular PDF and corresponds in space to the location of the known circular route. The length of this single probability ridge should match the perimeter of the underlying known circular route (subject to the effects of finite sampling effort), and this length will be determined by the parameters that control the periodic motion. It turns out that the length of this circular probability ridge can be calculated exactly by means of Bessel Functions. This means that we can directly compare the probability ridge lengths calculated for a finite dataset against the precise probability ridge lengths expected analytically for the corresponding stationary distribution. This creates an analytical baseline for assessing the method's performance in identifying ridges when they are known to exist. (Unfortunately, an analytical estimate of the expected ridge density is not calculable, but we can make the point easily enough using ridge length.)

The stationary probability density function for a 2-dimensional OUF stochastic process that follows a circular movement route of radius μ with standard deviation σ is expected to be symmetric with respect to the origin. The probability p at radius r can be expressed as

$$p(r,0) = \frac{1}{2\pi}\int_0^{2\pi} d\theta \, \frac{1}{2\pi\sigma^2} e^{-\left(\frac{(r-\mu cos\theta)^2+\mu^2 sin^2\theta}{2\sigma^2}\right)}$$

$$= \frac{1}{(2\pi)^2\sigma^2}\int_0^{2\pi} d\theta \, \frac{1}{2\pi\sigma^2} e^{-\left(\frac{r^2-2r\mu cos\theta+\mu^2}{2\sigma^2}\right)}$$

$$= \frac{1}{(2\pi)^2\sigma^2} e^{-\left(\frac{r^2+\mu^2}{2\sigma^2}\right)}\int_0^{2\pi} d\theta \, e^{\left(\frac{r\mu cos\theta}{\sigma^2}\right)}$$

$$= \frac{1}{2\pi\sigma^2} e^{-\left(\frac{r^2+\mu^2}{2\sigma^2}\right)} I_0\left(\frac{r\mu}{\sigma^2}\right)$$

in terms of the modified Bessel function I_α of order α (here zero). Given the circular movement process, we anticipate that the probability ridge atop the distribution of space use will also be annular in structure, and we next estimate the location of a probability ridge $\hat{r}$ where the probability distribution reaches a peak at $p(\hat{r},0)' = 0$. Taking the derivative, we have

$$0 = \frac{-2r}{2\sigma^2} I_0\left(\frac{r\mu}{\sigma^2}\right) + \frac{\mu}{\sigma^2} I_0'\left(\frac{r\mu}{\sigma^2}\right).$$

Simplifying, we have

$$r I_0\left(\frac{r\mu}{\sigma^2}\right) = \mu\, I_0'\left(\frac{r\mu}{\sigma^2}\right) = \mu\, I_1\left(\frac{r\mu}{\sigma^2}\right).$$

The Modified Bessel Functions can be evaluated numerically. When the variance in the movement process is non-negligible, we have asymptotically,

$$\frac{r}{\mu} = \frac{I_1(z)}{I_0(z)} = \frac{1 - \frac{3}{8z} + \ldots}{1 + \frac{1}{8z} + \ldots} \quad \text{for} \quad z = \frac{r\mu}{\sigma^2}$$

which limits to

$$r = \mu + \cdots$$

in the low noise case. For $\mu/\sigma < \sqrt{2}$ the probability density function (PDF) is unimodal, with one mode at the origin. For $\mu/\sigma = \sqrt{2}$ the PDF is degenerate, with a flat plateau at the origin. For $\mu/\sigma > \sqrt{2}$, the PDF has a circular ridge around the origin.

We used the R package *ctmm* to sample 6 sets of 100 sequences of points from an OUF Gaussian stochastic process with a circular movement model. These sets of sequences varied with respect to temporal duration, sampling frequency, and the timescale over which velocity was autocorrelated (τ_v) *(3)*. Provided $\mu/\sigma > \sqrt{2}$, we would expect to find that the probability ridge lengths evident in the sampled datasets were far from zero because the stationary distribution of the Alternative Ridge Model will always have a probability ridge corresponding to the location of the underlying circular movement path. The length of the probability ridges calculated for a given sampled sequence of points—and consequently the density of probability ridges—should vary, perhaps considerably, away from the expected value depending on the particular locations sampled and how those sampled locations influence the position of probability ridges in the range PDFs developed from the sampled tracks. We expect to see greater deviation away from the analytically determined probability ridge length values for simulated movement tracks that are of short duration.

We again considered the effect of track duration as a measure of dataset incompleteness, yielding an estimated distribution that deviated from the stationary distribution. To do this, we simulated from an OUF model with 24 samples/day (comparable to our dataset, which

had min-avg-max of 1-82-1440 locations/day, respectively), τ_v= 3600 seconds (comparable to our dataset, which had min-avg-max of 0-2376-86678 seconds, respectively), and the duration ranging from 32 to 1024 days (comparable to our dataset, which had min-avg-max of 30-294-3612 days, respectively). In this example, because $\mu/\sigma > \sqrt{2}$, the stationary distribution of the stochastic process includes a probability well, and the mean path forms a circle with perimeter ~6.28 km, which adjusts downward to a ~ 5.94 km ridge when accounting for the effects of stochasticity in the above derivation. In this Alternative Ridge Model, the anticipated value for our statistical estimation method is thus 5.94km times a factor of ~2 (for the computational aliasing artifacts discussed previously) plus the false positive estimation error due to finite sampling effort (see Table S5).

Our results for probability ridge length (km) (Table S6) generally matched our predictions, indicating that our methods consistently identify the existence of probability ridges at levels well away from zero when an underlying movement route is known to exist. Furthermore, our results demonstrate that the average value of the 100 simulations for each parameter combination approximates the specific value of probability ridge length expected on the basis of the analytical formula presented above. Artifacts due to finite sampling effort again underlie any deviations from the analytical expectations.

Figure S12 illustrates a range distribution calculated for an animal that stochastically patrols a region following a circular movement route via a Periodic OUF stochastic process. The circular movement route (which corresponds to the location of the single probability ridge) appears in panel A. The probability density function calculated from a finite sampled trajectory appears in panel B, along with the probability ridges estimated from this finite trajectory.

4) Comparison of results among the Null Model, the Alternative Ridge Model, and the empirical datasets

Figure S13 contrasts results from the Null Model, the Alternative Ridge Model, and the empirical datasets, demonstrating three important features. First, the ridge lengths calculated

from the individual-level empirical movement tracks substantially exceeded the low false positive values obtained from the Null Model (a stationary OUF process that lacked a movement model) (see Figure S11). These findings suggest that the probability ridges we identified in the empirical tracking datasets are real features of the animals' home range distributions rather than sampling artifacts. Second, the ridge lengths calculated from the individual-level empirical movement tracks were at least comparable to (and often greatly exceeded) those of the Alternative Ridge Model in which a known routeway was present (see Figure S12). The fact that the empirical ridge lengths exceeded those of the Alternative Ridge Model is expected because the real home range distributions exhibited substantially more complexity than would be expected in the case of the Alternative Ridge Model that was simple enough for an analytical calculation. Third, the relationships among the Null Model, the Alternative Ridge Model, and the empirical datasets were consistent regardless of whether we considered ridge length or ridge density.

5) Suggestions for future improvements to our statistical methods.

In calculating our area and ridge length estimates, we optimized the bandwidth for probability density estimation (11), but we did not invoke the area bias correction of (12), because it increased the numerical errors in the gradient and curvature calculations required for ridge estimation. An improved analysis would (a) include the bias correction for area estimation, but not for ridge estimation, and (b) optimize the bandwidth in three different ways — once for density estimation, once for gradient estimation, and once for curvature estimation, with the first for area estimation and the latter two for ridge estimation. In the context of mode estimation via KDE on independently sampled data, convergence can be optimized by minimizing the mean integrated square error of the gradient of the density function rather than the density function itself *(85)*. It should be a straightforward yet involved derivation to generalize the results from (11) to the gradient and curvature of the density function with autocorrelated data.

Supplemental discussion of particular species and natural history topics.

Species found in multiple landscapes.

The full dataset included GPS movement tracks for 11 species—six canids and five felids—that were each studied in at least 3 different landscapes. Table S3 provides detailed information about the studies used in this cross-landscape investigation and Fig. S2 presents ridge density data for all species x landscape combinations. Some tropical savannas include seasonally flooded grasslands.

Natural history pertaining to carnivore routeway usage and navigation

Published literature includes several mentions of felid species preferentially moving through their range on trails (including *Felis silvestris* (33), *Leopardus geoffroyi* (34), *Leopardus pardalis* (35), *Leptailurus serval* (36), and *Lynx rufus* (37)), and these species exhibited some of the highest ridge-associated probability mass in their family (Fig. S6).

In some species and landscapes, trails or navigational waypoints facilitating movement are persistent (or even actively maintained) among individuals and across generations via physical or chemical means (38-39). Whether ridge density and maps of ridge locations are similar across individuals residing in specific locations could be investigated in those species where territories are inherited after a resident dies (40).

Untested Alternative Interpretations

Limited evidence for magnetic cues exists in canids, which has been hypothesized to affect their foraging, orientation, and homing (41-42). However, questions about the generality and importance of these factors persist (43), raising questions about the potential of magnetic cues to assist in home range scale movements. No evidence yet suggests that any magnetic responsivity present in canids is as profound an adaptation as the well-known examples of magnetoreceptive animal migration (44) and tunneling (45). For felids, data regarding magnetoreception is apparently not available (43), but examples of long-range homing do exist (46), though these could involve non-magnetic cues (e.g., sun, polarized starlight, olfactory cues, landmarks).

Denning activity is common in both canids and felids, and would concentrate individuals' movements in a spatial area. However, unless individuals routinely used specific routes to access and leave a den site over an extended distance, denning would primarily result in a local probability peak (i.e., a statistical mode) in a home range distribution rather than a probability ridge. Data on the spatial locations of dens were not available for many individuals either due to the seasonality of the movement track (SI Potential phenological biases) or because it was not possible to systematically identify den sites by ground-truthing given the remote nature of many field sites. Communal latrines, including latrines used by multiple species, are another important part of carnivores' space use (47-50), but again such features would most likely yield modes rather than ridges within home range distributions.

Comments on species-level ridge density estimates

Three canid species (wolves, dhole (*Cuon alpinus*), and African wild dogs (*Lycaon pictus*)) exhibited lower mean ridge densities similar to average felids (Fig. S4). These three canids regularly hunt in groups and use a complex division of roles during hunting (24,25), traits that could influence their use of space through group-level decision-making. However, other canids that routinely (*Canis aureus*) or facultatively (*Canis latrans, Lupullela mesomelas, Cerdocyon thous*) hunt cooperatively did not have low ridge densities, and lions (*Panthera leo*), famed for their cooperative hunting, exhibited ridge densities no different than their solitarily hunting congeners (Fig. S3). Because sociality is not strongly connected to cognition in carnivores (51,52), an alternative interpretation would eschew cooperativity in favor of an explanation linked to the high metabolic and energetic costs of hyper-carnivory (53,54), a feeding trait that *C. lupus* (in many regions), *C. alpinus*, and *L. pictus* share with many felids, but not with several other canids that are more omnivorous. In contrast, two felid species (servals (*Leptailurus serval*) and jungle cats (*Felis chaus*)) had higher ridge densities more similar to average canids (Fig. S3). Upward deviations in ridge density for these two felids could be due to unmodeled environmental variables or differences in diet breadth. For example, jungle cats and servals have wide diet breadth (55,56), even within individuals, which could necessitate a more complex set of re-used travel routeways within their home ranges compared to other felids that have more specialized diets. Other, undiscovered aspects of these two species' behavior may also distinguish their reliance on re-used routeways from those of other wild felids.

Original funding for sources for the animal tracking data synthesized in this paper.

Original funding was provided by: the University of Washington Royalty Research Fund, Washington Research Foundation, Federal Aid in Wildlife Restoration Act, Safari Club International Foundation, and Safari Club International Michigan Involvement Committee; Canada Foundation for Innovation (no. 11578), the Natural Sciences and Engineering Research Council of Canada (no. 227080-2009, and the NSERC Discovery Grant Programme (to EHM), the Network of Centers of Excellence of Canada ArcticNet (no. 2007-WILDLIFE), Oregon Department of Fish and Wildlife and Federal Aid in Wildlife Restoration (Pittman-Robertson), the Army Public Health Center; Albert-Heim-Stiftung, Basler Stiftung für Biologische Forschung, Georges and Antoine Claraz Foundation, National Geographic Society, Parrotia-Stiftung, Stiftung Temperatio, Wilderness Wildlife Trust, Forschungskredit of the University of Zurich (no. FK-21-091), a Swiss National Science Foundation Grant (no.31003A_182286) to A. Ozgul, a Swiss National Science Foundation Grant (no. S-74334-06-01 to GC, and nos. 31003A_182286 and 310030_204478, Woolworths Holdings Limited, Conservation South Africa, The Cape Leopard Trust, ICMBio, Smithsonian Conservation Biology Institute, Morris Animal Foundation, Habitat Conservation Trust Foundation, Canada Foundation for Innovation, BC Ministry of Forests, World Wildlife Fund-Nedbank Green Trust (grant GT2251), the Institute for Communities and Wildlife in Africa (iCWild), the People's Trust for Endangered Species (PTES), Zoologische Gesellschaft für Arten- und Populationsschutz (ZGAP), Iranian Cheetah Society, Quagga Conservation Fund, Idea Wild and Association Francaise des Parcs Zoologiques (AFdPZ), US Army Corps of Engineers, Fort Drum Army Base, Schleswig-Holstein Agency for Coastal Defense, National Park and Marine Conservation – National Park, the Nationalpark Administration Lower Saxony, Wilhelmshaven, NIH (grant no. GM83863 to WMG), Etosha Ecological Institute at the Namibian Ministry of Environment and Tourism, Parks Canada, Alberta Fish and Wildlife, NSF LTREB grant (nos. 1556248 and 2038704), the Joint Russian-Mongolian complex biological expedition of the Russian Academy of Sciences, the Academy of Sciences of Mongolia, Russian Geographical Society, Ministry of Nature Resources Foundation, UNDP, WWF-Russia, National Science Foundation (BCS 99-03949 and BCS 1266389), LSB Leakey Foundation, Committee on Research, University of California, Davis, EU Horizon 2020 grant (nos. 641918 – AfricanBioServices), ARK Natuurontwikkeling,

Province of Limburg, United States Department of Defense, the Fort Bragg Wildlife Branch, the Fisheries, Wildlife, and Conservation Biology Program at North Carolina State University, Smithsonian Tropical Research Institute, National Geographic, San Diego Zoo Wildlife Alliance, Hessisches Landesamt für Naturschutz, Umwelt und Geologie (no. 15 b – 09 06/538 00/Zuw. Wildkatze) and RP Giessen (no. V-22b0500/90-2019/1), NSERC Integrated Landscape Management Chair, Petroleum Technology Alliance Canada, and the Alberta Conservation Association, Minnesota Zoo, Taronga Zoo, Point Defiance Zoo Society, United States Department of Agriculture, Utah State University, the Welder Wildlife Foundation, Texas Parks & Wildlife Department, USFWS Wildlife Restoration Grant no. W139T2-4, contributions of Texas Parks & Wildlife Department volunteers, Estonian Environmental Investment Centre, Fundação de Amparo à Pesquisa do Estado de São Paulo - FAPESP (no. 2013-10029-6 and 2013/50421-2), Cat Heaven Endangered Species-Project Survival, Dallas World Aquarium, Orient Express Hotels do Brasil, WWF Switzerland-Fundacion Vida Silvestre Argentina, Panthera Foundation, Rufford Small Grant Foundation, CNPq (Brazilian Government Research Council) via a research grant for Milton Cezar Ribeiro (no. 312045/2013-1), Research Council of Norway (grant nos. 251112, 281092, and 156810), the Norwegian Directorate for Nature Management, the Nature Protection Division of the County Governor's Office for Innlandet, Viken, Vestfold & Telemark, Trøndelag, Nordland, Troms & Finnmark County, Projeto Raposinha do Pontal/Juscelino F. Martins, Fundação Parque Zoológico de São Paulo, Cleveland Metropark Zoo, Neotropical Grassland Conservancy, Consórcio Capim Branco de Energia; HIDROEX (UNESCO/BID), Jaguar Land Rover España, Earthwatch Institute, Field Museum of Natural History, the Mohamed bin Zayed Species Conservation Fund, Panthera's Kaplan Graduate Award Program, Liz Claiborne and Art Ortenburg Foundation, Save the Tiger Fund, United States Fish and Wildlife Service Tiger Rhino Conservation Fund, University of Montana, Wildlife Conservation Society, NSF grant no. DEB-1652420 to LRP, University of KwaZulu-Natal, University of Nebraska Collaborative Research Initiative, Australian Wildlife Conservancy, Australian Government's National Environmental Science Program through the Threatened Species Recovery Hub, Foundation Segre, generous donors including Arkadaşlar, Bilge Bahar, Faruk Eczacıbaşı, Seha İşmen, Ömer Koç, Ömer Külahçıoğlu, Burak Över, Batubay Özkan, Emin Özgür, Suna Reyent, Faruk Yalçın Zoo, National Geographic Society, Sigrid Rausing Trust, STGM and TANAP, H. Batubay Özkan and Barbara Watkins, the

Biodiversity and Conservation Ecology Lab at the University of Utah School of Biological Sciences, Türkiye Department of Nature Conservation and National Parks and the Ministry of Agriculture (grant nos. 72784983-488.04-114100), the KuzeyDoğa Society, the Claude Leon Foundation, the University of Cape Town Research Council, Botanica Wines, Stellenbosch University, the National Research Foundation, Wildlife ACT, the City of Cape Town, Experiment, Big Cat Rescue, Peninsula Open Space Trust, Land Trust of Santa Cruz County, California Department of Fish and Wildlife, Santa Clara Open Space Authority, Prociencia 14-inv-208 from CONACYT Paraguay, Wellcome Trust DBT India Alliance Fellowship (no. IA/CPHI/15/1/502028 to ATV), an ISRO-IISc Space Technology Cell grant to MT, Swedish Nature Protection Board (no. DNR 15/155), Swedish Hunters Association (no. 5861/2016), Karl Erik Önnesjös Stiftelse, Sweden, and the Norwegian Directorate for Nature Management (grant nos. 13F6CC7, 15SA0283, 16SA3A43) and the Gotaas Fund, Norway (no. 13/00282), NSF grant (nos. 0963022 and 1255913), the Gordon and Betty Moore Foundation, Panthera, the UNDP GEF Small Grants Programme, MAS HoldingsLinea Intimo, The Leopard Trust—Sri Lanka, and numerous private donors.

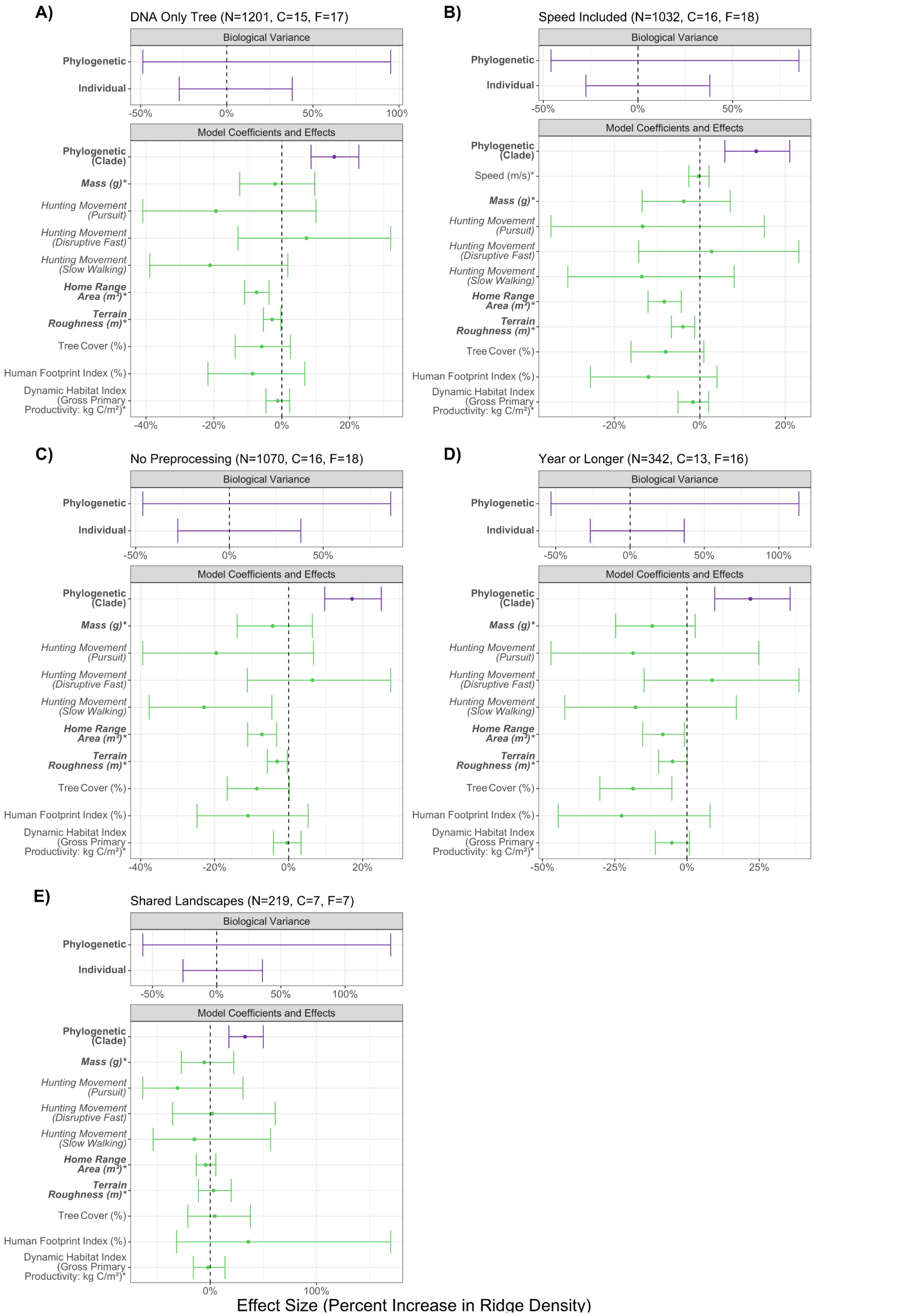

Figure S1. Effect size plots for ridge density for all subdatasets. Continuous variables were standardized so that the effect size corresponds to 1 standard deviation of the predictor, whereas for a variable expressed as a percentage, the effect size corresponds to the full effect of that predictor at 100%. Predictors in bold font and purple plotting represent biological variation, and the plots labeled Phylogenetic and Individual are prediction intervals. The plotting labeled Phylogenetic (Clade) is part of the overall phylogenetic variation, but it is expressed as a mean and confidence interval alongside other model coefficients. Model covariates are in green, including indicator variables (italics), variables log transformed for analysis (bold-italics), and standardized variables (asterisk). Effect size plots for the full dataset appear in Fig. 3A. Labels N, C, and F are the number of individuals, canid species, and felid species, respectively.

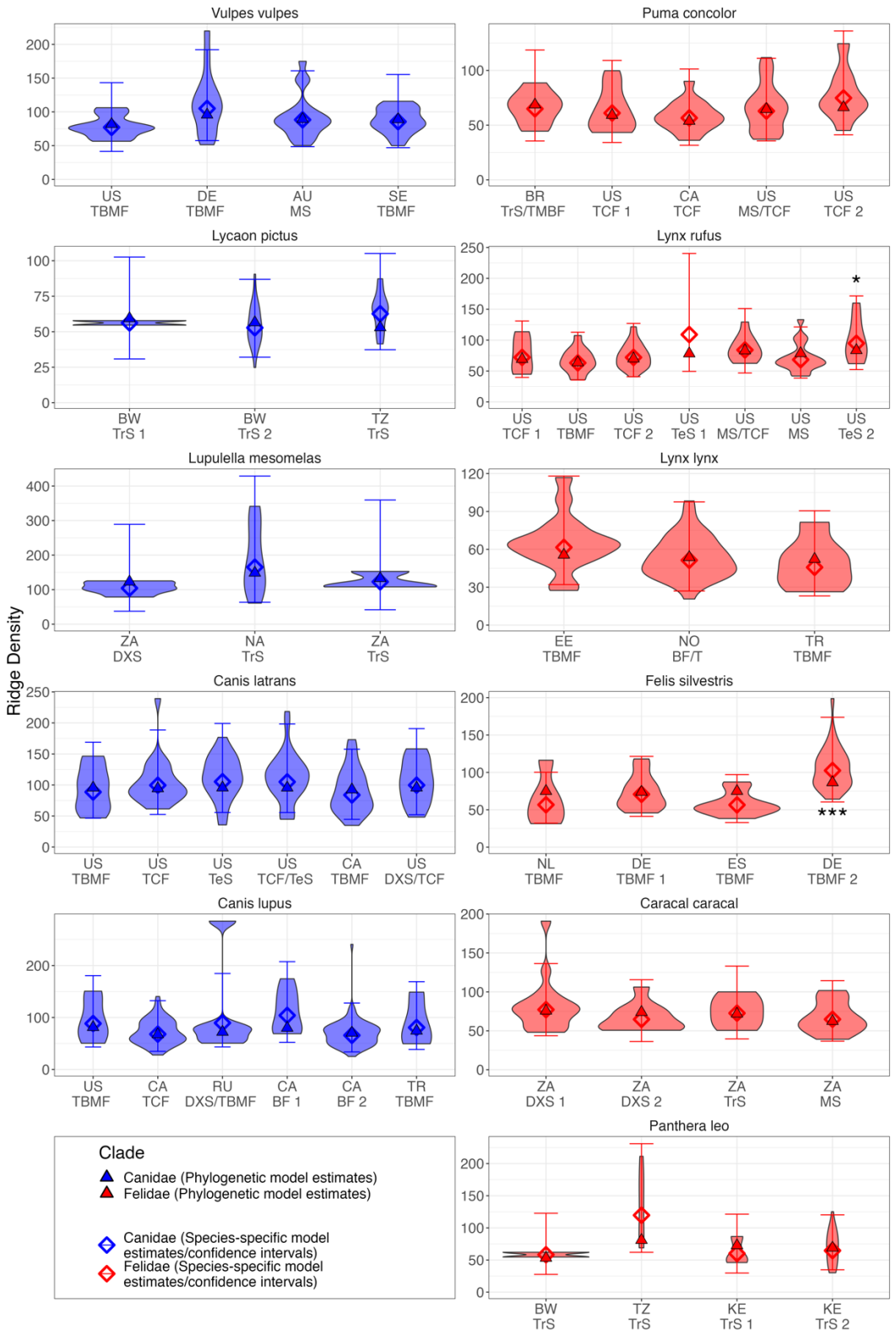

Figure S2. Empirical and fitted ridge densities for canid and felid species occurring in multiple landscapes. For each species × study site combination, the plot includes a violin plot of the empirical ridge density data (colored shapes), the predicted means from the full model (solid triangles), and the mean (±95%CI) estimates from a species-specific model (open diamonds). X-axes labels provide the Alpha2 country abbreviation (top row) and the biome (bottom row). Biomes (57), are: temperate broadleaf and mixed forest (TBMF), temperate coniferous forest (TCF), boreal forest (BF), tundra (T), tropical savanna (TrS), temperate savanna (TeS), tropical moist broadleaf forest (TMBF), Mediterranean scrub (MS), and desert and xeric scrublands (DXS). Asterisks (* $p < 0.05$, *** $p < 0.001$) identify the two instances in which a species studied in one landscape differed from the other landscapes for that species.

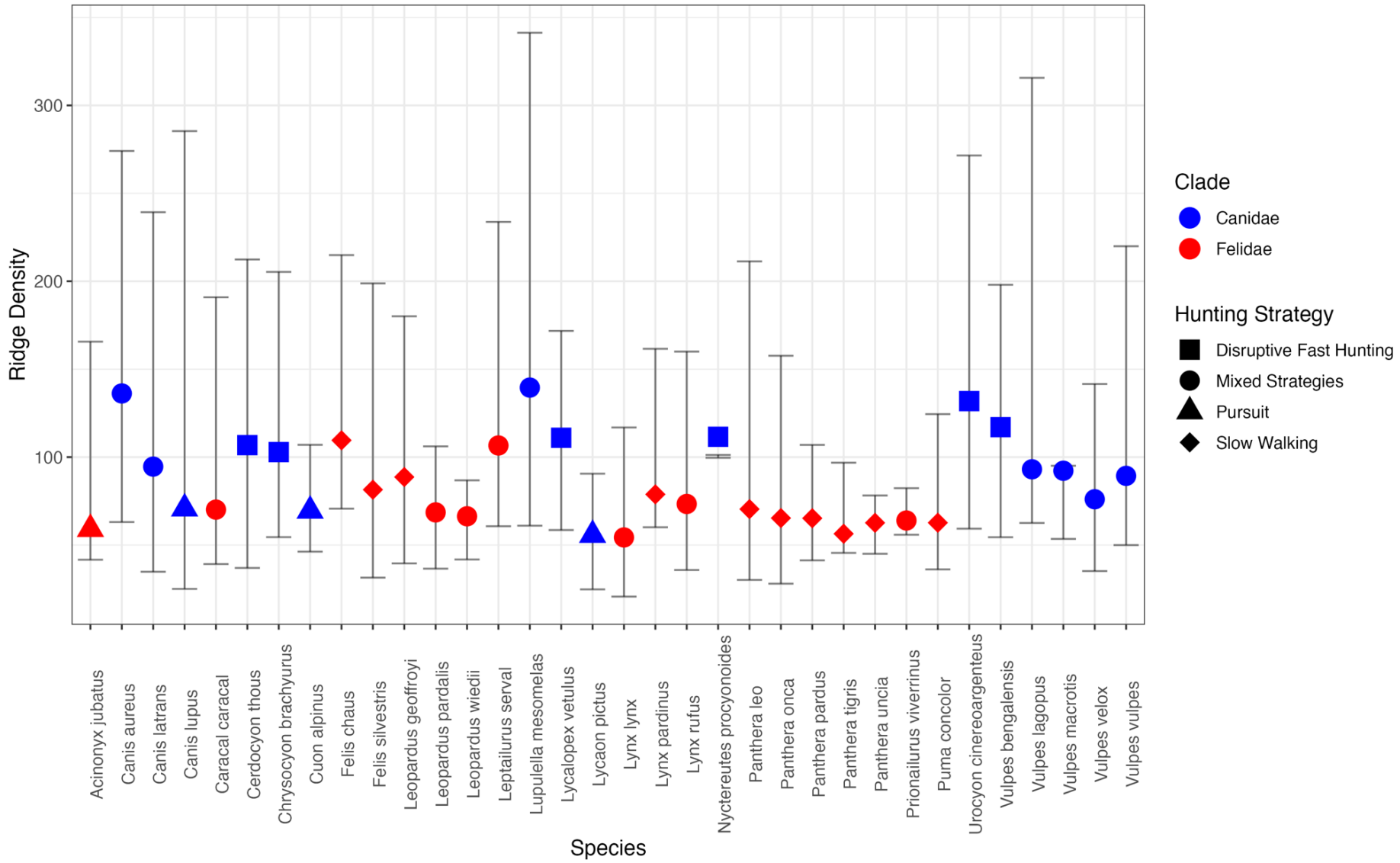

Figure S3. Empirical range of ridge density (vertical bars) and corresponding model-predicted means (symbols), labeled by clade (color) and movement strategy while hunting (shape) (see Tables S1, S2). The label 'Mixed strategies' indicates evidence of two or more strategies for movement while hunting.

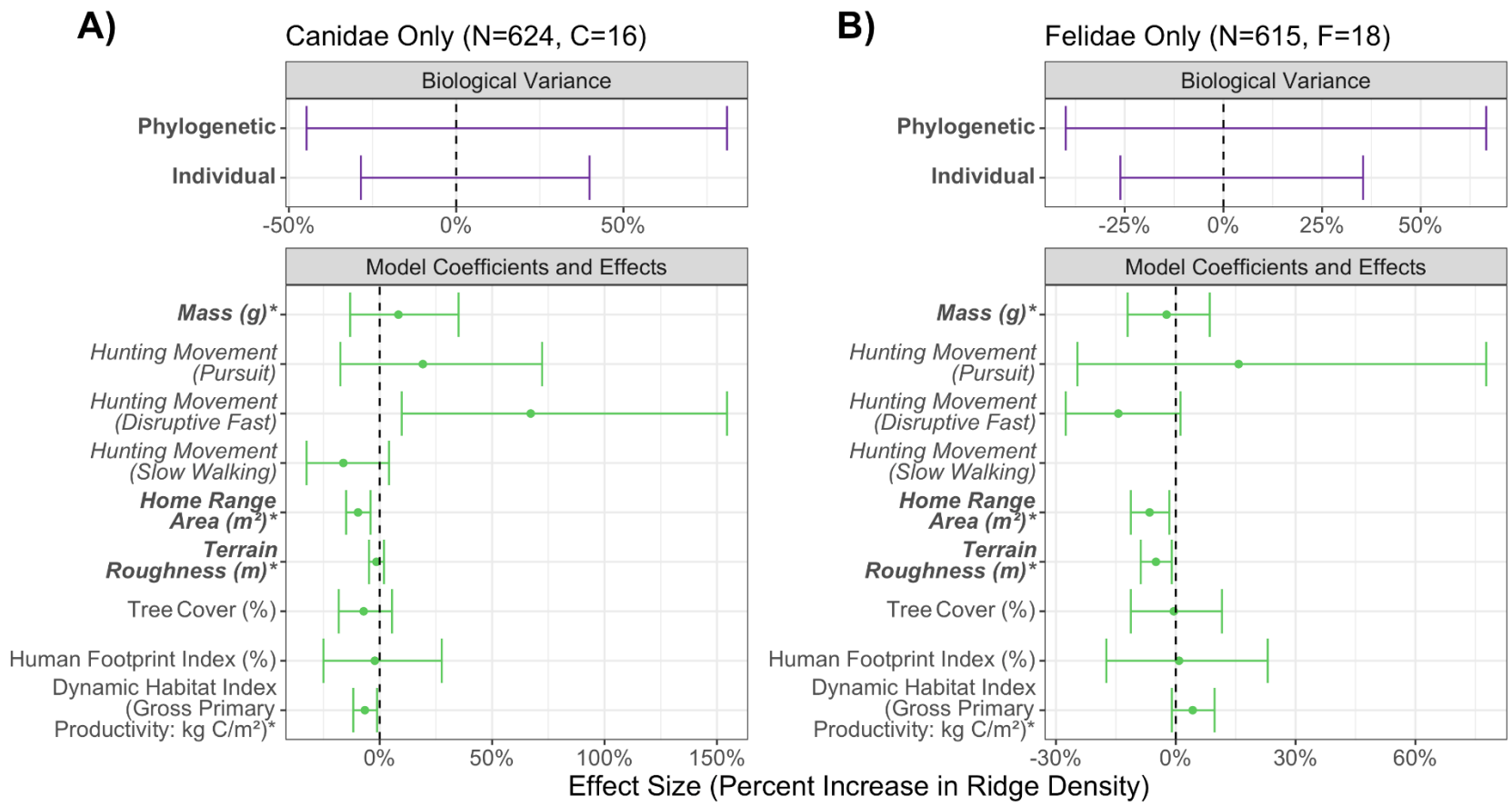

Figure S4. Effect size plots for ridge density of canids (A) and felids (B) analyzed separately, which represents an analysis comparable to placing all covariates in interaction with the clade-level effect in Fig. 3A. Continuous variables were standardized so that the effect size corresponds to 1 standard deviation of the predictor, whereas for a variable expressed as a percentage, the effect size corresponds to the full effect of that predictor at 100%. Predictors in bold font and purple plotting represent biological variation, and the plots labeled Phylogenetic and Individual are prediction intervals. The plotting labeled Phylogenetic (Clade) is part of the overall phylogenetic variation, but it is expressed as a mean and confidence interval alongside other model coefficients. Model covariates are in green, including indicator variables (italics), variables log transformed for analysis (bold-italics), and standardized variables (asterisk). Note: slow walking did not appear in the Felidae output because it proved a redundant predictor in the analysis (i.e., every felid species that exhibited the pursuit strategy did not exhibit the slow-walking strategy, and vice versa; Table S2). Labels N, C, and F are the number of individuals, canid species, and felid species, respectively.

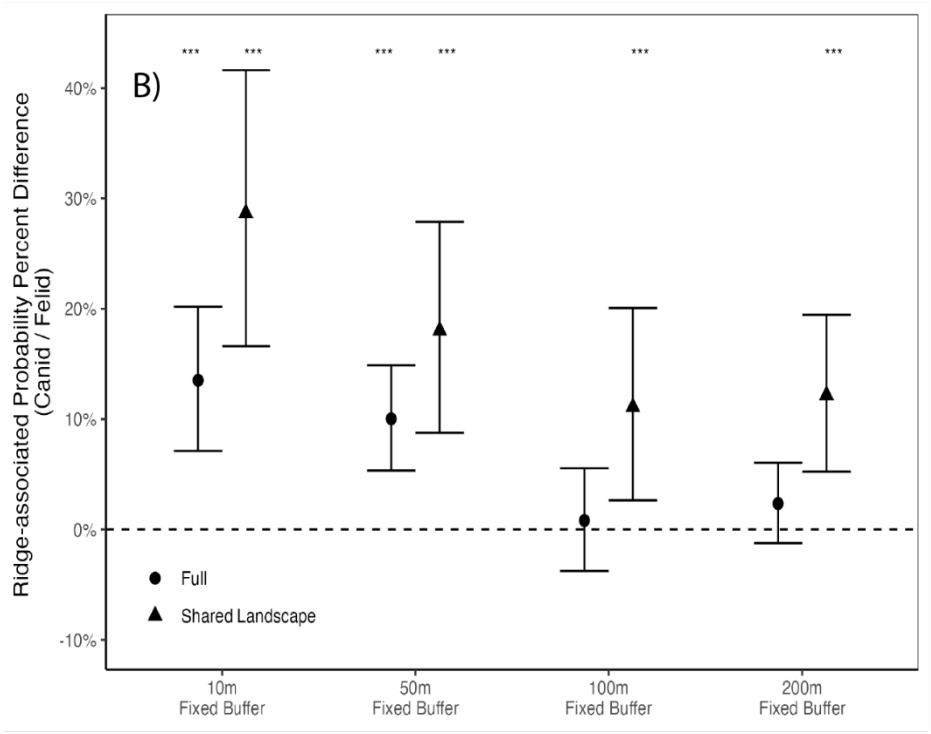

Figure S5. Clade effects for ridge-associated probability mass (calculated for fixed spatial buffers of 10 m, 50 m, 100 m, and 200 m on either side of all ridges for each individual) are plotted as a ratio, with y = 0.0 indicating no difference between clades and positive values indicating increased ridge-associated probability mass in canids. Clade effects are highly significant ($p < 0.00002$) for 10 m and 50 m buffer widths for the full dataset, and for all buffer widths ($p < 0.01$ for 100 m, $p < 0.0001$ for others) for the shared landscapes dataset.

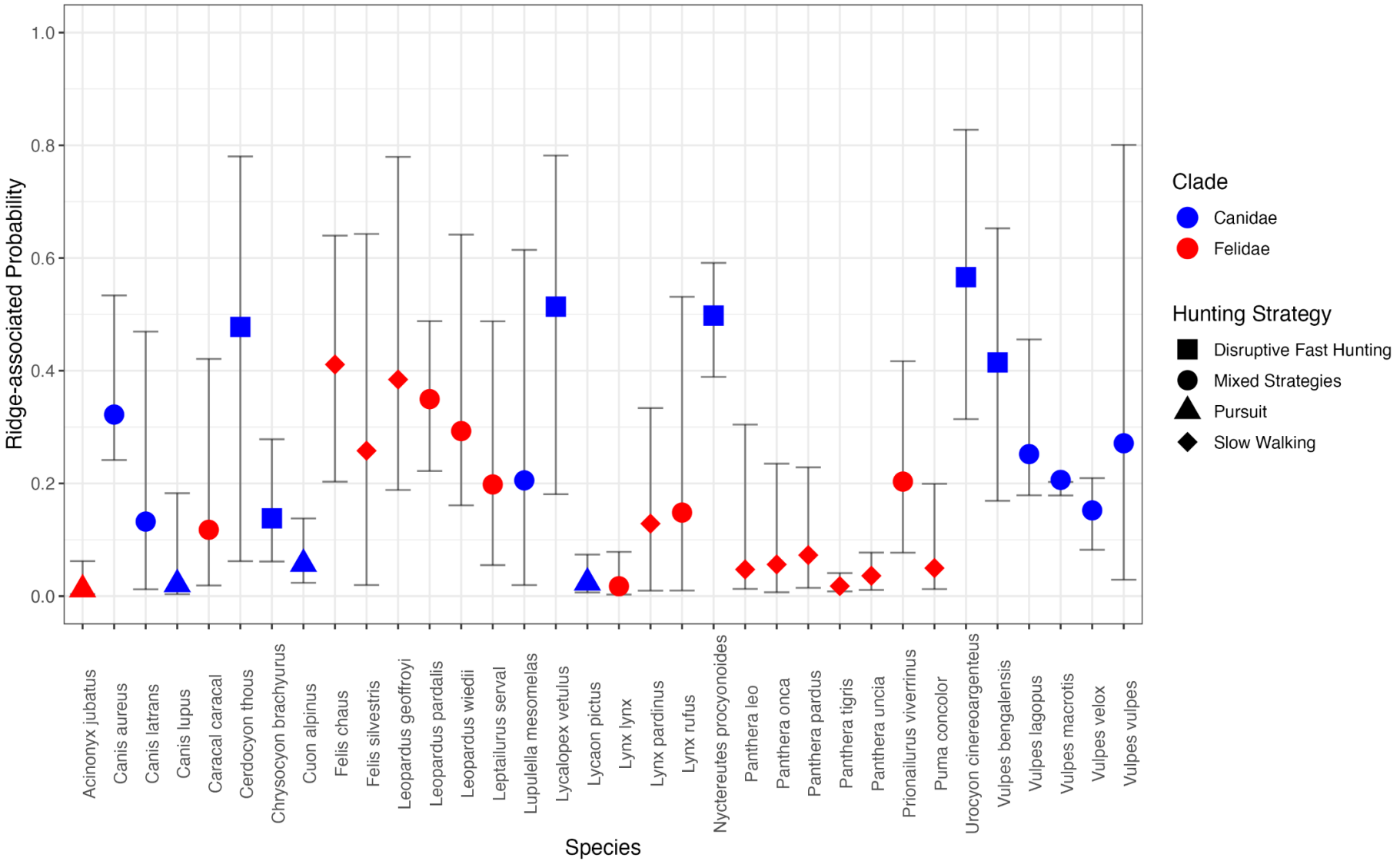

Figure S6. Empirical range of ridge-associated probability (vertical bars) and corresponding model-predicted means (symbols) for 50m ridge buffer widths, labeled by clade (color) and movement strategy while hunting (shape) (see Tables S1, S2). The label 'Mixed strategies' indicates evidence of two or more strategies for movement while hunting.

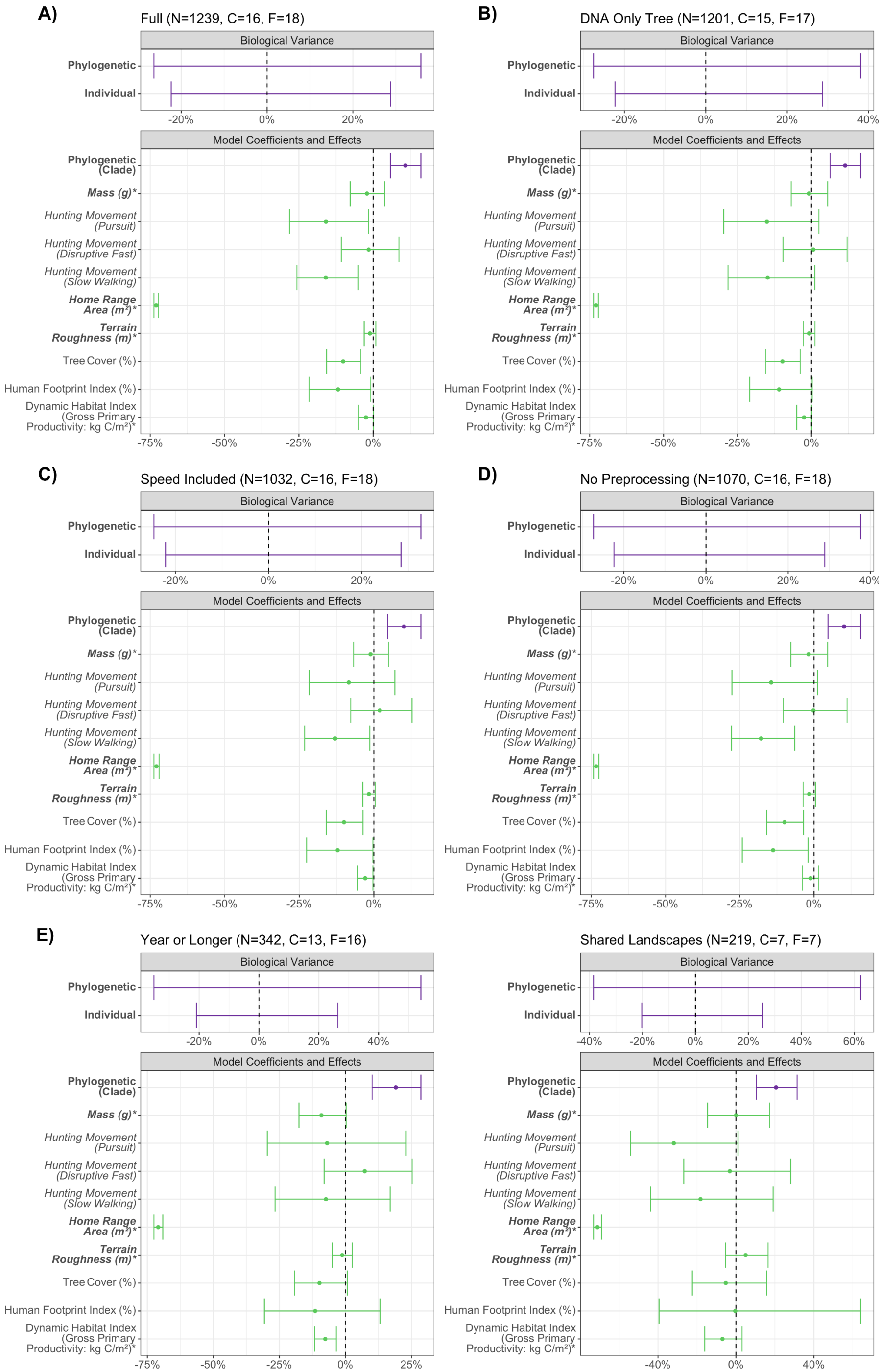

Figure S7. Effect size plots for ridge-associated probability mass density for the full dataset and all subdatasets for ridges with 50m buffer width. Continuous variables were standardized so that the effect size corresponds to 1 standard deviation of the predictor, whereas for a variable expressed as a percentage, the effect size corresponds to the full effect of that predictor at 100%. Predictors in bold font and purple plotting represent biological variation, and the plots labeled Phylogenetic and Individual are prediction intervals. The plotting labeled Phylogenetic (Clade) is part of the overall phylogenetic variation, but it is expressed as a mean and confidence interval alongside other model coefficients. Model covariates are in green, including indicator variables (italics), variables log transformed for analysis (bold-italics), and standardized variables (asterisk). Labels N, C, and F are the number of individuals, canid species, and felid species, respectively.

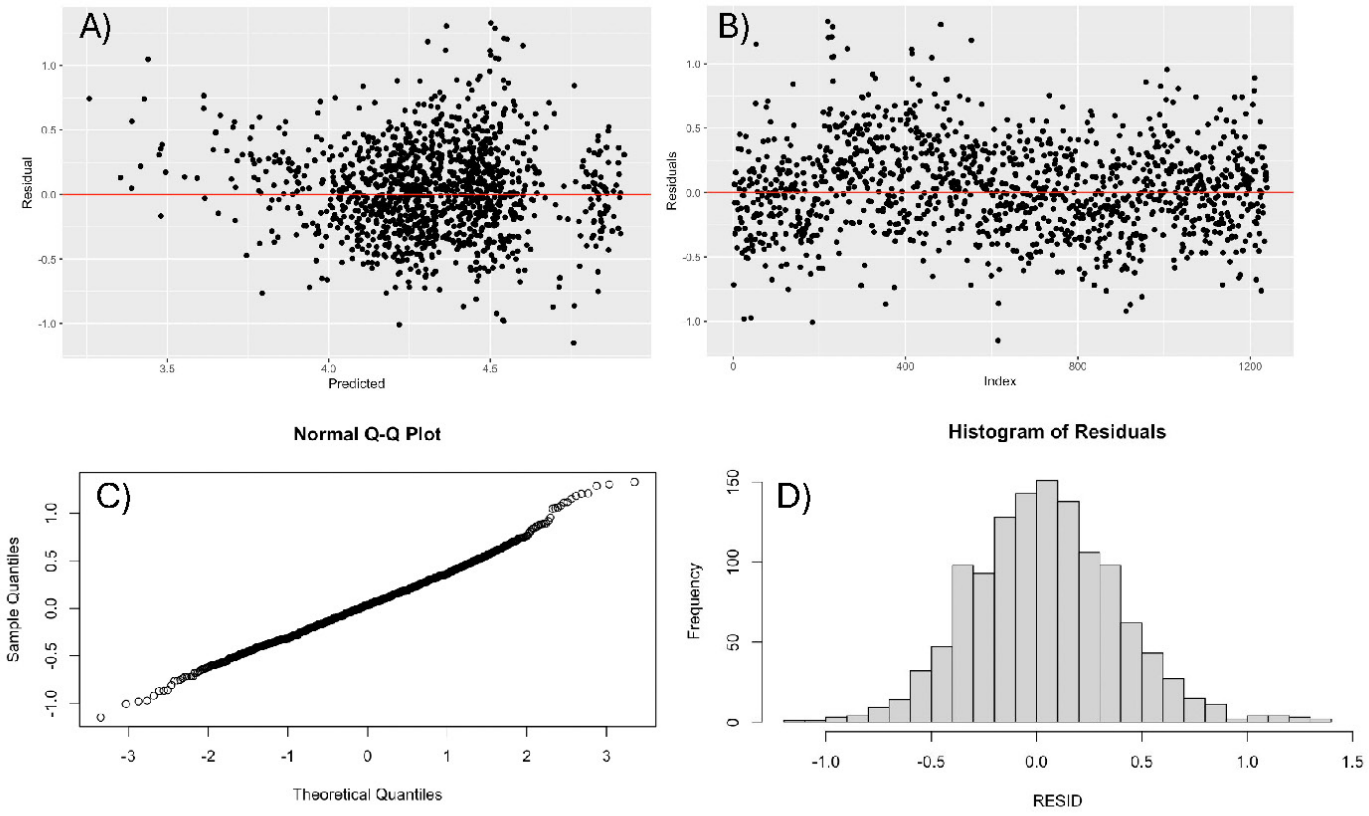

E)	log_mass_st	log_hr_st	inv_ess	log_roughness_st	mean_treecover	mean_hfi	seasonality_dhi_gpp_st
log_mass_st	1	0.6359	0.3126	0.0856	0.3772	-0.3476	-0.1353
log_hr_st	0.6359	1	0.4851	0.1513	0.3469	-0.4364	0.3199
inv_ess	0.3126	0.4851	1	0.0302	0.1403	-0.114	0.0557
log_roughness_st	0.0856	0.1513	0.0302	1	0.2971	-0.0231	0.2136
mean_treecover	0.3772	0.3469	0.1403	0.2971	1	-0.2584	0.2343
mean_hfi	-0.3476	-0.4364	-0.114	-0.0231	-0.2584	1	-0.1337
seasonality_dhi_gpp_st	-0.1353	0.3199	0.0557	0.2136	0.2343	-0.1337	1

Figure S8. Results from standard methods for assessing model adequacy for the analyses of ridge density that comprise Figure 3A in the main text, demonstrating that the linear modeling assumptions were satisfactorily met. Subpanels provide plots of A) residuals against predicted values, B) residuals against an index of the underlying individual movement datasets (see Supplementary Dataset S1), C) the quantile-quantile (Q-Q) relationship, and D) the histogram of residuals. Subpanel E presents results from an analysis of collinearity of the linear regression terms.

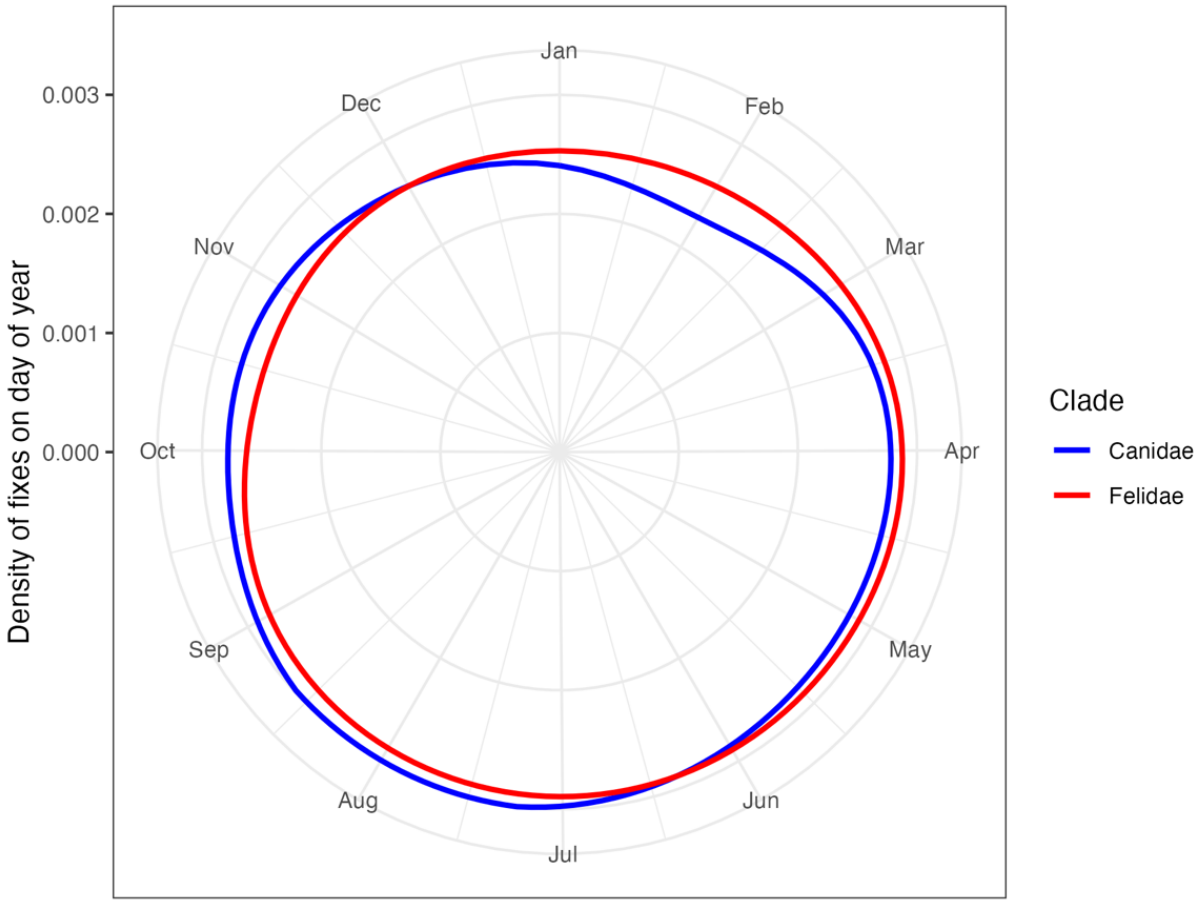

Figure S9. Comparative availability of canid and felid GPS fixes (across all species and individuals) as a function of time of year.

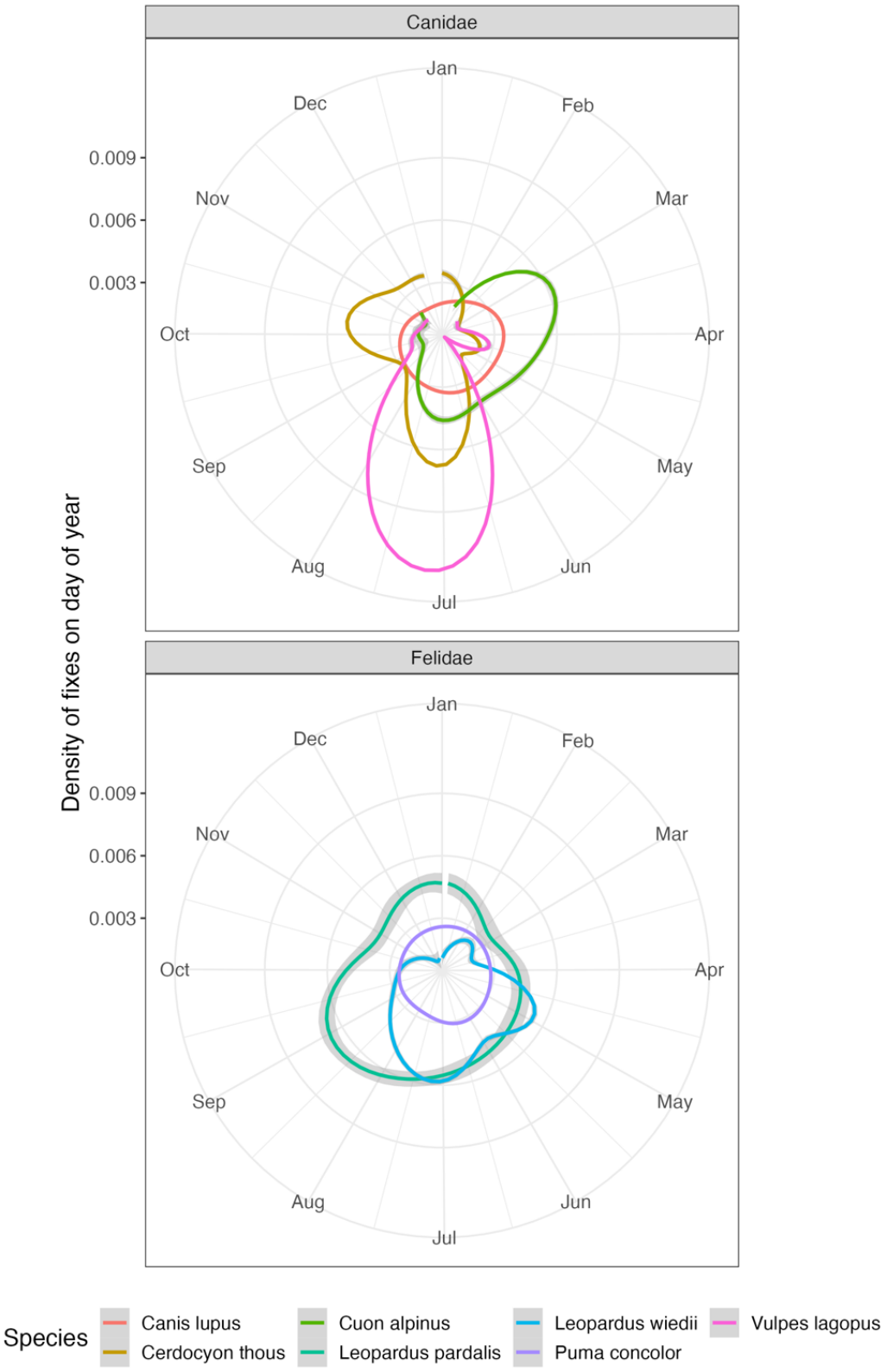

Figure S10. Pronounced species-level deviations in seasonal data availability away from annual circularity.

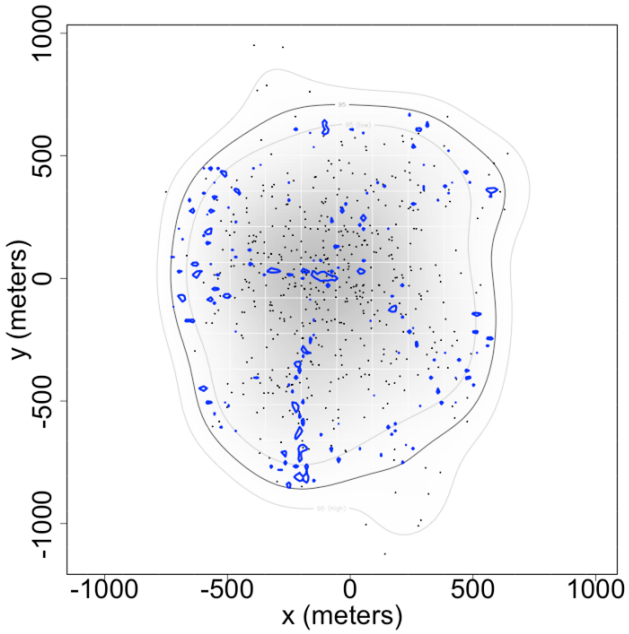

Figure S11. Probability ridges identified for a Null OUF Gaussian stochastic process without a movement model. The parameters of the model were: τ_p = 86400 sec, τ_v = 1350 sec, σ^2 = 100000 m^2, μ = c(0,0), Days: 64, Fixes/day: 8. Sampled locations are in black and calculated probability ridges are in blue. The scattershot of small probability ridges are false positives that appear by virtue of finite sampling effort and represent deviations from the true value of zero probability ridge density expected in the stationary distribution. The probability ridges were calculated via the computationally fast *ctmm* algorithm so that at this visual resolution, individual ridges may appear 'doubled,' as 'parallel lines', or as 'closed loops' due to the statistically inconsequential computational 'aliasing' discussed earlier.

Figure S12. Probability ridges identified for the Alternative Ridge Model based on a periodic OUF Gaussian stochastic process that includes circular movement. The parameters of the Alternative Ridge Model were: τ_p = 86400 sec, τ_v = 1350 sec, σ^2 = 100000 m^2, Days: 32, Fixes/day: 8. The movement model was defined as having a circular mean trajectory with radius 1 km. Parametrically this is expressed in *ctmm* as : μ= c(0, 0, 1000, 0, 1000, 0), Mean = "periodic", Harmonic = c(1,0), Period= 86400 sec. The circumference of the mean path is ~5.94 km (blue circle), and the true length of the probability ridge in the stationary distribution for this stochastic process is ~6.28 km (green circle) as determined by the Bessel function calculation above. Panel A shows sampled GPS points and trajectory, and the analytically determined expected ridge locations. The long probability ridges appearing in B in a roughly circular form in the interior of the range distribution provide good approximations to both the expected location and the expected length of the true probability ridge in A. The scattershot of small probability ridges beyond the two long probability ridges are false positives that appear by virtue of finite sampling effort. The probability ridges were calculated via the computationally fast *ctmm* algorithm so that at this visual resolution, individual ridges may appear 'doubled,' as 'parallel lines', or as 'closed loops' due to the statistically inconsequential computational 'aliasing artifacts' discussed at length earlier.

A

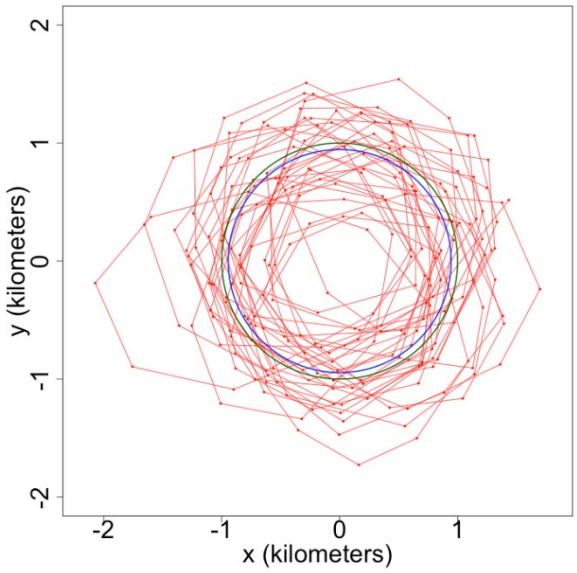

B

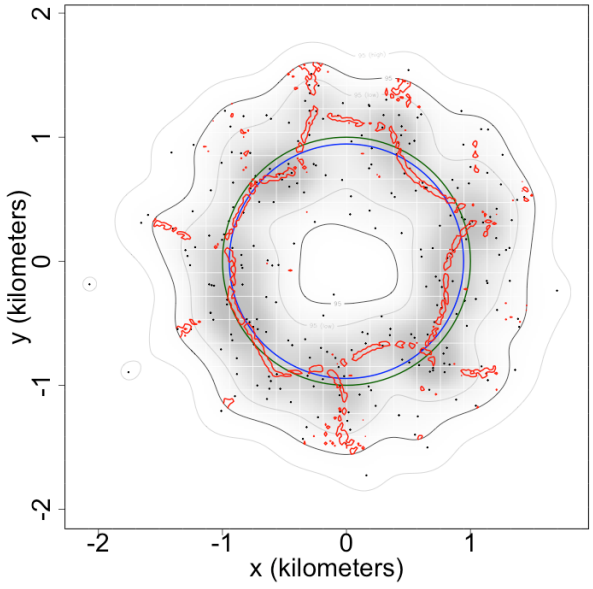

Figure S13. Contrasting results from the Null Model, the Alternative Ridge Model, and the empirical datasets in terms of ridge length (A) and ridge density (B). Ridge length and ridge density are zero in the stationary distribution of the Null Model, and any deviations above that value are false positives due to the effects of finite sampling effort. Ridge length and ridge density are expected to be above zero in the stationary distribution of the Alternative Ridge Model (see Table S6). In the empirical datasets, values for both ridge length and ridge density are generally well above the levels expected due to estimation error. Note quasi-logarithmic histogram bins in A.

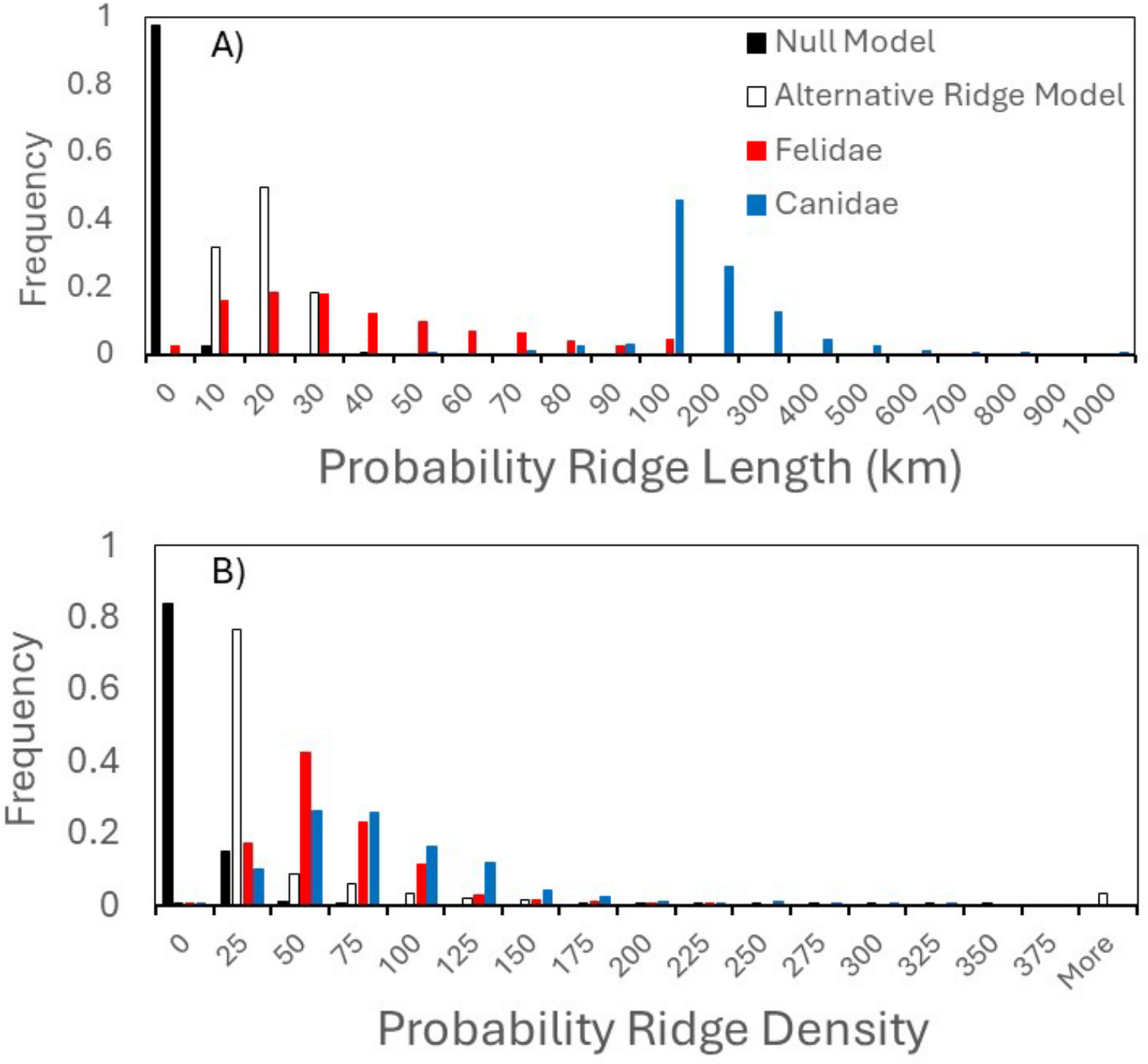

Table S1. Fixed effects hypothesized to contribute to variation in ridge density.

Fixed Effect	Statistical Aspects	Level	Abbreviation, Description, and Justification	References
Body mass	Log transformed / standardized	Species	Key driver of interspecific variation in mammals that could also affect routeway use on biomechanical grounds. Sourced from Elton Traits 1.0.	59
Movement strategy while hunting	Categorical	Species	Distinguishes among carnivore species that routinely engage in long-distance pursuits, disruptive fast hunting to flush prey, slow walking to surprise prey, or a mix of these strategies. Different strategies could translate into differential re-use of space.	See Table S2
Terrain roughness	Log transformed / standardized	Individual	May influence animal movement routeways when individuals conserve energy by favoring locations with reduced physical gradients when available (thus concentrating their space use in flatter areas) or when animals choose rougher terrain as a protection against human persecution.	60-61
Tree cover	Not transformed	Individual	Could affect ease of landscape navigation via perceptual, biomechanical, and physiological mechanisms	62
Human footprint index	Not transformed	Individual	HFI; Composite measure reflecting several ways in which humans alter landscapes. Known to shape movements by mammals globally	17, 23, 63-64
Variation dynamic habitat index for gross primary productivity	Log transformed / standardized	Individual	Var DHI GPP; Measure of the intensity of seasonality in a region, used to evaluate the potential importance of seasonal differences in movement conditions (e.g., snow depth; flooding), which could influence an individual's tendency to reuse travel routeways	65
Home range size	Log transformed / standardized	Individual	HR; Estimated as the mean 95% contour of an autocorrelated kernel density estimation with small sample size correction (AKDEc) applied to GPS movement data via the R package *ctmm*. Included to quantify any residual effects of an individual's spatial scale of movement beyond those captured in the standardization of total ridge length (Eq. S1). E.g., larger home ranges may feature lower ridge density due to limitations on how extensively travel routeways can be remembered and thus re-used.	2
Effective sample size	Inverse	Individual	ESS; A bias-correction term quantifying data robustness for spatial modeling, accounting for GPS sampling interval, sampling duration, and home range crossing time (measures mobility relative to home range size); calculated via *ctmm*	2
Speed	Not transformed / standardized	Individual	Scale-insensitive continuous time measure; calculated via *ctmm,* but only for individuals best fit by OUF models, which have continuous velocity. Tests the hypothesis that travel speed is related to ridge density, such as if fast travel reduced opportunities for memory formation.	5

Table S2. Movement strategies while hunting hypothesized to contribute to variation in ridge density

Species	Movement strategy while hunting	References
Canis aureus	Disruptive fast hunting + Slow walking	24, 25, 29-31
Canis latrans	Disruptive fast hunting + Slow walking	24, 25, 29-31
Canis lupus	Pursuit	24, 25, 29-31
Cerdocyon thous	Disruptive fast hunting	24, 25, 29
Chrysocyon brachyurus	Disruptive fast hunting	24, 29, 70
Cuon alpinus	Pursuit	24, 25, 30
Lupulella mesomelas	Pursuit + Disruptive fasting hunting	24, 66-68
Lycalopex vetulus	Disruptive fast hunting	24, 76
Lycaon pictus	Pursuit	24, 25, 29, 30
Nyctereutes procyonoides	Disruptive fast hunting	24, 25, 29-31
Urocyon cinereoargenteus	Disruptive Fast hunting	24, 30
Vulpes bengalensis	Disruptive fast hunting	24, 77
Vulpes lagopus	Disruptive fast hunting + Slow walking	24, 78
Vulpes macrotis	Disruptive fast hunting + Slow walking	24, 79, 80
Vulpes velox	Disruptive fast hunting + Slow walking	24, 81, 82
Vulpes vulpes	Disruptive fast hunting + Slow walking	24, 29, 30
Acinonyx jubatus	Pursuit	29, 31
Caracal caracal	Disruptive fast hunting + Slow walking	24, 26, 27, 29, 69
Felis chaus	Slow walking	24, 27, 30, 71
Felis silvestris	Slow walking	24, 27
Leopardus geoffroyi	Slow walking	24-27, 72
Leopardus pardalis	Disruptive fast hunting + Slow walking	29, 24, 27, 30, 73
Leopardus wiedii	Disruptive fast hunting + Slow walking	24, 27, 74
Leptailurus serval	Disruptive fast hunting + Slow walking	29, 26, 24, 27, 30
Lynx lynx	Disruptive fast hunting + Slow walking	24, 27
Lynx pardinus	Slow walking	24, 27
Lynx rufus	Disruptive fast hunting + Slow walking	24, 27, 29
Panthera leo	Slow walking	24, 26, 27, 30, 75
Panthera onca	Slow walking	24, 27, 29
Panthera pardus	Slow walking	24, 27, 29, 30
Panthera tigris	Slow walking	24, 27, 29, 30
Panthera uncia	Slow walking	24, 27, 29
Prionailurus viverrinus	Disruptive fast hunting + Slow walking	24, 27, 30
Puma concolor	Slow walking	24, 27, 29, 30

Note: In the *pursuit* strategy, prey are actively chased, sometimes for many hundreds of meters. *Slow walking* includes sit-and-wait predation, and upon discovery of a prey individual, typically involves some elements of stalking, ambushing, and pouncing behaviors that are terminology appearing in other works. Lastly, *disruptive fast hunting* corresponds to carnivores moving quickly through an area attempting to startle and flush prey. We treated these strategies as indicator variables, which meant that (unlike previous categorizations) a species could be classified as employing more than one strategy.

Table S3. Detailed information regarding the studies represented in Figure S2. Biomes from (57).

Species	Study Identifier	Country	Biome Full Name	Country Alpha2 Code	Biome Abbreviation	Country-Biome Deconfliction Identifier
Canis latrans	Belant-Beyer	United States	Temperate Broadleaf & Mixed Forest	US	TBMF	
Canis latrans	Clark	United States	Temperate Conifer Forest	US	TCF	
Canis latrans	Kays	United States	Temperate Savanna	US	TeS	
Canis latrans	Prugh	United States	Temperate Conifer Forest + Temperate Savanna	US	TCF + TeS	
Canis latrans	Wheeldon	Canada	Temperate Broadleaf & Mixed Forest	CA	TBMF	
Canis latrans	Young	United States	Desert & Xeric Scrubland + Temperate Conifer Forest	US	DXS + TCF	
Canis lupus	Belant-Beyer	United States	Temperate Broadleaf & Mixed Forest	US	TBMF	
Canis lupus	Hebblewhite	Canada	Temperate Conifer Forest	CA	TCF	
Canis lupus	Hernandez-Blanco	Russia	Desert &Xeric Scrubland + Temperate Broadleaf & Mixed Forest	RU	DXS + TBMF	
Canis lupus	Lantham	Canada	Boreal Forest/Taiga	CA	BF	1
Canis lupus	Patterson.B	Canada	Boreal Forest/Taiga	CA	BF	2
Canis lupus	Şekercioğlu	Türkiye	Temperate Broadleaf & Mixed Forest	TR	TBMF	
Lupulella mesomelas	Drouilly	South Africa	Desert & Xeric Scrubland	ZA	DXS	
Lupulella mesomelas	Getz-Bellan	Namibia	Tropical Savanna	NA	TrS	
Lupulella mesomelas	Ramesh	South Africa	Tropical Savanna	ZA	TrS	
Caracal caracal	Cristescu	South Africa	Desert & Xeric Scrubland	ZA	DXS	1
Caracal caracal	Drouilly	South Africa	Desert & Xeric Scrubland	ZA	DXS	2
Caracal caracal	Ramesh	South Africa	Tropical Savanna	ZA	TrS	
Caracal caracal	Serieys	South Africa	Mediterranean Scrub	ZA	MS	
Felis silvestris	Janssen-Dekker	Netherlands	Temperate Broadleaf & Mixed Forest	NL	TBMF	
Felis silvestris	Lang	Germany	Temperate Broadleaf & Mixed Forest	DE	TBMF	1
Felis silvestris	Palomares	Spain	Temperate Broadleaf & Mixed Forest	ES	TBMF	
Felis silvestris	STHG	Germany	Temperate Broadleaf & Mixed Forest	DE	TBMF	2
Lycaon pictus	Abrahms	Botswana	Tropical Savanna	BW	TrS	1
Lycaon pictus	Cozzi	Botswana	Tropical Savanna	BW	TrS	2
Lycaon pictus	Jackson	Tanzania	Tropical Savanna	TZ	TrS	
Lynx lynx	Mannil-Kont	Estonia	Temperate Broadleaf & Mixed Forest	EE	TBMF	
Lynx lynx	Odden	Norway	Boreal Forest + Tundra	NO	BF + T	
Lynx lynx	Şekercioğlu	Türkiye	Temperate Broadleaf & Mixed Forest	TR	TBMF	
Lynx rufus	Clark	United States	Temperate Conifer Forest	US	TCF	1
Lynx rufus	Farrell	United States	Temperate Broadleaf & Mixed Forest	US	TBMF	
Lynx rufus	Prugh	United States	Temperate Conifer Forest	US	TCF	2
Lynx rufus	Ranglack	United States	Temperate Savanna	US	TeS	1
Lynx rufus	Serieys.AromasHills	United States	Mediterranean Scrub + Temperate Conifer Forest	US	MS + TCF	
Lynx rufus	Serieys.CoyoteValley	United States	Mediterranean Scrub	US	MS	
Lynx rufus	Young	United States	Temperate Savanna	US	TeS	2
Panthera leo	Abrahms	Botswana	Tropical Savanna	BW	TrS	
Panthera leo	Fryxell	Tanzania	Tropical Savanna	TZ	TrS	
Panthera leo	Patterson.BD	Kenya	Tropical Savanna	KE	TrS	1
Panthera leo	Wilmers	Kenya	Tropical Savanna	KE	TrS	2
Puma concolor	Clark	United States	Temperate Conifer Forest	US	TCF	1
Puma concolor	Darlington	Canada	Temperate Conifer Forest	CA	TCF	
Puma concolor	Azevedo.Lemos	Brasil	Tropical Savanna + Tropical Moist Broadleaf Forest	BR	TrS + TMBF	
Puma concolor	Wilmers	United States	Mediterranean Scrub + Temperate Conifer Forest	US	MS + TCF	
Puma concolor	Young	United States	Temperate Conifer Forest	US	TCF	2
Vulpes vulpes	Frair	United States	Temperate Broadleaf & Mixed Forest	US	TBMF	
Vulpes vulpes	Garthe	Germany	Temperate Broadleaf & Mixed Forest	DE	TBMF	
Vulpes vulpes	Roshier	Australia	Mediterranean Scrub	AU	MS	
Vulpes vulpes	Walton	Sweden	Temperate Broadleaf & Mixed Forest	SE	TBMF	

Table S4. Results from additional supplemental analyses conducted to ensure the robustness of results to changes in the threshold for defining a ridge (14) and to other subsetting procedures beyond those discussed in the main text.

# Tracks	Dataset Subset Analyzed	Ridge Threshold	Mean (± 95% CI) of Clade Effect	P value of Clade Effect
1239	All individuals	0.1	1.22 (±0.08)	$p < 10^{-8}$
		0.5	1.15 (±0.07)	$p < 10^{-5}$
		0.9	1.13 (±0.11)	$p < 0.03$
1201	DNA-only tree	0.1	1.22 (±0.08)	$p < 10^{-9}$
		0.5	1.16 (±0.08)	$p < 10^{-5}$
		0.9	1.13 (±0.12)	$p < 0.03$
1032	Speed Included	0.1	1.18 (±0.09)	$p < 10^{-5}$
		0.5	1.13 (±0.07)	$p < 10^{-3}$
		0.9	1.12 (±0.13)	$p < 0.05$
1070	No Preprocessing	0.1	1.25 (±0.09)	$p < 10^{-10}$
		0.5	1.17 (±0.08)	$p < 10^{-5}$
		0.9	1.13 (±0.13)	$p < 0.05$
342	Year or Longer	0.1	1.52 (±0.17)	$p < 10^{-7}$
		0.5	1.22 (±0.13)	$p < 10^{-3}$
		0.9	1.17 (±0.21)	$p = 0.07$
219	Shared Landscapes	0.1	1.42 (±0.18)	$p < 10^{-8}$
		0.5	1.33 (±0.16)	$p < 10^{-5}$
		0.9	1.24 (±0.24)	$p < 0.03$
1231	All species except ocelot (*Leopardus pardalis*) whose collars provided high resolution VHF data instead of GPS	0.5	1.14 (±0.07)	$p < 0.0001$
1089	All tracks except the ultra-high resolution tracks that we resampled to 1-minute intervals	0.5	1.15 (±0.08)	$p < 0.0001$

Table S5. Probability ridge *length* calculated for simulations from the Null Model.

	AKDE Probability Ridge Length (km)		
Duration (days)	Mean	2.5 Percentile	97.5 Percentile
32	7.9	3.9	12.0
64	6.5	3.9	9.1
128	5.6	3.4	7.8
256	4.5	3.0	6.1
512	3.7	2.4	5.1
1024	3.1	1.9	4.2

Note: The Null Model consisted of a stationary OUF stochastic Gaussian process. The expected value for all simulations is zero because the stationary distribution of an OUF Gaussian process will not have any probability ridges. Nonzero values of probability ridge length reflect low values of false positives attributable to finite sampling effort.

Table S6. Probability ridge *length* calculated for simulations from the Alternative Ridge Model

		AKDE Probability Ridge Length (km)			
		Anticipated Value	Mean	2.5 Percentile	97.5 Percentile
Duration (days)	32	19.8	33.4	28.1	38.6
	64	18.4	28.2	23.7	32.7
	128	17.5	24.2	19.0	29.4
	256	16.4	21.5	17.6	25.4
	512	15.6	18.8	15.2	22.3
	1024	15.0	16.9	13.7	20.1

Note: The Alternative Ridge Model consisted of a Gaussian stochastic process with a circular mean path. From Figure S12, the parameters were: τ_p = 86400 sec, τ_v = 1350 sec, σ^2 = 100000 m^2, Days: 32, Fixes/day: 8. The movement model was defined as having a circular mean trajectory with radius 1 km. Parametrically this is expressed in *ctmm* as : μ= c(0, 0, 1000, 0, 1000, 0), Mean = "periodic", Harmonic = c(1,0), Period= 86400 sec. The probability ridge length that exists in the stationary distribution for this stochastic process can be calculated analytically using Bessel functions. The probability ridge expected for this model is a circle with a diameter of 945m, which yields the Anticipated Value after the corrections discussed previously. The Mean column indicates that our method does a good job of approximating the analytical expected value despite vagaries introduced by finite sampling effort, and that the match between anticipated and observed values improves with increasing track duration. The 2.5 and 97.5 percentile columns indicate that when probability ridges should exist based on the existence of a known underlying circular movement route, our methods consistently identified their existence at levels well above zero.

Dataset S1 (separate file). Detailed individual-level information about the canid and felid GPS tracks evaluated (1528) and used (1239) for this analysis.

Dataset S2 (separate file). Detailed information regarding the original sources of animal tracking data, the movement tracks used in this analysis (including their sources and availability), animal care and permit authorizations, and track-specific funding acknowledgements.

SI References

1. Kays, R., et al., The Movebank system for studying global animal movement and demography. Methods in Ecology and Evolution, 13(2), 419-431. (2022)
2. Calabrese, J.M., Fleming, C.H. and Gurarie, E., ctmm: An R package for analyzing animal relocation data as a continuous-time stochastic process. Methods in Ecology and Evolution, 7(9), 1124-1132. (2016)
3. Silva, I., Fleming, C.H., Noonan, M.J., Alston, J., Folta, C., Fagan, W.F. and Calabrese, J.M., Autocorrelation-informed home range estimation: A review and practical guide. Methods in Ecology and Evolution, 13(3), 534-544. (2022)
4. Fleming, C.H., et al., From fine-scale foraging to home ranges: a semivariance approach to identifying movement modes across spatiotemporal scales. American Naturalist 183(5), E154-E167. (2014)
5. Noonan, M.J., et al., Scale-insensitive estimation of speed and distance traveled from animal tracking data. Movement Ecology, 7(1), 1-15. (2019)
6. Uhlenbeck, G.E. and Ornstein, L.S., On the theory of the Brownian motion. Physical Review, 36(5), p.823. (1930)
7. Fleming, C. H., et al., Non-Markovian maximum likelihood estimation of autocorrelated movement processes. Methods in Ecology and Evolution 5, 462-472. (2014)
8. Fleming, C.H., Subaşi, Y. and Calabrese, J.M., Maximum-entropy description of animal movement. Physical Review E, 91(3), p. 032107. (2015)
9. Noonan, M.J., et al. A comprehensive analysis of autocorrelation and bias in home range estimation. Ecological Monographs. 89, e01344. (2019)
10. Fleming, C.H., Noonan, M.J., Medici, E.P. and Calabrese, J.M., Overcoming the challenge of small effective sample sizes in home-range estimation. Methods in Ecology and Evolution, 10(10), 1679-1689. (2019)
11. Fleming, C.H., et al., Rigorous home range estimation with movement data: a new autocorrelated kernel density estimator. Ecology, 96(5), 1182-1188. (2015)
12. Fleming, C.H. and Calabrese, J.M., A new kernel density estimator for accurate home-range and species-range area estimation. Methods in Ecology and Evolution, 8(5), 571-579. (2017)
13. Burt, W.H., Territoriality and home range concepts as applied to mammals. Journal of Mammalogy, 24(3), 346-352. (1943)
14. Genovese, C.R., Perone-Pacifico, M., Verdinelli, I. and Wasserman, L., Nonparametric ridge estimation. The Annals of Statistics, 42(4), 1511-1545. (2014)
15. Chacón, J.E. and Duong, T., Multivariate kernel smoothing and its applications. CRC Press. (2018)
16. Alavi, S.E., et al., A quantitative framework for identifying patterns of route-use in animal movement data. Frontiers in Ecology and Evolution, 9, p.743014. (2022)
17. Dickie, M., Serrouya, R., McNay, R. S., and Boutin, S. Faster and farther: Wolf movement on linear features and implications for hunting behaviour. Journal of Applied Ecology, 54, 253e263. (2017)
18. Dunford, C.E., et al., Surviving in steep terrain: a lab-to-field assessment of locomotor costs for wild mountain lions (*Puma concolor*). Movement Ecology, 8, 1-12. (2020)
19. Rosenbaum, R., et al., Spatial ecology of snow leopards (*Panthera uncia*) in the Altai Mountains of western Mongolia. PLoS ONE 18(1): e0280011. (2023)

20. Upham, N.S., Esselstyn, J.A. and Jetz, W., Inferring the mammal tree: species-level sets of phylogenies for questions in ecology, evolution, and conservation. PLoS Biology, 17(12), p.e3000494. (2019)
21. Paradis, E. and Schliep, K., ape 5.0: an environment for modern phylogenetics and evolutionary analyses in R. Bioinformatics, 35(3), 526-528. (2019)
22. Revell, L. J. phytools: An R package for phylogenetic comparative biology (and other things). Methods in Ecology and Evolution, 3, 217-223. (2012)
23. Tucker, M. A., et al., Moving in the Anthropocene: Global reductions in terrestrial mammalian movements. Science, 359(6374), pp.466-469. (2018)
24. Mittermeier, R.A. and Wilson, D.E., Handbook of the Mammals of the World: vol. 1: Carnivores, Lynx Ediciones, Barcelona, Spain. (2009)
25. Alderton, D. and Tanner, B., Foxes, wolves, and wild dogs of the world. Facts on File. (1994)
26. Hunter, L., Cats of Africa: Behavior, ecology, and conservation. Johns Hopkins University Press. Baltimore. (2006)
27. Sunquist, M. and Sunquist, F., Wild Cats of the World. University of Chicago Press. Chicago. (2017)
28. Venter, O., et al. Sixteen years of change in the global terrestrial human footprint and implications for biodiversity conservation Nature Communications, 7(1), p.12558. (2016)
29. Van Valkenburgh, B., Locomotor diversity within past and present guilds of large predatory mammals. Paleobiology, 11(4), 406-428 (1985)
30. Schwab, J.A., Kriwet, J., Weber, G.W. and Pfaff, C., Carnivoran hunting style and phylogeny reflected in bony labyrinth morphometry. Scientific Reports, 9(1), 1-9. (2019)
31. Hirt, M.R., Tucker, M., Müller, T., Rosenbaum, B. and Brose, U., Rethinking trophic niches: speed and body mass colimit prey space of mammalian predators. Ecology and Evolution, 10(14), 7094-7105. (2020)
32. Yonelinas, A.P., Ranganath, C., Ekstrom, A.D. and Wiltgen, B.J., A contextual binding theory of episodic memory: systems consolidation reconsidered. Nature Reviews Neuroscience, 20(6), 364-375 (2019).
33. Nowak, R.M. and J.L. Paradiso. Walker's Mammals of the World, 4th edition. Volume 2. Johns Hopkins University Press. Baltimore. (1983)
34. Barlow, J.C., Land mammals from Uruguay: ecology and zoogeography. PhD Dissertation, University of Kansas. (1967)
35. Murray, J.L. and Gardner, G.L., *Leopardus pardalis*. Mammalian Species, (548), 1-10. (1997)
36. Geertsema, A.A., Aspects of the ecology of the serval *Leptailurus serval* in the Ngorongoro Crater, Tanzania. Netherlands Journal of Zoology, 35(4), 527-610. (1984)
37. Rollings, C.T., Habits, foods and parasites of the bobcat in Minnesota. The Journal of Wildlife Management, 9(2), 131-145. (1945)
38. Naumov, N.P., Signal (biological) fields and their significance for animals, Zhurnal Obshchei Biologii, 34 (6), 808–817. (1973)
39. Kashetsky, T., Avgar, T. and Dukas, R., The cognitive ecology of animal movement: evidence from birds and mammals. Frontiers in Ecology and Evolution, 9, p.724887. (2021)

40. Moehlman, P.D., Intraspecific variation in canid social systems. Carnivore Behavior, Ecology, and Evolution, J.L. Gittleman, ed., pp.143-163. Springer Science & Business Media. (1989)
41. Červený, J., Begall, S., Koubek, P., Nováková, P. and Burda, H., Directional preference may enhance hunting accuracy in foraging foxes. Biology Letters, 7(3), 355-357. (2011)
42. Benediktová, K., Adamkova, J., Svoboda, J., Painter, M.S., Bartoš, L., Novakova, P., Vynikalova, L., Hart, V., Phillips, J. and Burda, H., Magnetic alignment enhances homing efficiency of hunting dogs. Elife, 9, p.e55080. (2020)
43. Schneider, W.T., Holland, R.A. and Lindecke, O., Over 50 years of behavioural evidence on the magnetic sense in animals: what has been learnt?. The European Physical Journal Special Topics. 232, 269–278. (2023)
44. Wynn, J., Padget, O., Mouritsen, H., Morford, J., Jaggers, P. and Guilford, T., Magnetic stop signs signal a European songbird's arrival at the breeding site after migration. Science, 375(6579), 446-449. (2022)
45. Wegner, R.E., Begall, S. and Burda, H., Magnetic compass in the cornea: local anaesthesia impairs orientation in a mammal. Journal of Experimental Biology, 209(23), 4747-4750. (2006)
46. Linnell, J.D., Aanes, R., Swenson, J.E., Odden, J. and Smith, M.E., Translocation of carnivores as a method for managing problem animals: a review. Biodiversity & Conservation, 6, 1245-1257. (1997)
47. Macdonald, D.W., The ecology of carnivore social behaviour. Nature, 301(5899), 379-384. (1983)
48. Rodgers, T.W., Giacalone, J., Heske, E.J., Pawlikowski, N.C. and Schooley, R.L., Communal latrines act as potentially important communication centers in ocelots *Leopardus pardalis*. Mammalian Biology, 80, 380-384. (2015)
49. Potts, J.R., Fagan, W.F. and Mourao, G., Deciding when to intrude on a neighbour: quantifying behavioural mechanisms for temporary territory expansion. Theoretical Ecology, 12, 307-318. (2019)
50. Buesching, C.D. and Jordan, N.R., The function of carnivore latrines: review, case studies, and a research framework for hypothesis testing. pp.131-171. In: *Small Carnivores: Evolution, Ecology, Behaviour, and Conservation*, E.D.L. San, J.J. Sato, J.L. Belant, and M.J. Somers, eds. (2022)
51. Holekamp, K.E., Dantzer, B., Stricker, G., Yoshida, K.C.S. and Benson-Amram, S., Brains, brawn and sociality: a hyaena's tale. Animal Behaviour, 103, 237-248. (2015)
52. Holekamp, K.E. and Benson-Amram, S., The evolution of intelligence in mammalian carnivores. Interface focus, 7(3), p.20160108. (2017)
53. Benson-Amram, S., Griebling, H.J. and Sluka, C.M., The current state of carnivore cognition. Animal Cognition, 26(1), 37-58. (2023)
54. Carbone C, Teacher A, and Rowcliffe JM The costs of carnivory. PLoS Biology 5(2):e22. (2007)
55. Ramesh, T and Downs, C.T. Diet of serval (*Leptailurus serval*) on farmlands in the Drakensberg Midlands, South Africa. Mammalia,79, 399-407 (2014)
56. Parchizadeh, J., Schooler, S.L., Adibi, M.A., Arias, M.G., Rezaei, S. and Belant, J.L., A review of caracal and jungle cat diets across their geographical ranges during 1842–2021. Ecology and Evolution, 13(5), p.e10130. (2023)
57. ESRI 2017. https://hub.arcgis.com/datasets/esri::resolve-ecoregions-and-biomes/about

58. Katna, A., Kulkarni, A., Thaker, M., and Vanak, A. T. Habitat specificity drives differences in space-use patterns of multiple mesocarnivores in an agroecosystem. Journal of Zoology, 316(2), 92-103. (2022)
59. Wilman, H., Belmaker, J., Simpson, J., de la Rosa, C., Rivadeneira, M.M. and Jetz, W., EltonTraits 1.0: Species-level foraging attributes of the world's birds and mammals: Ecological Archives E095-178. Ecology, 95(7), 2027-2027. (2014)
60. Amatulli, G., Domisch, S., Tuanmu, M.N., Parmentier, B., Ranipeta, A., Malczyk, J. and Jetz, W., A suite of global, cross-scale topographic variables for environmental and biodiversity modeling. Scientific Data, 5(1), 1-15. (2018)
61. Dunford, C.E., Marks, N.J., Wilmers, C.C., Bryce, C.M., Nickel, B., Wolfe, L.L., Scantlebury, D.M. and Williams, T.M., Surviving in steep terrain: a lab-to-field assessment of locomotor costs for wild mountain lions (*Puma concolor*). Movement Ecology, 8, pp.1-12. (2020)
62. Tuanmu, M.N. and Jetz, W., A global 1-km consensus land-cover product for biodiversity and ecosystem modelling. Global Ecology and Biogeography, 23(9), pp.1031-1045. (2014)
63. Venter, O., Sanderson, E.W., Magrach, A., Allan, J.R., Beher, J., Jones, K.R., Possingham, H.P., Laurance, W.F., Wood, P., Fekete, B.M. and Levy, M.A., Sixteen years of change in the global terrestrial human footprint and implications for biodiversity conservation. Nature Communications, 7(1), p.12558. (2016)
64. Zimmermann, B., Nelson, L., Wabakken, P., Sand, H. and Liberg, O., Behavioral responses of wolves to roads: scale-dependent ambivalence. Behavioral Ecology, 25(6), 1353-1364. (2014)
65. Radeloff, V.C., Dubinin, M., Coops, N.C., Allen, A.M., Brooks, T.M., Clayton, M.K., Costa, G.C., Graham, C.H., Helmers, D.P., Ives, A.R. and Kolesov, D., The dynamic habitat indices (DHIs) from MODIS and global biodiversity. Remote Sensing of Environment, 222, pp. 204-214. (2019)
66. Kamler, J.F., Foght, J.L. and Collins, K., Single black-backed jackal (*Canis mesomelas*) kills adult impala (*Aepyceros melampus*). African Journal of Ecology, 48(3), pp.847-848. (2010)
67. Botha, A.E., Bruns, A.C. and le Roux, A., The spatial ecology of black-backed jackals (*Canis mesomelas*) in a protected mountainous grassland area. African Zoology, 57(1), pp.43-55. (2022)
68. Ferguson, J.W.H., Nel, J.A.J. and Wet, M.D., Social organization and movement patterns of black-backed jackals *Canis mesomelas* in South Africa. Journal of Zoology, 199(4), pp.487-502. (1983)
69. Drouilly, M., Nattrass, N., and O'Riain, M. J. Global positioning system location clusters vs. scats: comparing dietary estimates to determine mesopredator diet in a conflict framework. Journal of Zoology, 310(2), pp. 83-94. (2020)
70. Dietz, J.M., *Chrysocyon brachyurus*. American Society of Mammalogists: Mammalian Species. (1985)
71. Mishra, R., Gautam, B., Shah, S.K., Subedi, N., Pokheral, C.P. and Lamichhane, B.R., Opportunistic records of jungle cat (*Felis chaus*) and their activity pattern in Koshi Tappu Wildlife Reserve, Nepal. Nepalese Journal of Zoology, 4(1), pp.50-55. (2020)
72. Canepuccia, A.D., Martinez, M.M. and Vassallo, A.I., Selection of waterbirds by Geoffroy's cat: effects of prey abundance, size, and distance. Mammalian Biology, 72(3), pp.163-173. (2007)

73. Murray, J.L. and Gardner, G.L., *Leopardus pardalis*. Mammalian Species, (548), pp.1-10. (1997)
74. Solorzano-Filho, J.A. Mobbing of *Leopardus wiedii* while hunting by a group of *Sciurus ingrami* in an Araucaria forest of Southeast Brazil. Mammalia: 2006, pp. 156–157. (2006)
75. Loarie, S. R., Tambling, C. J., and Asner, G. P. Lion hunting behaviour and vegetation structure in an African savanna. Animal Behaviour, 85(5), pp. 899-906. (2013)
76. Dalponte, J.C., *Lycalopex vetulus* (Carnivora: Canidae). Mammalian Species, (847), pp.1-7. (2009)
77. Gompper, M.E. and Vanak, A.T., *Vulpes bengalensis*. Mammalian Species, (795), pp.1-5. (2006)
78. Bahr, J., The hunting ecology of Arctic foxes (*Alopex lagopus*) near Cape Churchill, Manitoba (Master's thesis). University of Manitoba. (1989)
79. Egoscue, H.J., Ecology and life history of the kit fox in Tooele County, Utah. Ecology, 43(3), pp.481-497. (1962)
80. Snow, C., San Joaquin Kit Fox, *Vulpes macrotis mutica*: Related Subspecies and the Swift Fox, *Vulpes velox* (No. 6). US Bureau of Land Management. Denver, CO. (1973)
81. Bremner-Harrison, S., Prodohl, P.A. and Elwood, R.W. Behavioural trait assessment as a release criterion: boldness predicts early death in a reintroduction programme of captive-bred swift fox (*Vulpes velox*). In Animal Conservation Forum, 7(3), pp. 313-320. Cambridge University Press. (2004)
82. Butler, A.R., Bly, K.L., Harris, H., Inman, R.M., Moehrenschlager, A., Schwalm, D. and Jachowski, D.S., Winter movement behavior by swift foxes (*Vulpes velox*) at the northern edge of their range. Canadian Journal of Zoology, 97(10), pp.922-930. (2019)
83. Williams, C. K., and Rasmussen, C. E. *Gaussian processes for machine learning* (Vol. 2, No. 3, p. 4). Cambridge, MA: MIT press. (2006)
84. Péron, G., Fleming, C. H., de Paula, R. C., Mitchell, N., Strohbach, M., Leimgruber, P., & Calabrese, J. M. (2017). Periodic continuous-time movement models uncover behavioral changes of wild canids along anthropization gradients. *Ecological Monographs*, *87*(3), 442-456.
83. Vieu, P. A note on density mode estimation. Statistics & Probability Letters 26:4, 297-307 (1996)